

Ustroń, 18 Sept. 2012

Andreev scattering :

from the nano- to macroscale

T. Domański

**Marie Curie–Skłodowska University,
Lublin, Poland**

<http://kft.umcs.lublin.pl/doman/lectures>

Outline

Outline

1. **Introduction**

/ underlying idea /

Outline

1. Introduction

/ underlying idea /

2. Andreev transport via quantum dots

/ correlations versus superconductivity /

Outline

1. **Introduction**

/ underlying idea /

2. **Andreev transport via quantum dots**

/ correlations versus superconductivity /

3. **Further extensions**

/ quantum interference and decoherence /

Outline

1. **Introduction**

/ underlying idea /

2. **Andreev transport via quantum dots**

/ correlations versus superconductivity /

3. **Further extensions**

/ quantum interference and decoherence /

4. **Andreev spectroscopy in bulk superconductors**

/ probe of the pair coherence /

Outline

1. **Introduction**

/ underlying idea /

2. **Andreev transport via quantum dots**

/ correlations versus superconductivity /

3. **Further extensions**

/ quantum interference and decoherence /

4. **Andreev spectroscopy in bulk superconductors**

/ probe of the pair coherence /

5. **Andreev scattering in ultracold gasses**

/ interplay between closed and open channels /

1. Introduction

Andreev reflections

– **the main concept**

Andreev reflections

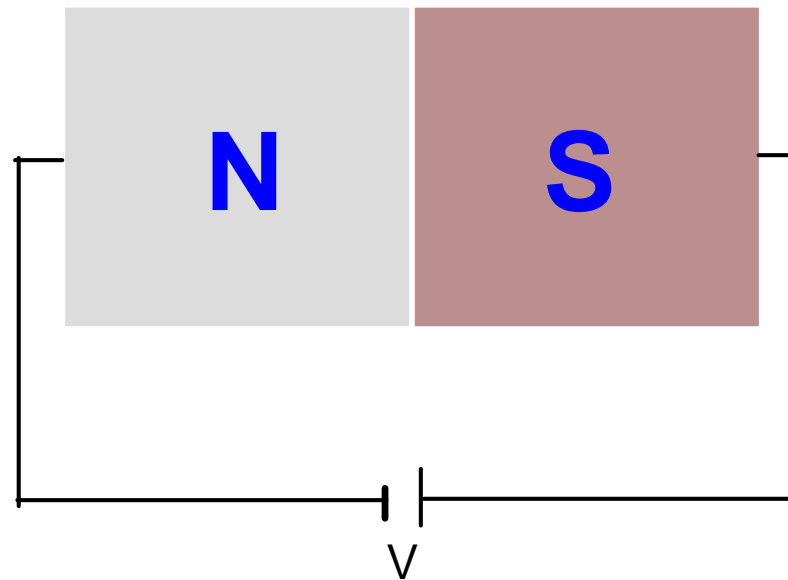
– the main concept

Let us consider the process of electron tunneling from the normal conductor **N** (e.g. metallic lead) to the superconducting electrode **S**

Andreev reflections

– the main concept

Let us consider the process of electron tunneling from the normal conductor **N** (e.g. metallic lead) to the superconducting electrode **S**

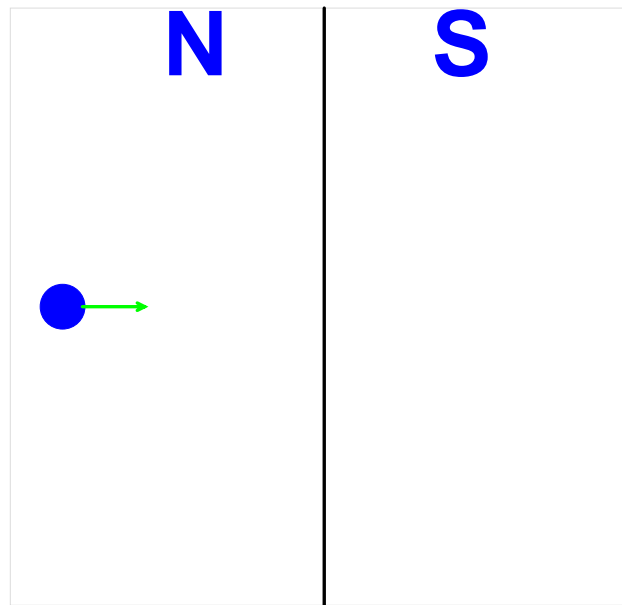


Let us restrict to the subgap regime $|eV| \ll \Delta$ of an applied bias V .

Andreev reflections

– the main concept

Let us consider the process of electron tunneling from the normal conductor **N** (e.g. metallic lead) to the superconducting electrode **S**

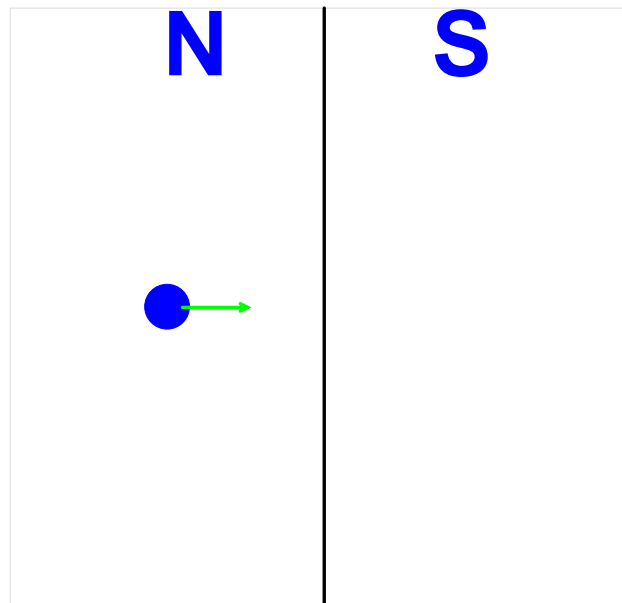


electron

Andreev reflections

– the main concept

Let us consider the process of electron tunneling from the normal conductor **N** (e.g. metallic lead) to the superconducting electrode **S**

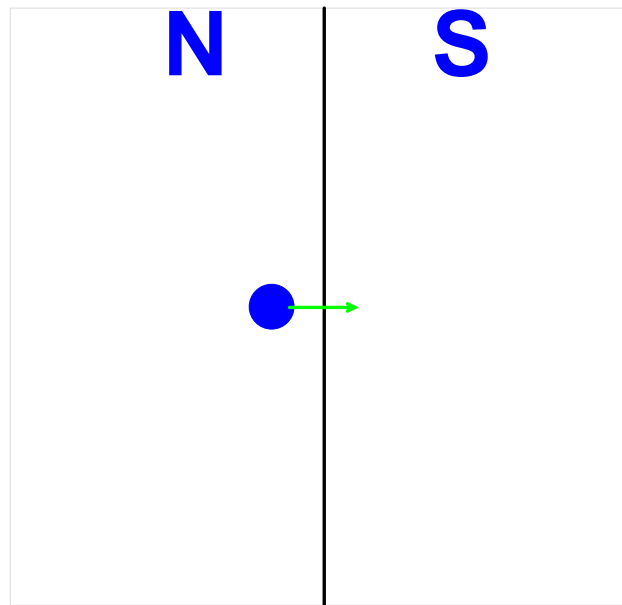


electron

Andreev reflections

– the main concept

Let us consider the process of electron tunneling from the normal conductor **N** (e.g. metallic lead) to the superconducting electrode **S**

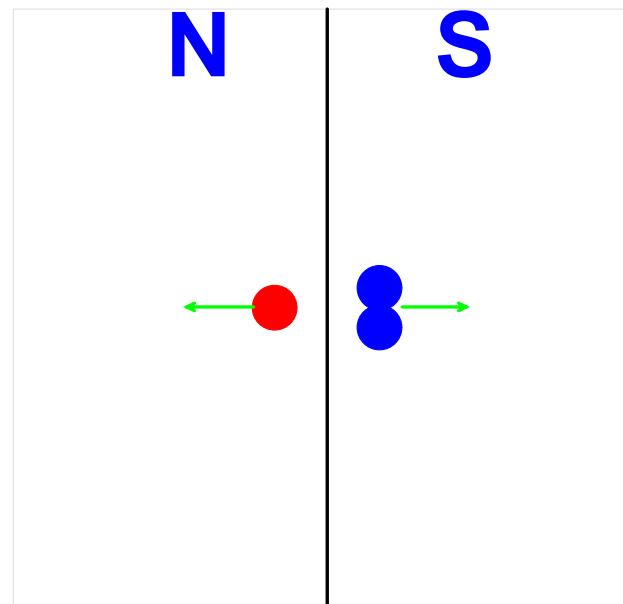


electron

Andreev reflections

– the main concept

Let us consider the process of electron tunneling from the normal conductor **N** (e.g. metallic lead) to the superconducting electrode **S**



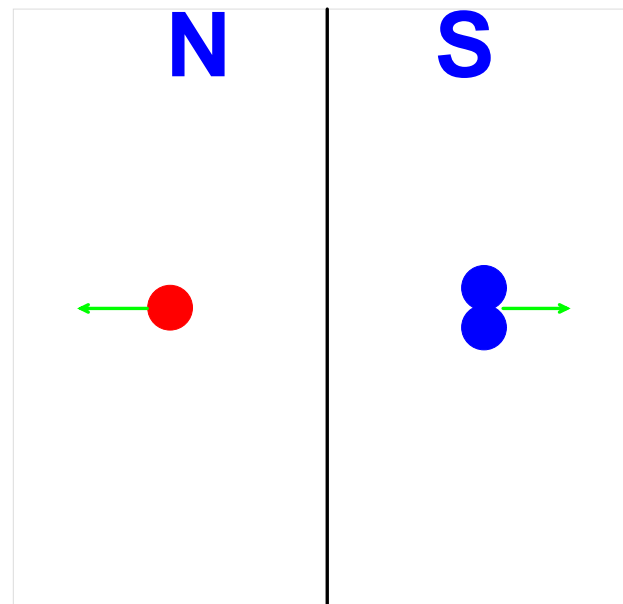
hole

Cooper pair

Andreev reflections

– the main concept

Let us consider the process of electron tunneling from the normal conductor **N** (e.g. metallic lead) to the superconducting electrode **S**



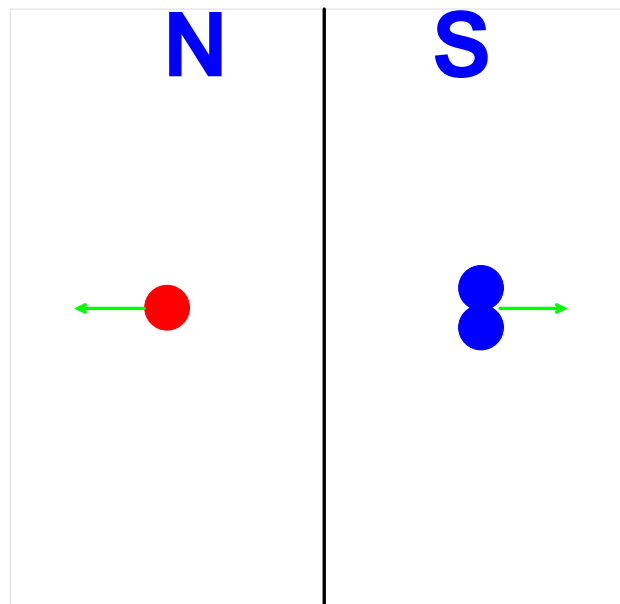
hole

Cooper pair

Andreev reflections

– the main concept

Let us consider the process of electron tunneling from the normal conductor **N** (e.g. metallic lead) to the superconducting electrode **S**



hole

Cooper pair

Such double-charge exchange is named the Andreev reflection (scattering).

Andreev reflections

–

historical remark

Andreev reflections

–

historical remark

This *anomalous* transport channel allows for a finite subgap current across the N-S interface even though the single-particle transmissions are forbidden. Its original idea has been suggested by

Andreev reflections

– historical remark

This *anomalous* transport channel allows for a finite subgap current across the N-S interface even though the single-particle transmissions are forbidden. Its original idea has been suggested by



A.F. Andreev

/ P. Kapitza Institute, Moscow (Russia) /

A.F. Andreev, Sov. Phys. JETP **19**, 1228 (1964).

2. Andreev transport via quantum dot

Physical situation

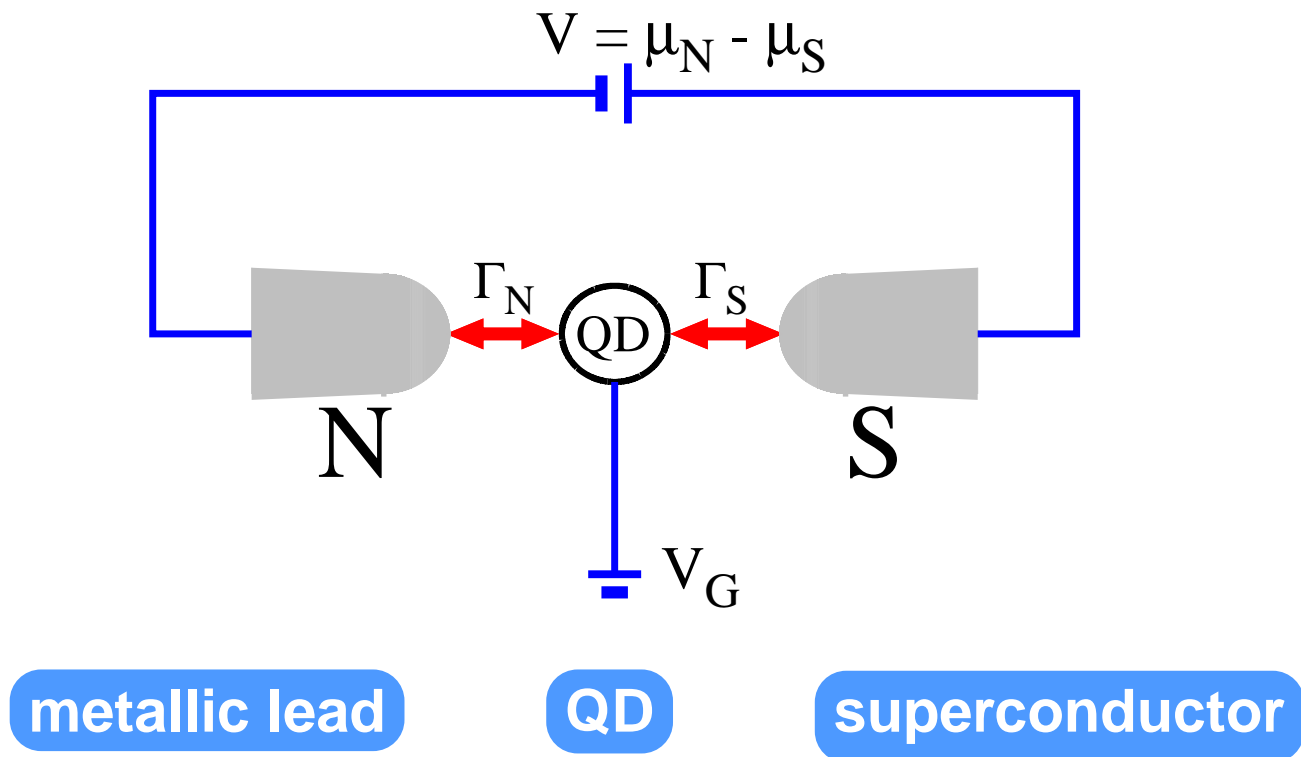
N-QD-S scheme

Let us consider the quantum dot (QD) on an interface between the external metallic (N) and superconducting (S) leads

Physical situation

N-QD-S scheme

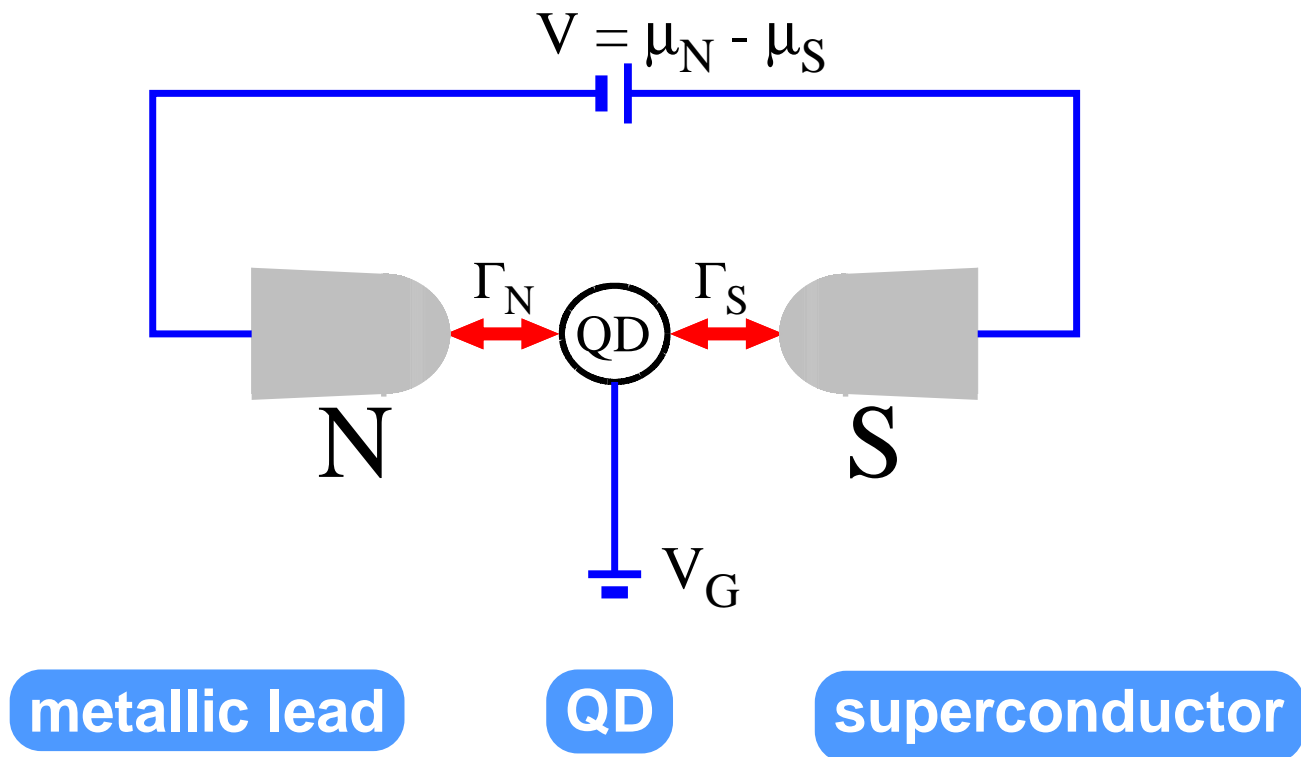
Let us consider the quantum dot (QD) on an interface between the external metallic (N) and superconducting (S) leads



Physical situation

N-QD-S scheme

Let us consider the quantum dot (QD) on an interface between the external metallic (N) and superconducting (S) leads



This setup can be thought of as a particular version of the SET.

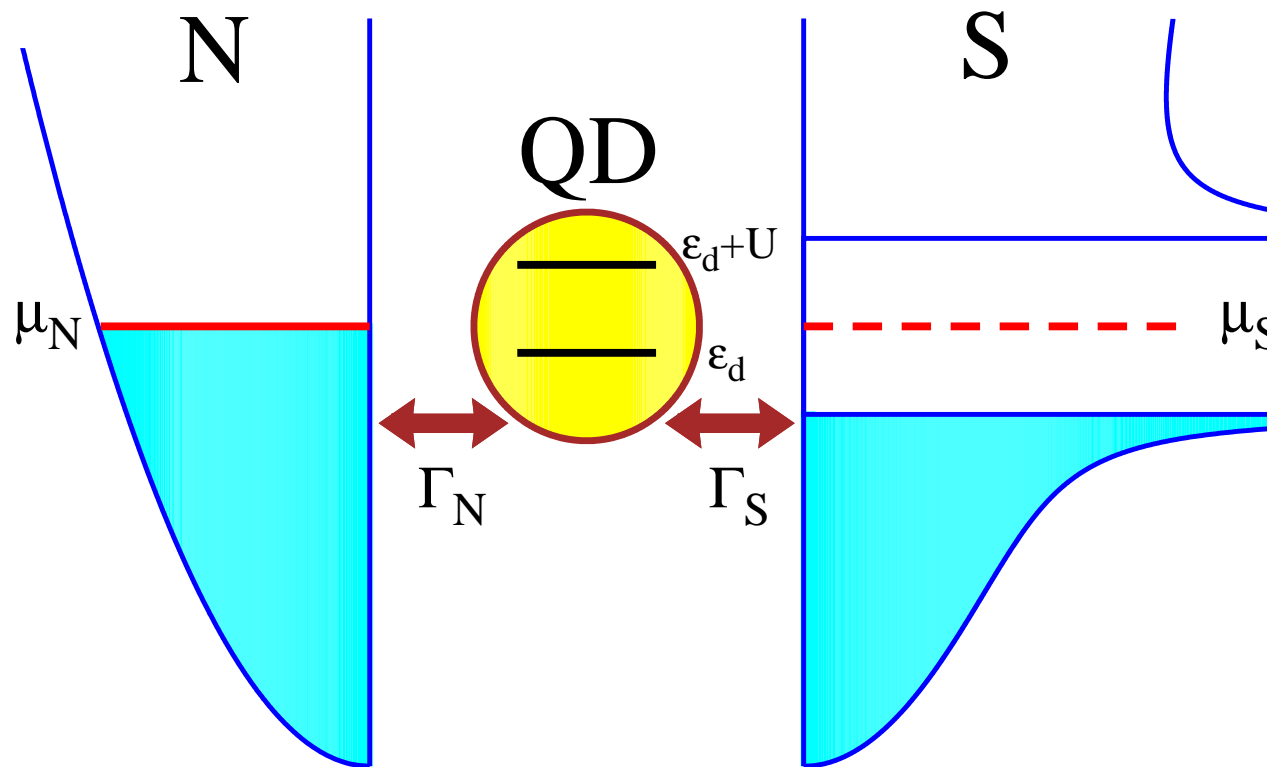
Physical situation – energy spectrum

Physical situation – energy spectrum

Components of the N-QD-S heterostructure have the following spectra

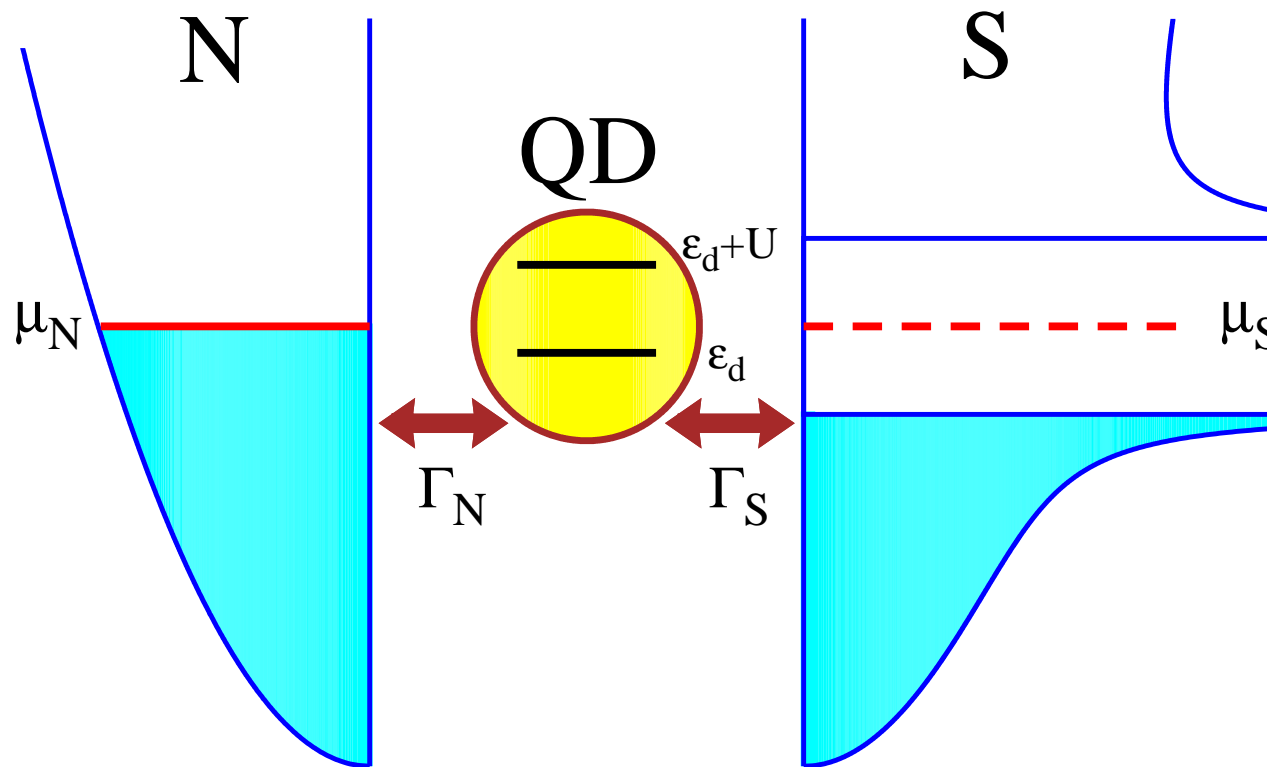
Physical situation – energy spectrum

Components of the N-QD-S heterostructure have the following spectra



Physical situation – energy spectrum

Components of the N-QD-S heterostructure have the following spectra



External bias $eV = \mu_N - \mu_S$ induces the current(s) through QD.

Microscopic model

The correlation effects

Microscopic model

The correlation effects

$$\hat{H}_{QD} = \sum_{\sigma} \epsilon_d \hat{d}_{\sigma}^{\dagger} \hat{d}_{\sigma} + U \hat{n}_{d\uparrow} \hat{n}_{d\downarrow}$$

Microscopic model

The correlation effects

$$\hat{H}_{QD} = \sum_{\sigma} \epsilon_d \hat{d}_{\sigma}^{\dagger} \hat{d}_{\sigma} + U \hat{n}_{d\uparrow} \hat{n}_{d\downarrow}$$

are expected to affect the transport properties of the system

Microscopic model

The correlation effects

$$\hat{H}_{QD} = \sum_{\sigma} \epsilon_d \hat{d}_{\sigma}^{\dagger} \hat{d}_{\sigma} + U \hat{n}_{d\uparrow} \hat{n}_{d\downarrow}$$

are expected to affect the transport properties of the system

$$\begin{aligned} \hat{H} = & \sum_{\sigma} \epsilon_d \hat{d}_{\sigma}^{\dagger} \hat{d}_{\sigma} + U \hat{n}_{d\uparrow} \hat{n}_{d\downarrow} + \hat{H}_N + \hat{H}_S \\ & + \sum_{\mathbf{k}, \sigma} \sum_{\beta=N, S} \left(V_{\mathbf{k}\beta} \hat{d}_{\sigma}^{\dagger} \hat{c}_{\mathbf{k}\sigma\beta} + V_{\mathbf{k}\beta}^* \hat{c}_{\mathbf{k}\sigma, \beta}^{\dagger} \hat{d}_{\sigma} \right) \end{aligned}$$

Microscopic model

The correlation effects

$$\hat{H}_{QD} = \sum_{\sigma} \epsilon_d \hat{d}_{\sigma}^{\dagger} \hat{d}_{\sigma} + U \hat{n}_{d\uparrow} \hat{n}_{d\downarrow}$$

are expected to affect the transport properties of the system

$$\begin{aligned} \hat{H} = & \sum_{\sigma} \epsilon_d \hat{d}_{\sigma}^{\dagger} \hat{d}_{\sigma} + U \hat{n}_{d\uparrow} \hat{n}_{d\downarrow} + \hat{H}_N + \hat{H}_S \\ & + \sum_{k,\sigma} \sum_{\beta=N,S} \left(V_{k\beta} \hat{d}_{\sigma}^{\dagger} \hat{c}_{k\sigma\beta} + V_{k\beta}^* \hat{c}_{k\sigma,\beta}^{\dagger} \hat{d}_{\sigma} \right) \end{aligned}$$

where

$$\hat{H}_N = \sum_{k,\sigma} (\epsilon_{k,N} - \mu_N) \hat{c}_{k\sigma N}^{\dagger} \hat{c}_{k\sigma N}$$

Microscopic model

The correlation effects

$$\hat{H}_{QD} = \sum_{\sigma} \epsilon_d \hat{d}_{\sigma}^{\dagger} \hat{d}_{\sigma} + U \hat{n}_{d\uparrow} \hat{n}_{d\downarrow}$$

are expected to affect the transport properties of the system

$$\begin{aligned} \hat{H} = & \sum_{\sigma} \epsilon_d \hat{d}_{\sigma}^{\dagger} \hat{d}_{\sigma} + U \hat{n}_{d\uparrow} \hat{n}_{d\downarrow} + \hat{H}_N + \hat{H}_S \\ & + \sum_{k,\sigma} \sum_{\beta=N,S} \left(V_{k\beta} \hat{d}_{\sigma}^{\dagger} \hat{c}_{k\sigma\beta} + V_{k\beta}^* \hat{c}_{k\sigma,\beta}^{\dagger} \hat{d}_{\sigma} \right) \end{aligned}$$

where

$$\hat{H}_S = \sum_{k,\sigma} (\epsilon_{k,S} - \mu_S) \hat{c}_{k\sigma S}^{\dagger} \hat{c}_{k\sigma S} - \sum_k \left(\Delta \hat{c}_{k\uparrow S}^{\dagger} \hat{c}_{k\downarrow S}^{\dagger} + \text{h.c.} \right)$$

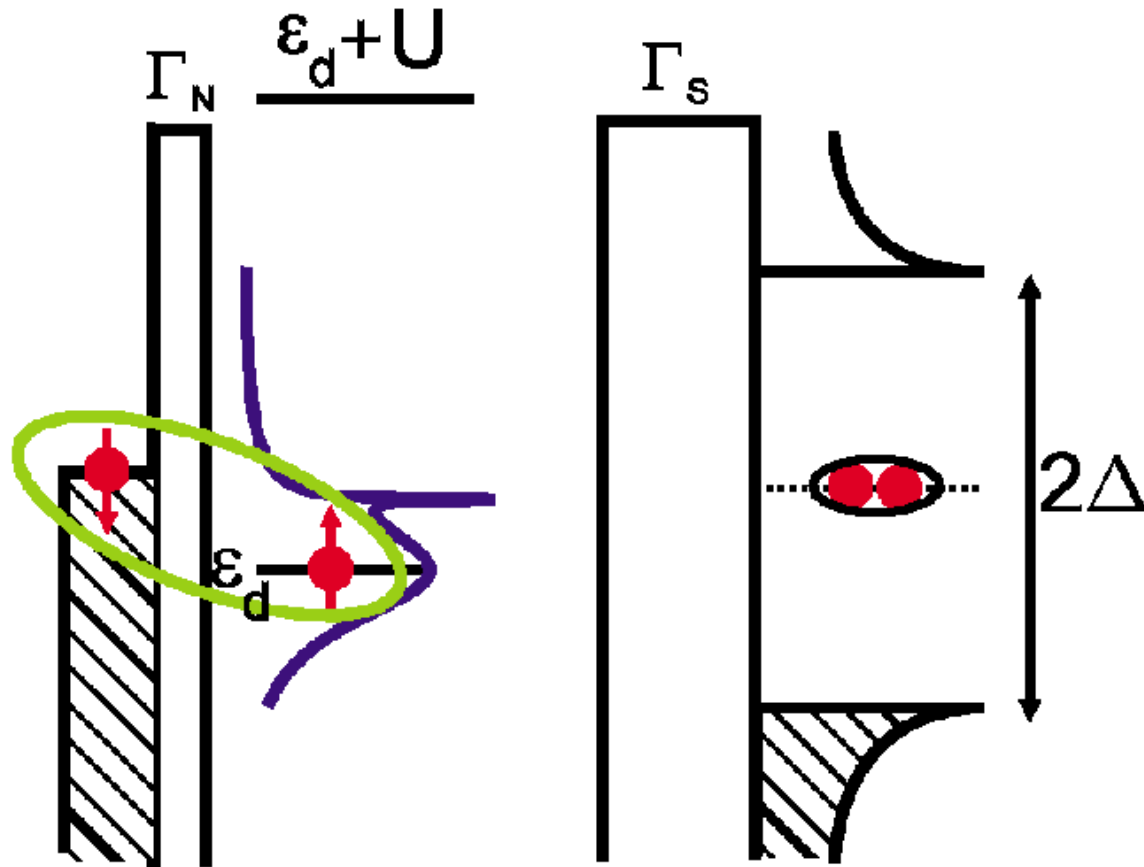
Relevant problems : **issue # 1**

Relevant problems : issue # 1

Hybridization of QD to the metallic lead is responsible for:

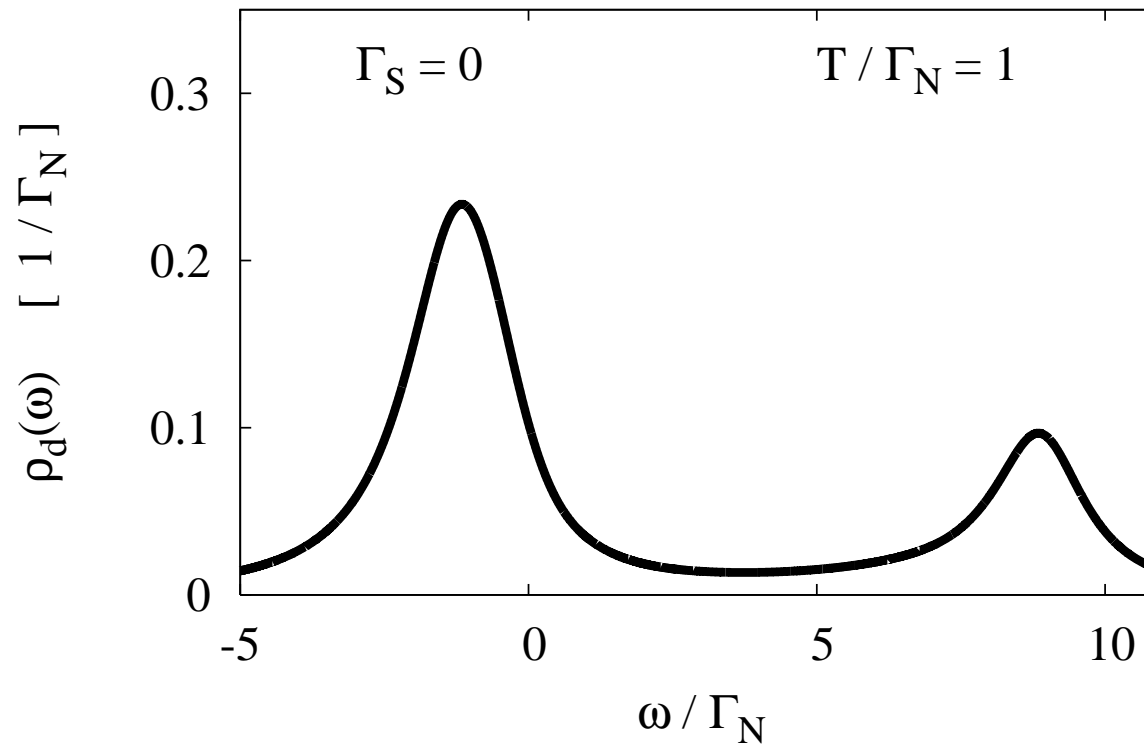
Relevant problems : issue # 1

Hybridization of QD to the metallic lead is responsible for:



Relevant problems : issue # 1

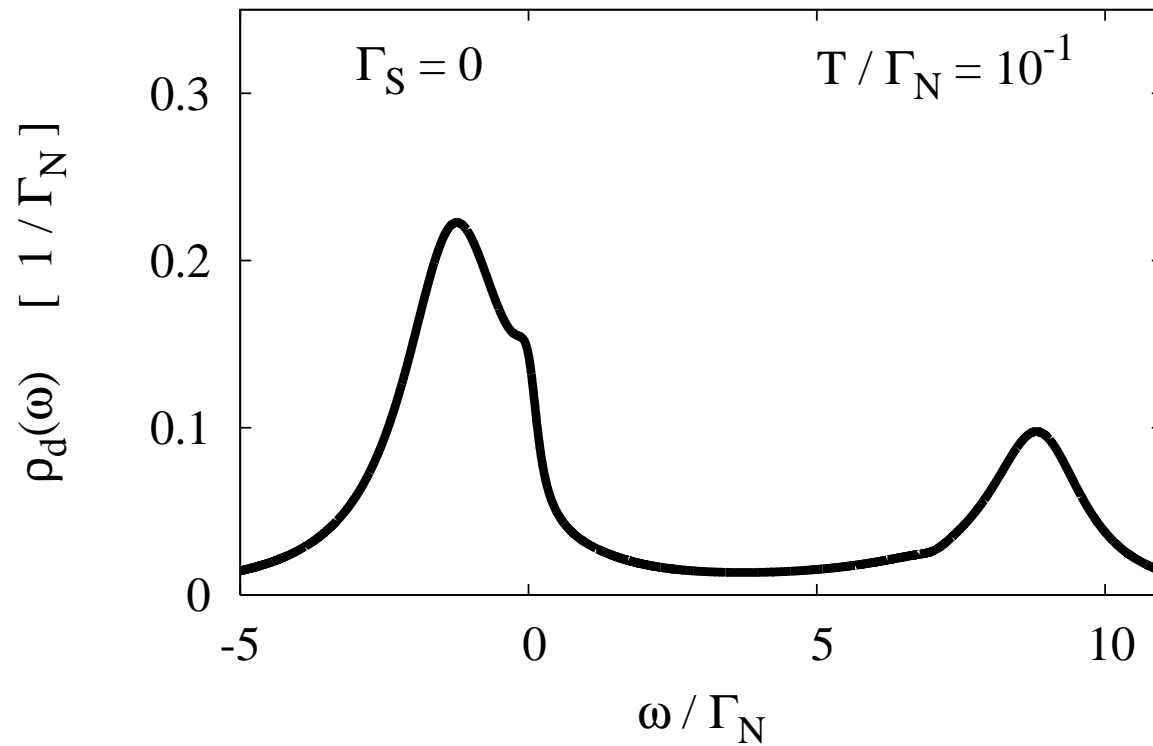
Hybridization of QD to the metallic lead is responsible for:



a broadening of QD levels

Relevant problems : issue # 1

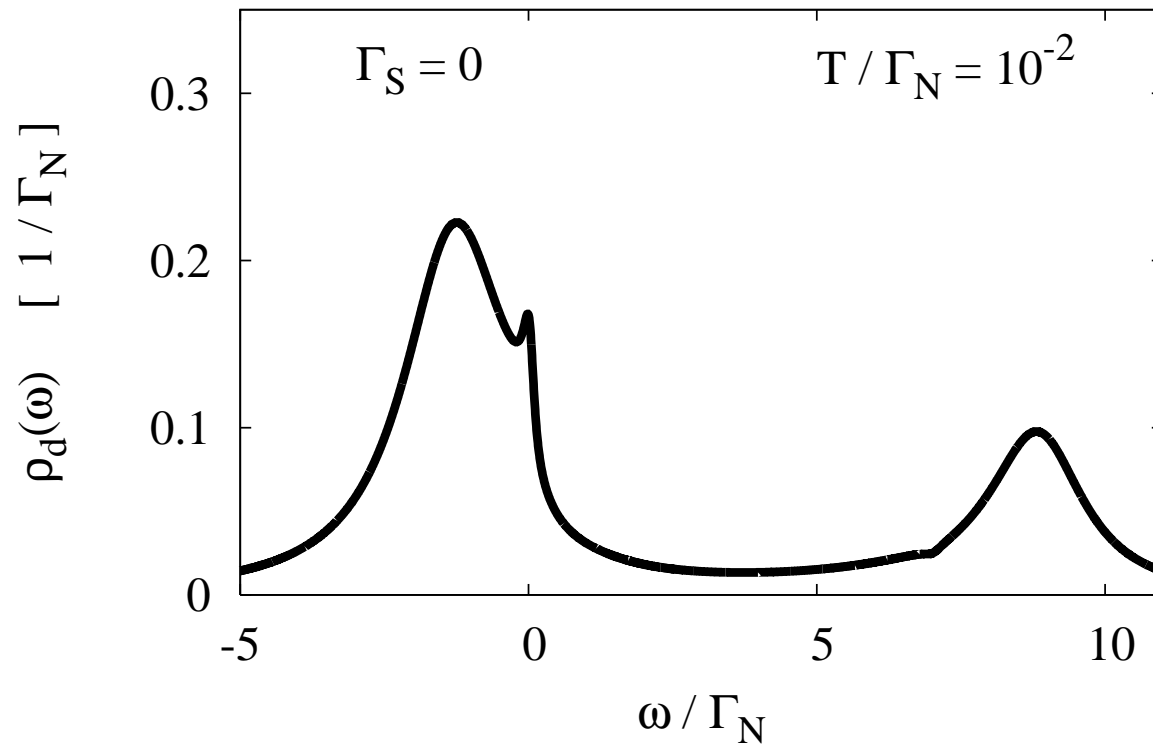
Hybridization of QD to the metallic lead is responsible for:



a broadening of QD levels and ...

Relevant problems : issue # 1

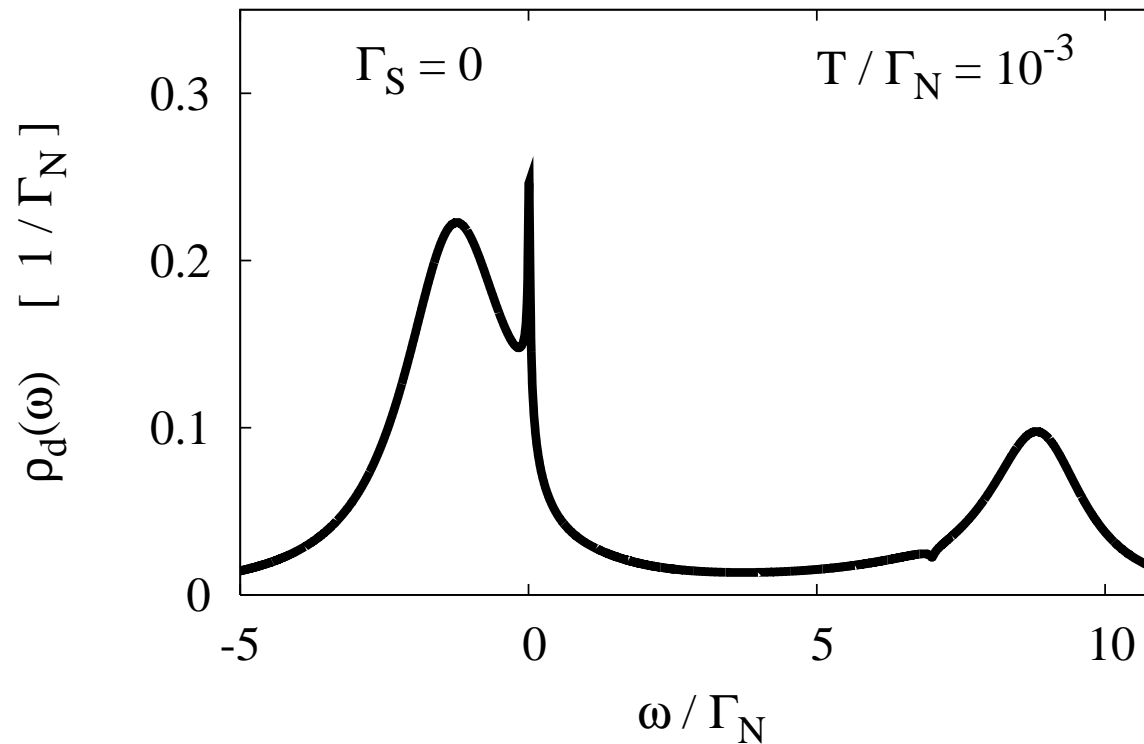
Hybridization of QD to the metallic lead is responsible for:



a broadening of QD levels and ...

Relevant problems : issue # 1

Hybridization of QD to the metallic lead is responsible for:

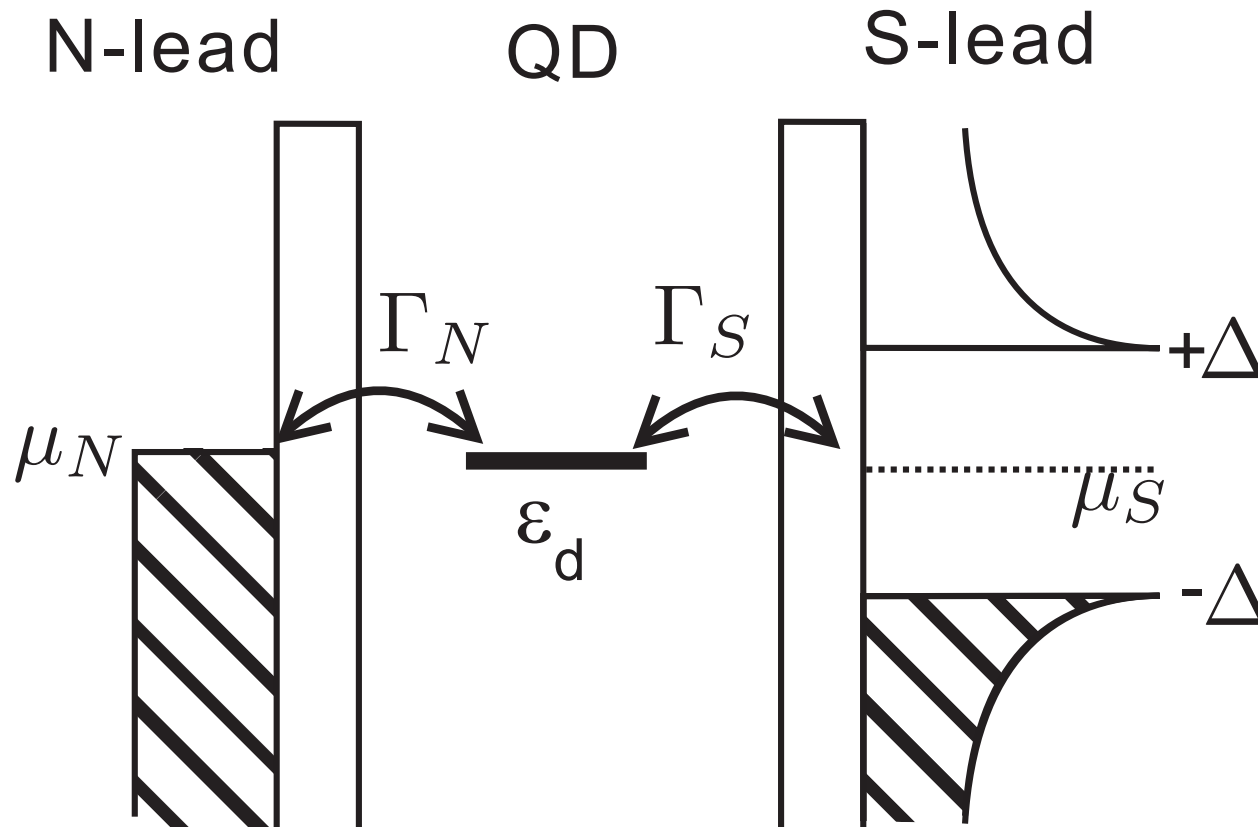


- ★ a broadening of QD levels and
- ★ appearance of the Kondo resonance below T_K .

Relevant problems : **issue # 2**

Relevant problems : issue # 2

Hybridization of QD to the superconducting lead



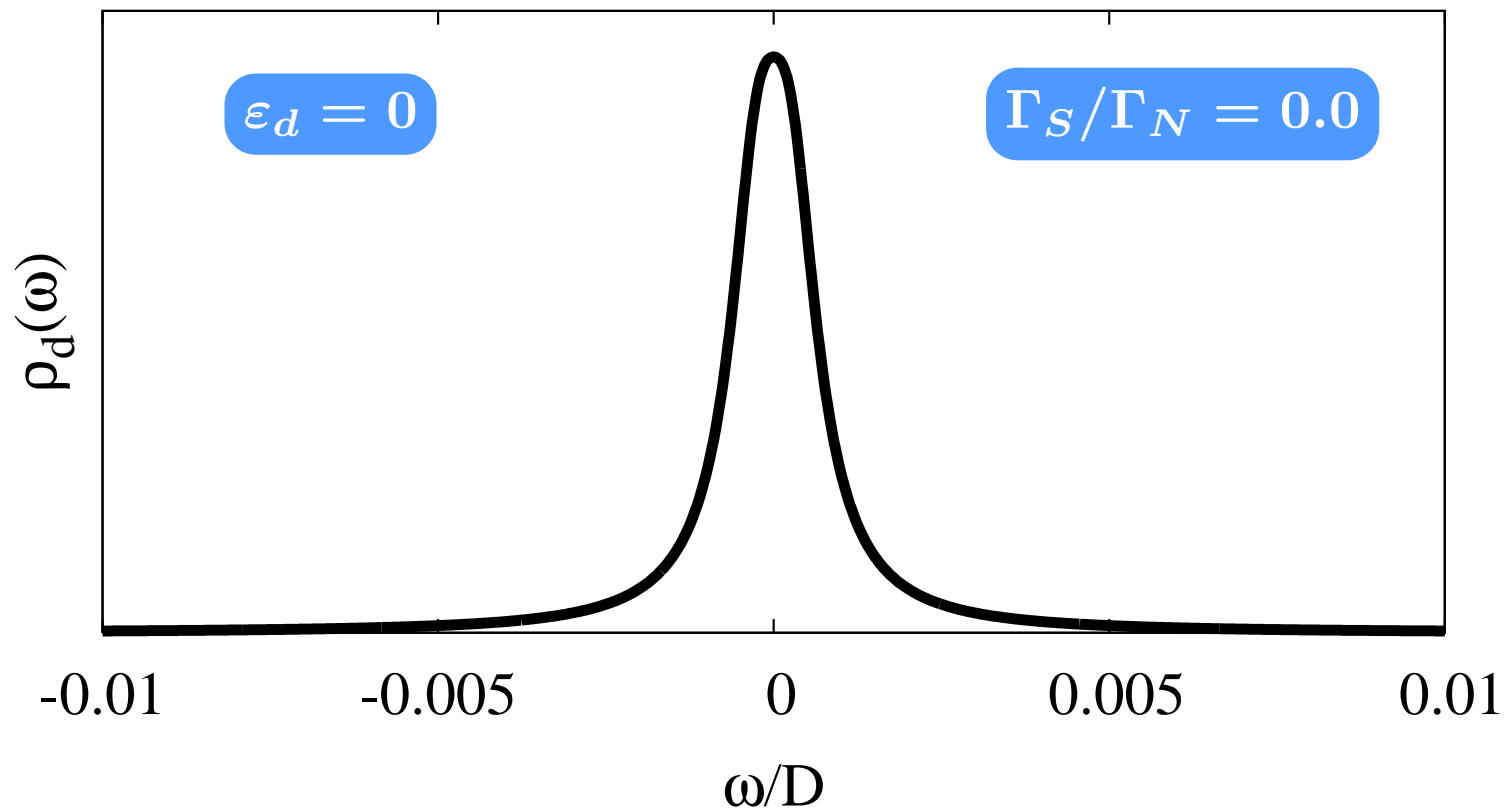
Relevant problems : issue # 2

Hybridization of QD to S transmits the **on-dot pairing** (*proximity effect*).

Relevant problems : issue # 2

Hybridization of QD to S transmits the **on-dot pairing** (*proximity effect*).

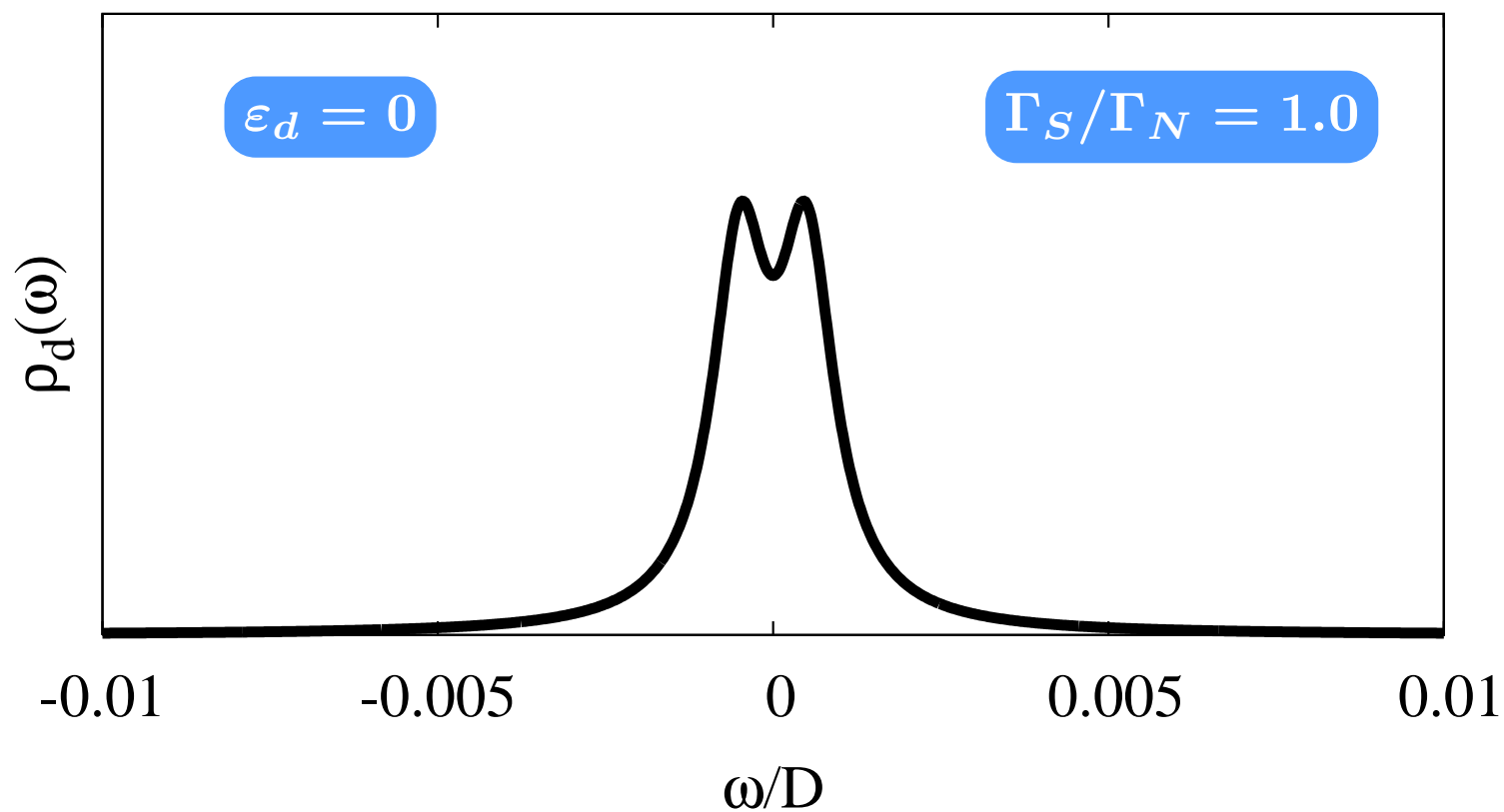
$$U = 0$$



Relevant problems : issue # 2

Hybridization of QD to S transmits the **on-dot pairing** (*proximity effect*).

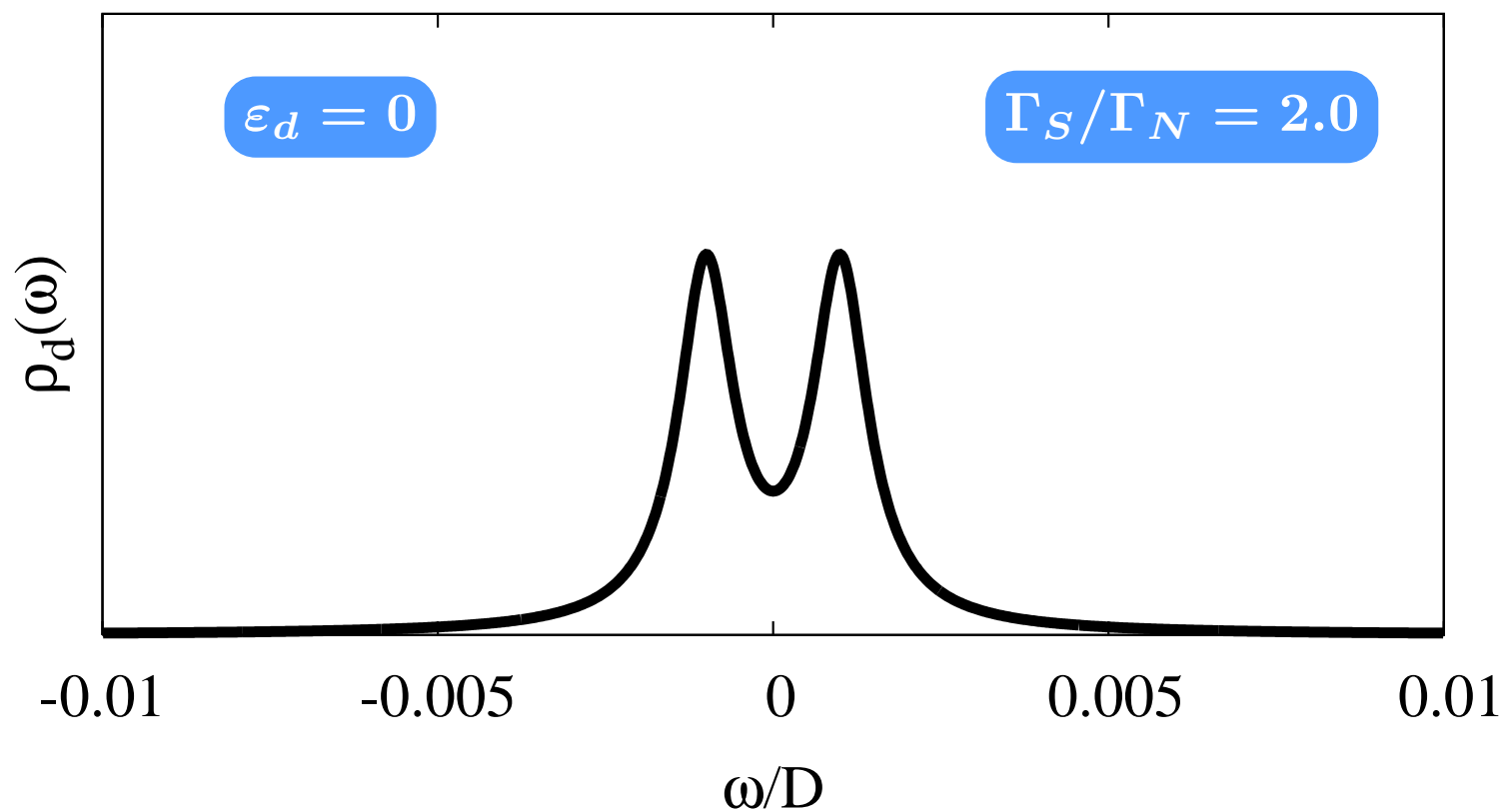
$$U = 0$$



Relevant problems : issue # 2

Hybridization of QD to S transmits the **on-dot pairing** (*proximity effect*).

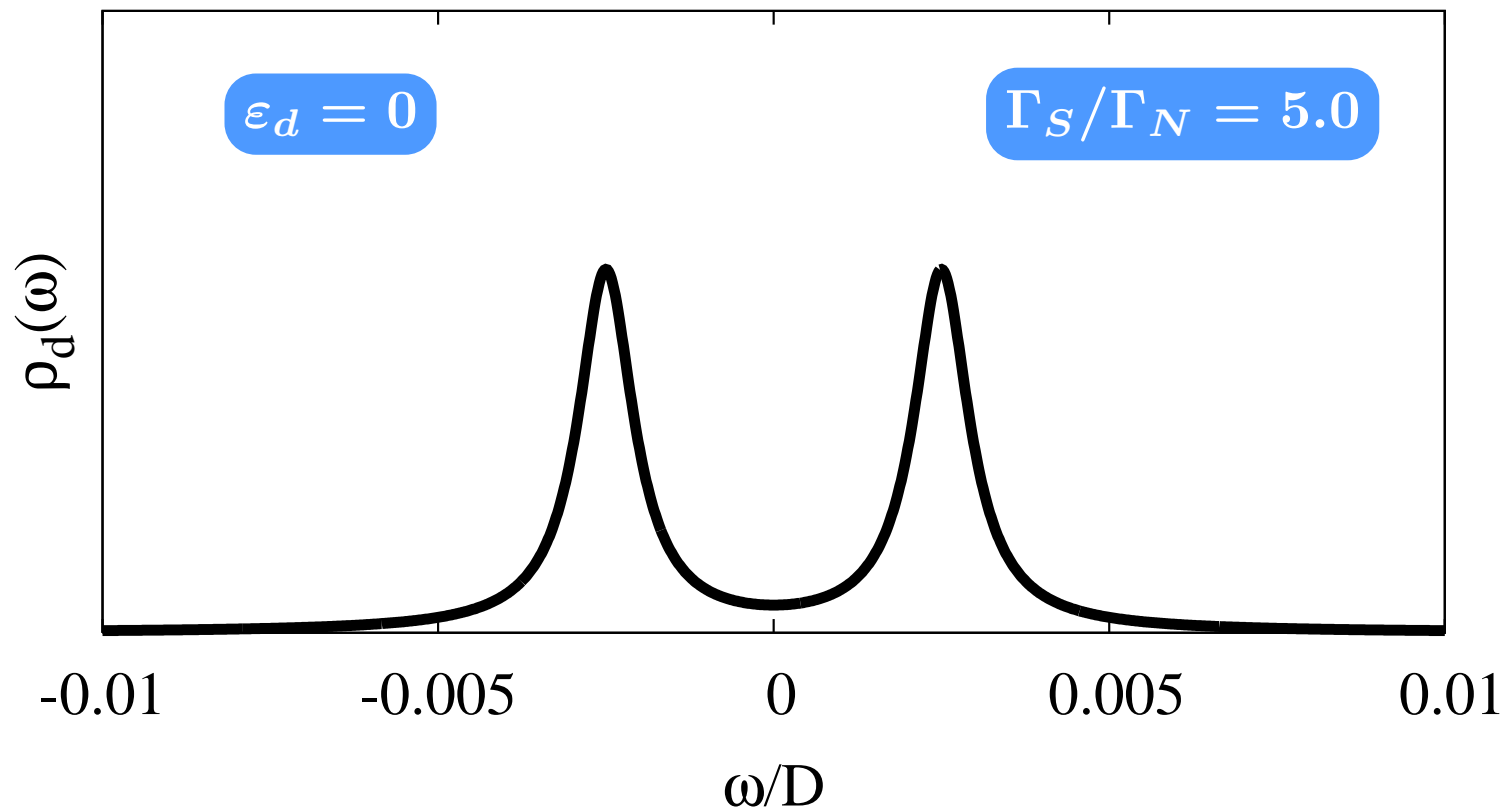
$$U = 0$$



Relevant problems : issue # 2

Hybridization of QD to S transmits the **on-dot pairing** (*proximity effect*).

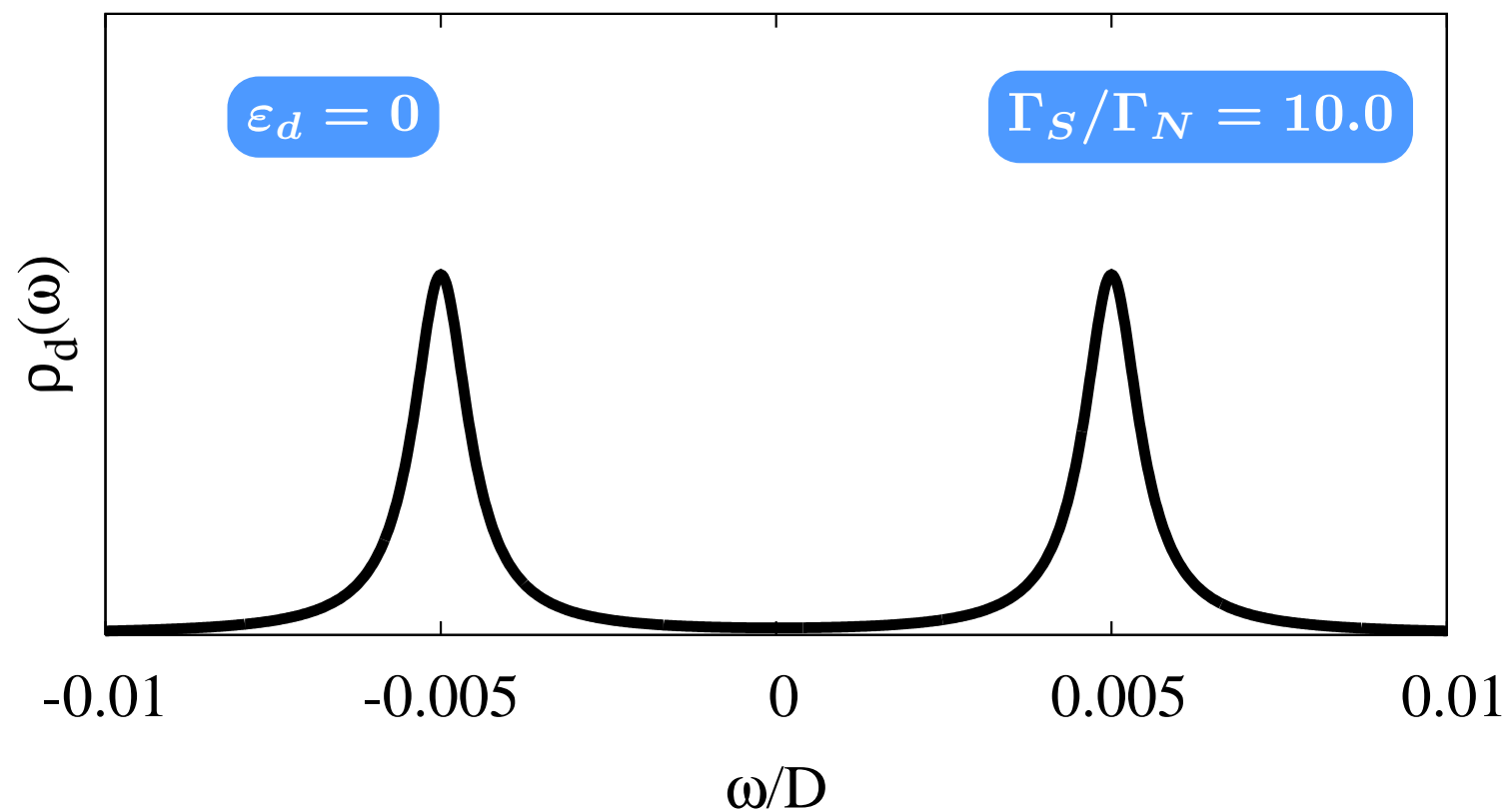
$$U = 0$$



Relevant problems : issue # 2

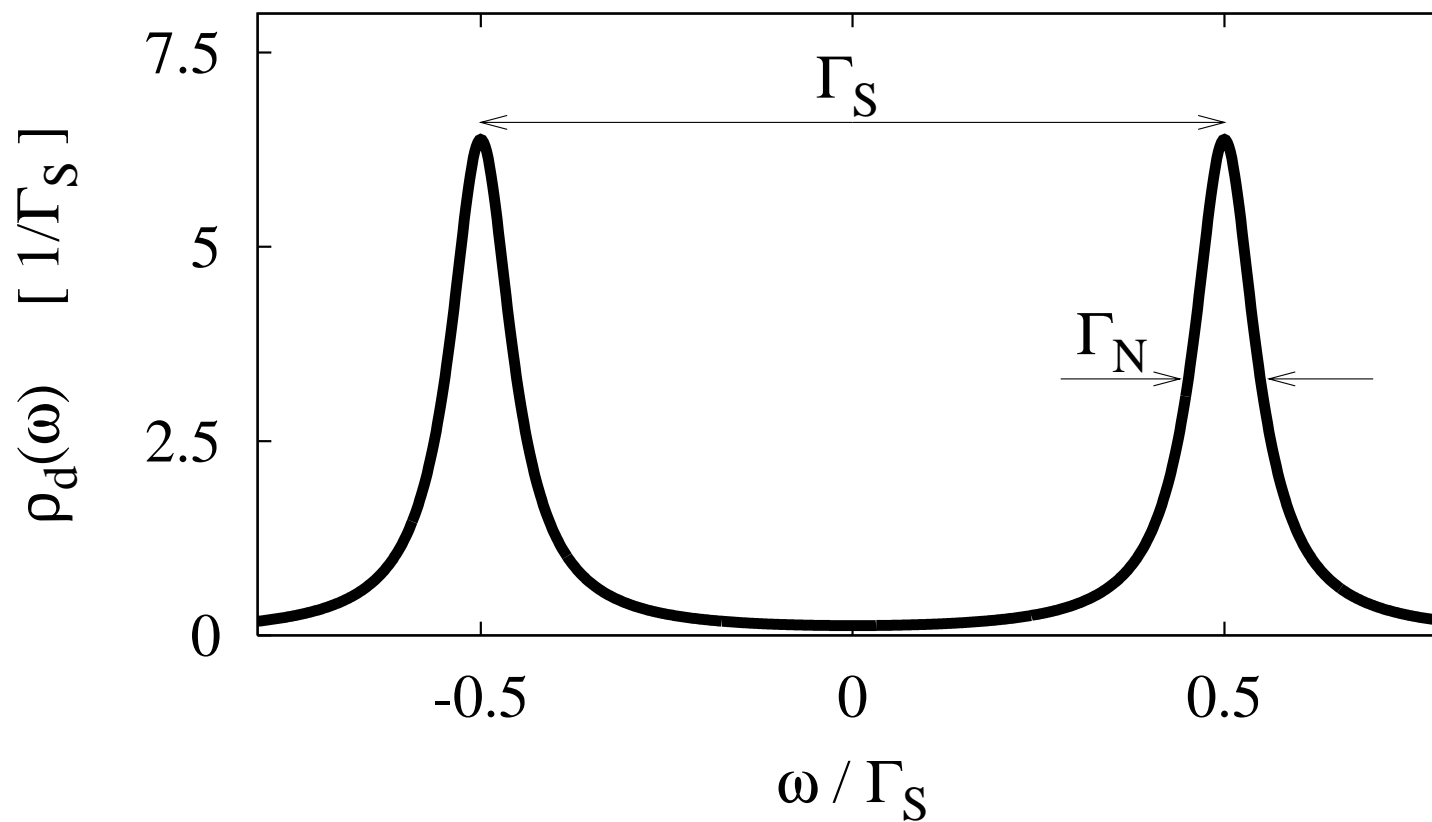
Hybridization of QD to S transmits the **on-dot pairing** (*proximity effect*).

$$U = 0$$



Relevant problems : issue # 2

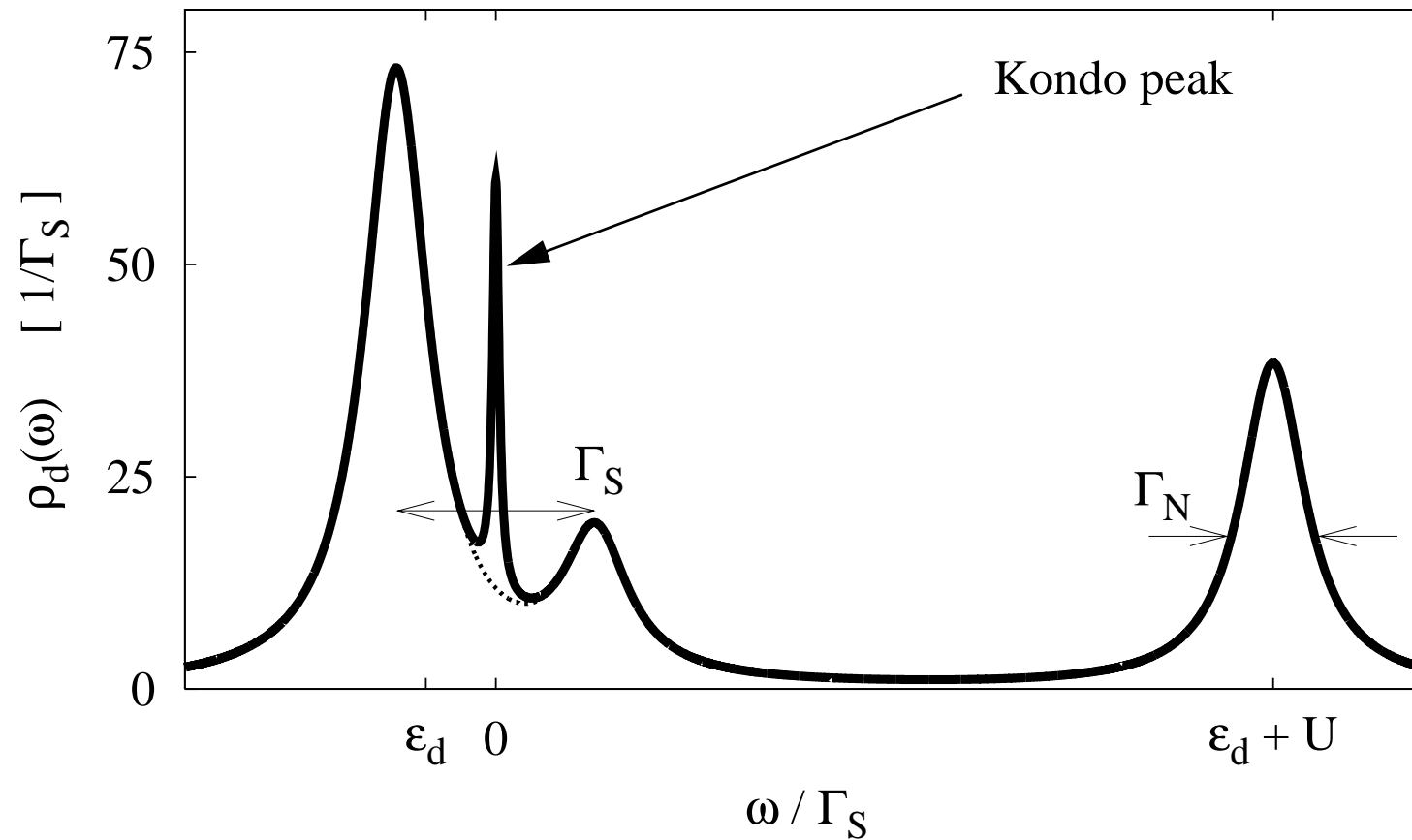
Hybridization of QD to S transmits the **on-dot pairing** (*proximity effect*).



Relevant problems : # 1 + 2

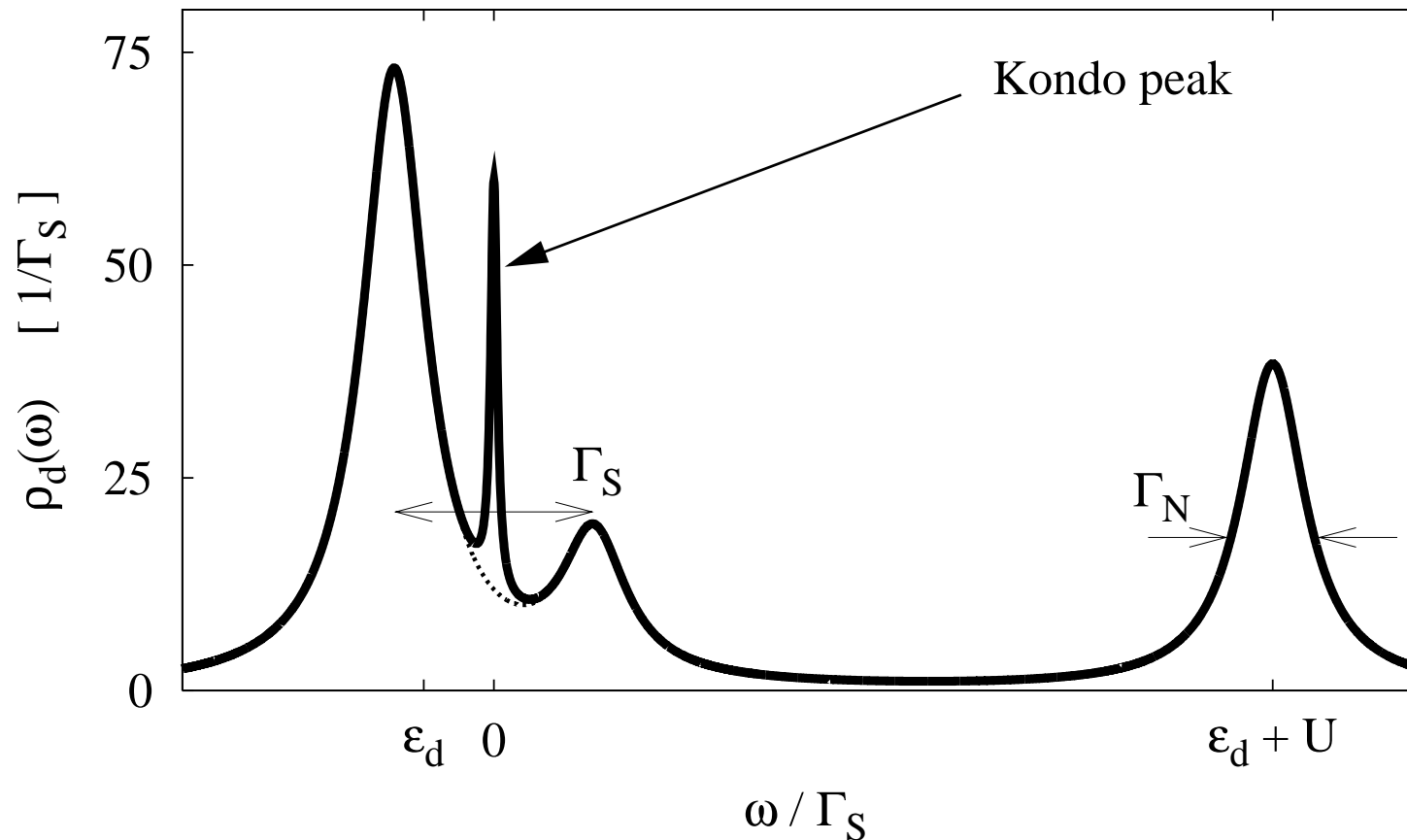
Relevant problems : # 1 + 2

Hybridizations Γ_N and Γ_S are thus effectively leading to



Relevant problems : # 1 + 2

Hybridizations Γ_N and Γ_S are thus effectively leading to



/ interplay between the Kondo effect and superconductivity /

Questions:

Questions:

- ★ What kind of interplay occurs between superconductivity (transmitted onto the QD) and the Kondo effect ?

Questions:

- ★ What kind of interplay occurs between superconductivity (transmitted onto the QD) and the Kondo effect ?

Do they cooperate or compete ?

Questions:

★ What kind of interplay occurs between superconductivity (transmitted onto the QD) and the Kondo effect ?

Do they cooperate or compete ?

★ How do these effects show up in the charge current through N-QD-S junction ?

Questions:

- ★ What kind of interplay occurs between superconductivity (transmitted onto the QD) and the Kondo effect ?

Do they cooperate or compete ?

- ★ How do these effects show up in the charge current through N-QD-S junction ?

Are there any particular features ?

Formal aspects

Formal aspects

To account for both, the proximity effect and the correlations, we have to deal with the Nambu (2×2 matrix) Green's function

Formal aspects

To account for both, the proximity effect and the correlations, we have to deal with the Nambu (2×2 matrix) Green's function

$$G_d(\tau, \tau') = - \begin{pmatrix} \hat{T}_\tau \langle \hat{d}_\uparrow(\tau) \hat{d}_\uparrow^\dagger(\tau') \rangle & \hat{T}_\tau \langle \hat{d}_\uparrow(\tau) \hat{d}_\downarrow(\tau') \rangle \\ \hat{T}_\tau \langle \hat{d}_\downarrow^\dagger(\tau) \hat{d}_\uparrow^\dagger(\tau') \rangle & \hat{T}_\tau \langle \hat{d}_\downarrow^\dagger(\tau) \hat{d}_\downarrow(\tau') \rangle \end{pmatrix}$$

Formal aspects

To account for both, the proximity effect and the correlations, we have to deal with the Nambu (2×2 matrix) Green's function

$$G_d(\tau, \tau') = - \begin{pmatrix} \hat{T}_\tau \langle \hat{d}_\uparrow(\tau) \hat{d}_\uparrow^\dagger(\tau') \rangle & \hat{T}_\tau \langle \hat{d}_\uparrow(\tau) \hat{d}_\downarrow(\tau') \rangle \\ \hat{T}_\tau \langle \hat{d}_\downarrow^\dagger(\tau) \hat{d}_\uparrow^\dagger(\tau') \rangle & \hat{T}_\tau \langle \hat{d}_\downarrow^\dagger(\tau) \hat{d}_\downarrow(\tau') \rangle \end{pmatrix}$$

In equilibrium its Fourier transform obeys the Dyson equation

Formal aspects

To account for both, the proximity effect and the correlations, we have to deal with the Nambu (2×2 matrix) Green's function

$$G_d(\tau, \tau') = - \begin{pmatrix} \hat{T}_\tau \langle \hat{d}_\uparrow(\tau) \hat{d}_\uparrow^\dagger(\tau') \rangle & \hat{T}_\tau \langle \hat{d}_\uparrow(\tau) \hat{d}_\downarrow(\tau') \rangle \\ \hat{T}_\tau \langle \hat{d}_\downarrow^\dagger(\tau) \hat{d}_\uparrow^\dagger(\tau') \rangle & \hat{T}_\tau \langle \hat{d}_\downarrow^\dagger(\tau) \hat{d}_\downarrow(\tau') \rangle \end{pmatrix}$$

In equilibrium its Fourier transform obeys the Dyson equation

$$G_d(\omega)^{-1} = \begin{pmatrix} \omega - \varepsilon_d & 0 \\ 0 & \omega + \varepsilon_d \end{pmatrix} - \Sigma_d^0(\omega) - \Sigma_d^U(\omega)$$

Formal aspects

To account for both, the proximity effect and the correlations, we have to deal with the Nambu (2×2 matrix) Green's function

$$G_d(\tau, \tau') = - \begin{pmatrix} \hat{T}_\tau \langle \hat{d}_\uparrow(\tau) \hat{d}_\uparrow^\dagger(\tau') \rangle & \hat{T}_\tau \langle \hat{d}_\uparrow(\tau) \hat{d}_\downarrow(\tau') \rangle \\ \hat{T}_\tau \langle \hat{d}_\downarrow^\dagger(\tau) \hat{d}_\uparrow^\dagger(\tau') \rangle & \hat{T}_\tau \langle \hat{d}_\downarrow^\dagger(\tau) \hat{d}_\downarrow(\tau') \rangle \end{pmatrix}$$

In equilibrium its Fourier transform obeys the Dyson equation

$$G_d(\omega)^{-1} = \begin{pmatrix} \omega - \varepsilon_d & 0 \\ 0 & \omega + \varepsilon_d \end{pmatrix} - \Sigma_d^0(\omega) - \Sigma_d^U(\omega)$$

with

$$\Sigma_d^0(\omega) \quad \text{the selfenergy for } U = 0$$

Formal aspects

To account for both, the proximity effect and the correlations, we have to deal with the Nambu (2×2 matrix) Green's function

$$G_d(\tau, \tau') = - \begin{pmatrix} \hat{T}_\tau \langle \hat{d}_\uparrow(\tau) \hat{d}_\uparrow^\dagger(\tau') \rangle & \hat{T}_\tau \langle \hat{d}_\uparrow(\tau) \hat{d}_\downarrow(\tau') \rangle \\ \hat{T}_\tau \langle \hat{d}_\downarrow^\dagger(\tau) \hat{d}_\uparrow^\dagger(\tau') \rangle & \hat{T}_\tau \langle \hat{d}_\downarrow^\dagger(\tau) \hat{d}_\downarrow(\tau') \rangle \end{pmatrix}$$

In equilibrium its Fourier transform obeys the Dyson equation

$$G_d(\omega)^{-1} = \begin{pmatrix} \omega - \varepsilon_d & 0 \\ 0 & \omega + \varepsilon_d \end{pmatrix} - \Sigma_d^0(\omega) - \Sigma_d^U(\omega)$$

with

$$\Sigma_d^U(\omega) \quad \text{correction due to } U \neq 0.$$

Non-equilibrium phenomena

Non-equilibrium phenomena

The steady current $J_L = -J_R$ is found to consist of two contributions

$$J(V) = J_1(V) + J_A(V)$$

Non-equilibrium phenomena

The steady current $J_L = -J_R$ is found to consist of two contributions

$$J(V) = J_1(V) + J_A(V)$$

which can be expressed by the Landauer-type formula

$$J_1(V) = \frac{2e}{h} \int d\omega \, T_1(\omega) [f(\omega + eV, T) - f(\omega, T)]$$

$$J_A(V) = \frac{2e}{h} \int d\omega \, T_A(\omega) [f(\omega + eV, T) - f(\omega - eV, T)]$$

with the transmittance

$$T_1(\omega) = \Gamma_N \Gamma_S \left(|G_{11}^r(\omega)|^2 + |G_{12}^r(\omega)|^2 - \frac{2\Delta}{|\omega|} \text{Re} G_{11}^r(\omega) G_{12}^r(\omega) \right)$$

Non-equilibrium phenomena

The steady current $J_L = -J_R$ is found to consist of two contributions

$$J(V) = J_1(V) + J_A(V)$$

which can be expressed by the Landauer-type formula

$$J_1(V) = \frac{2e}{h} \int d\omega \, T_1(\omega) [f(\omega + eV, T) - f(\omega, T)]$$

$$J_A(V) = \frac{2e}{h} \int d\omega \, T_A(\omega) [f(\omega + eV, T) - f(\omega - eV, T)]$$

with the transmittance

$$T_A(\omega) = \Gamma_N^2 |G_{12}(\omega)|^2$$

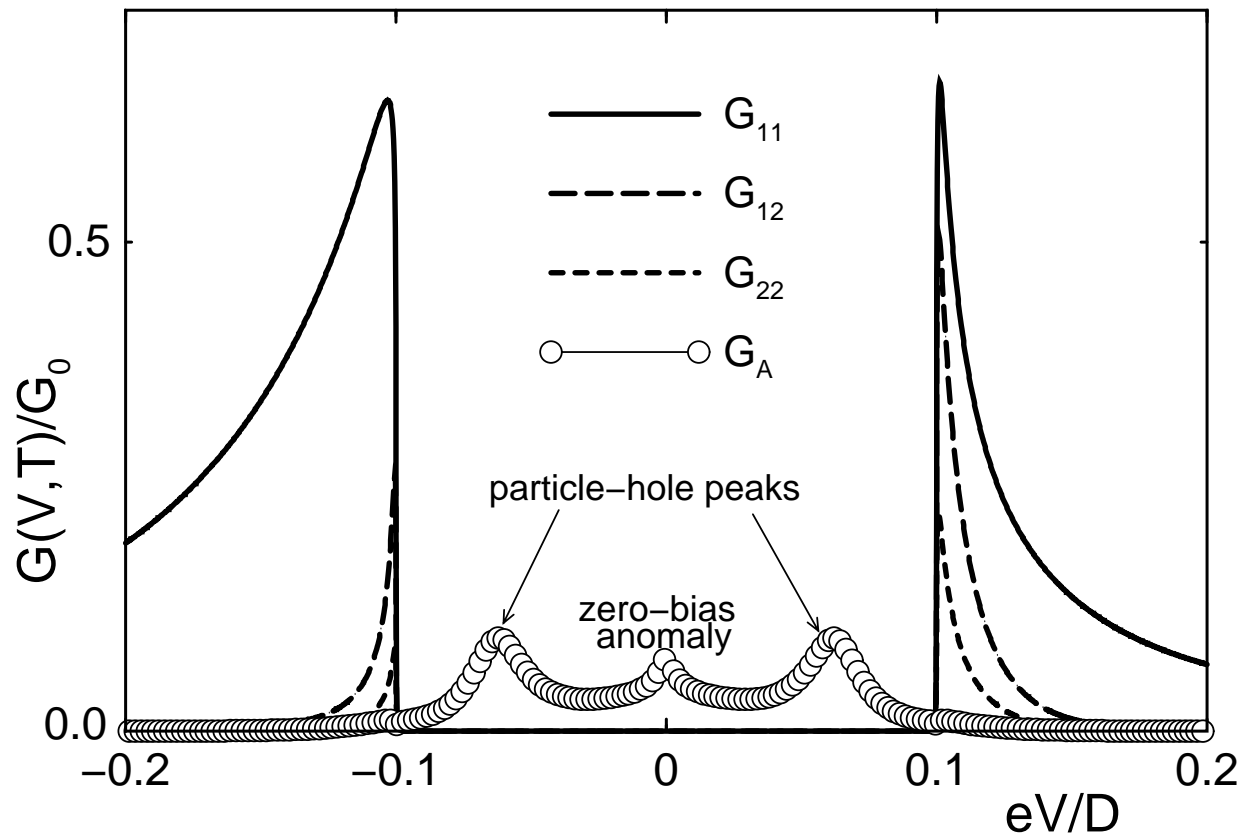
Transport channels

Transport channels

Qualitative features in the differential conductance $G(V) = \frac{\partial J(V)}{\partial V}$

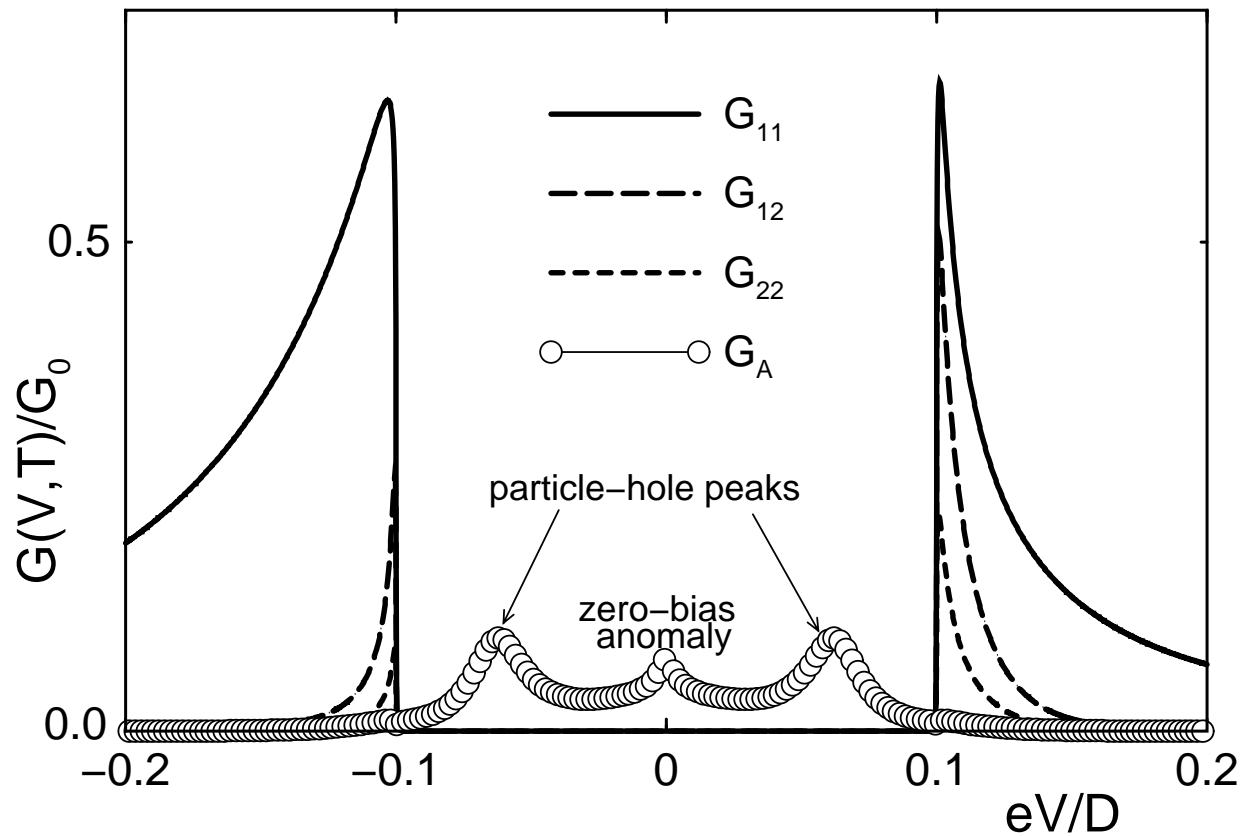
Transport channels

Qualitative features in the differential conductance $G(V) = \frac{\partial J(V)}{\partial V}$



Transport channels

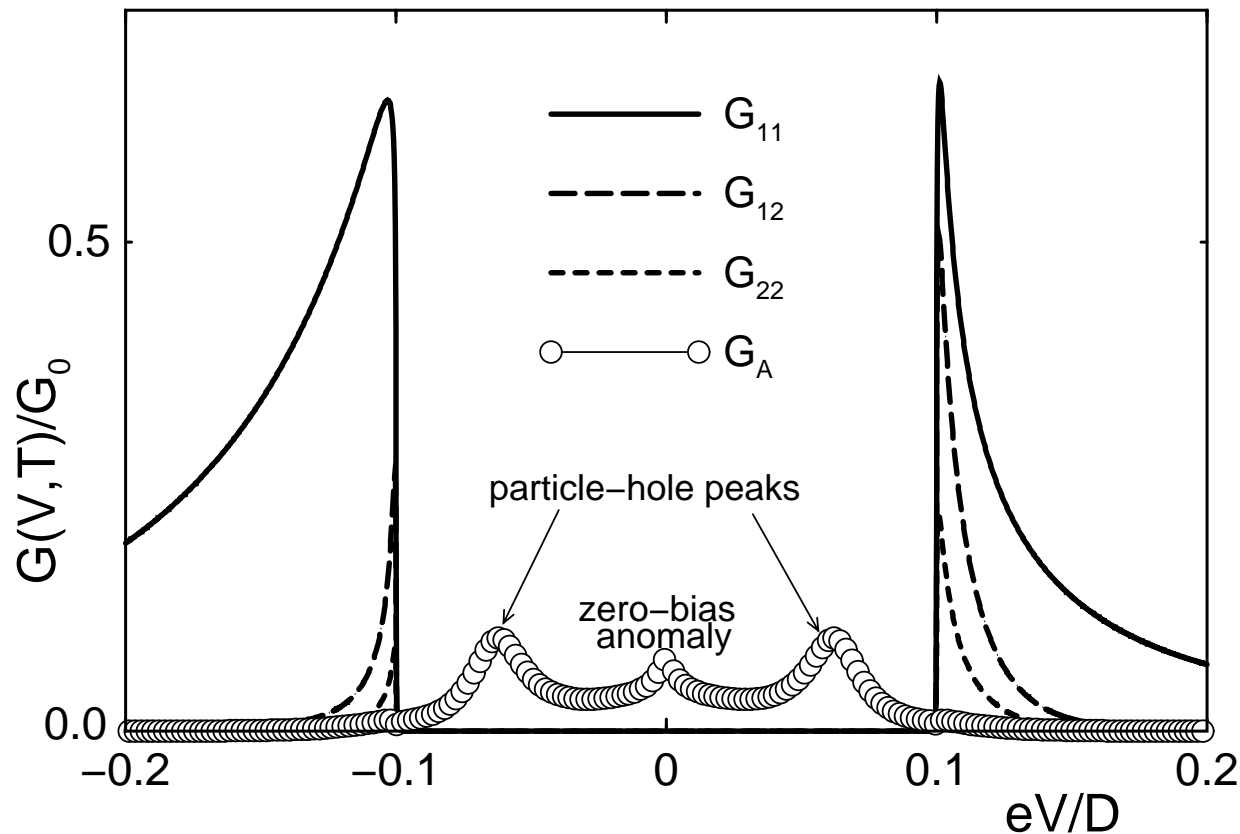
Qualitative features in the differential conductance $G(V) = \frac{\partial J(V)}{\partial V}$



T. Domański, A. Donabidowicz, K.I. Wysokiński, PRB **76**, 104514 (2007).

Transport channels

Qualitative features in the differential conductance $G(V) = \frac{\partial J(V)}{\partial V}$



T. Domański, A. Donabidowicz, K.I. Wysokiński, PRB **76**, 104514 (2007).

We shall now focus on the subgap Andreev conductance.

Correlated QD

– effect of the asymmetry Γ_S/Γ_N

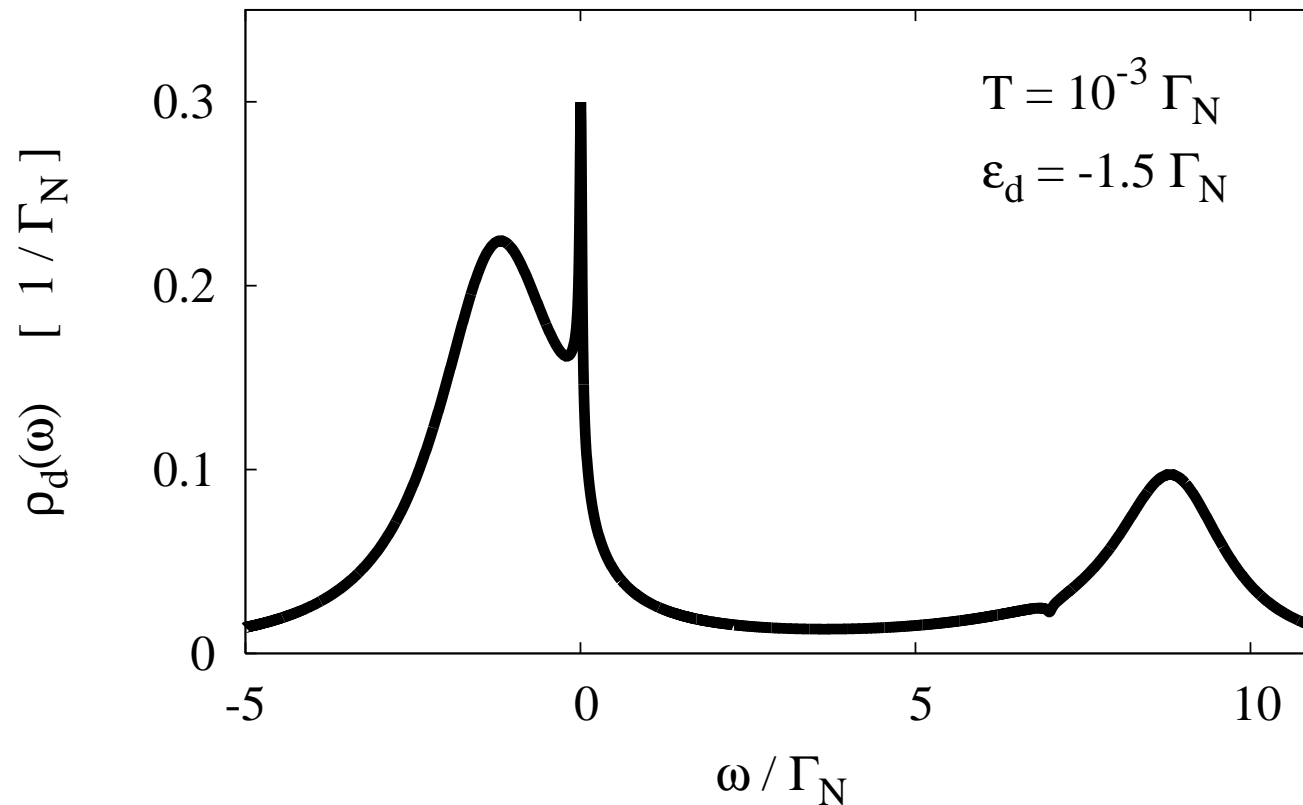
Correlated QD – effect of the asymmetry Γ_S/Γ_N

Spectral function obtained below T_K for $U = 10\Gamma_N$

Correlated QD

– effect of the asymmetry Γ_S/Γ_N

Spectral function obtained below T_K for $U = 10\Gamma_N$

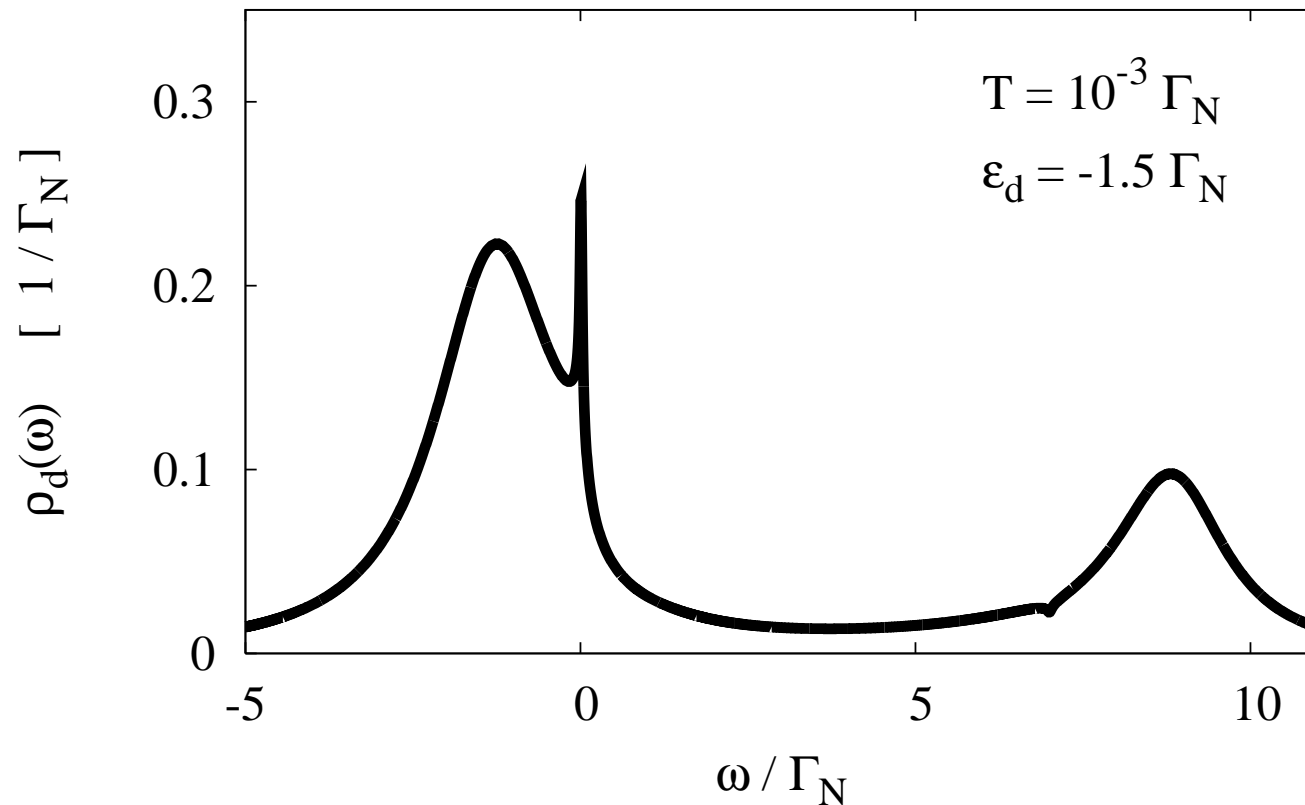


$$\Gamma_S/\Gamma_N = 0$$

Correlated QD

– effect of the asymmetry Γ_S/Γ_N

Spectral function obtained below T_K for $U = 10\Gamma_N$

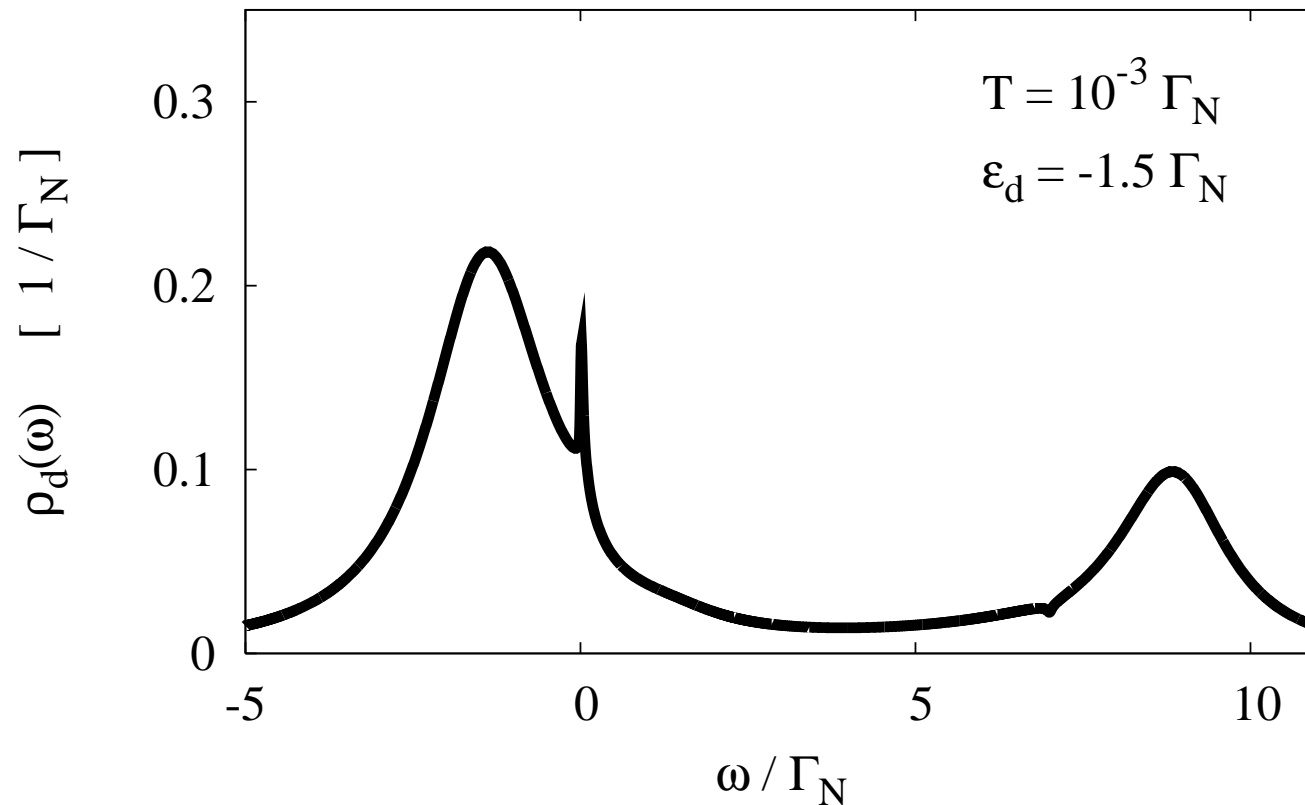


$$\Gamma_S/\Gamma_N = 1$$

Correlated QD

– effect of the asymmetry Γ_S/Γ_N

Spectral function obtained below T_K for $U = 10\Gamma_N$

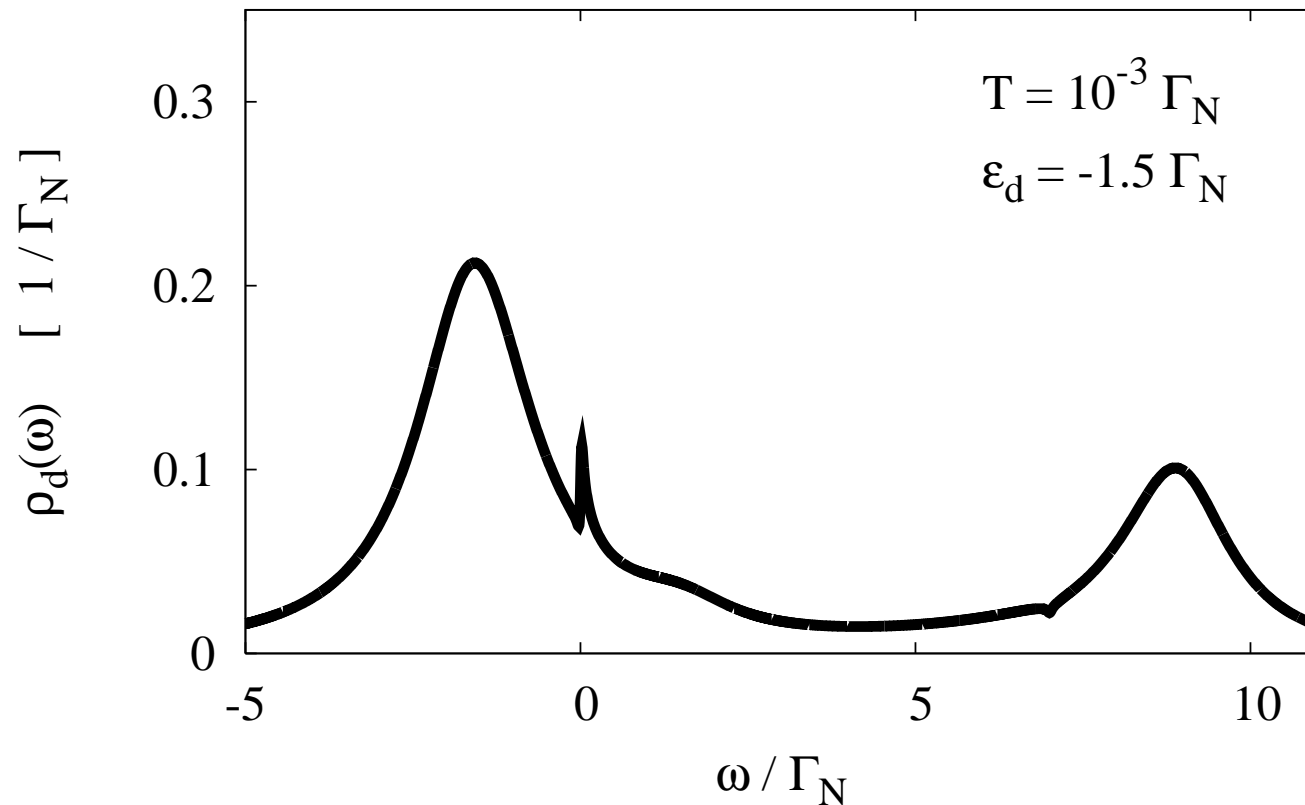


$$\Gamma_S/\Gamma_N = 2$$

Correlated QD

– effect of the asymmetry Γ_S/Γ_N

Spectral function obtained below T_K for $U = 10\Gamma_N$

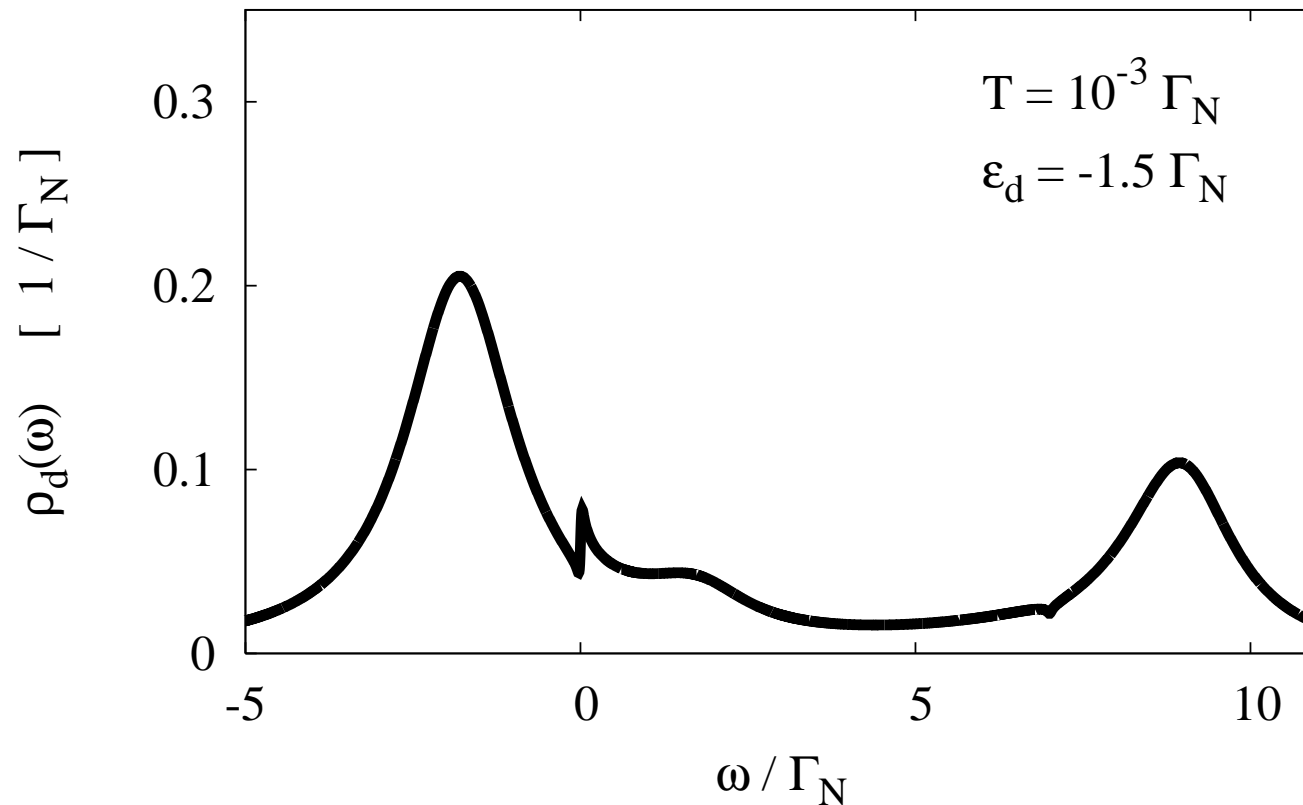


$$\Gamma_S/\Gamma_N = 3$$

Correlated QD

– effect of the asymmetry Γ_S/Γ_N

Spectral function obtained below T_K for $U = 10\Gamma_N$

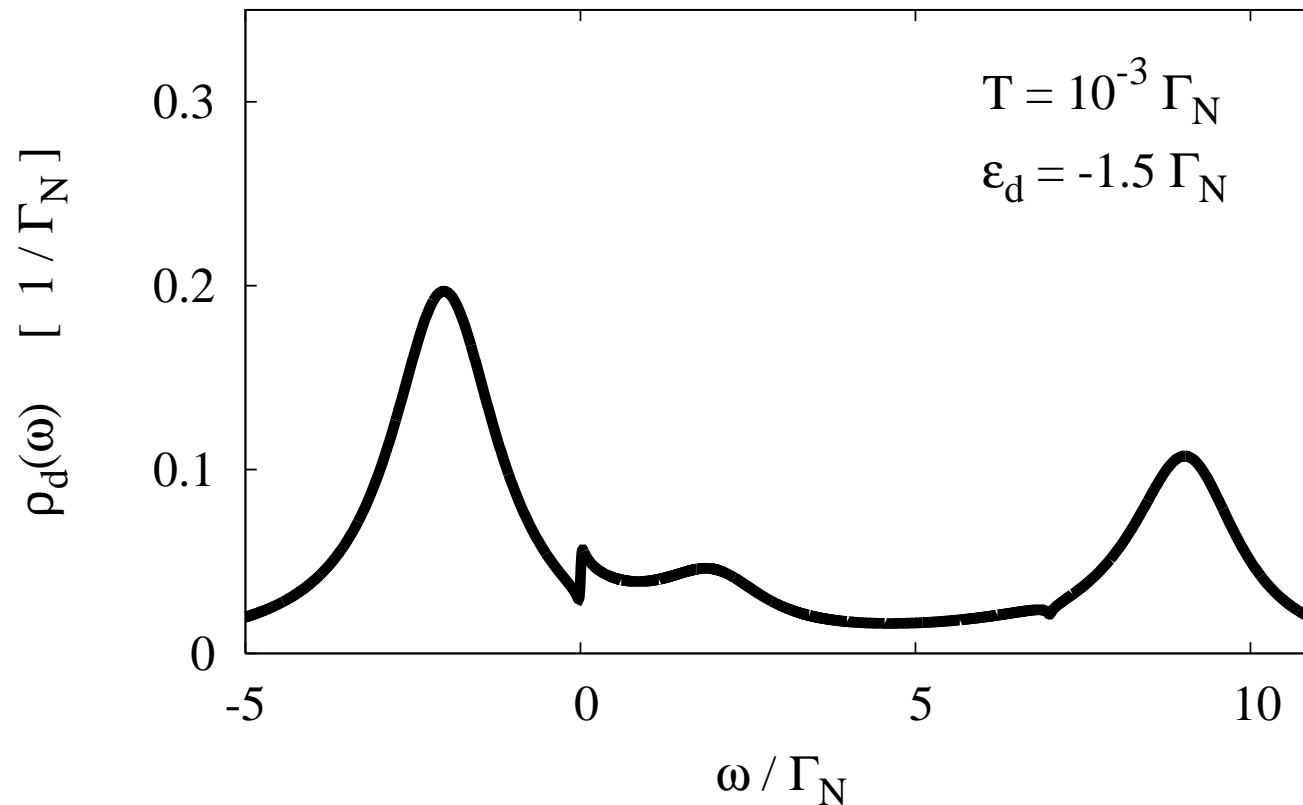


$$\Gamma_S/\Gamma_N = 4$$

Correlated QD

– effect of the asymmetry Γ_S/Γ_N

Spectral function obtained below T_K for $U = 10\Gamma_N$

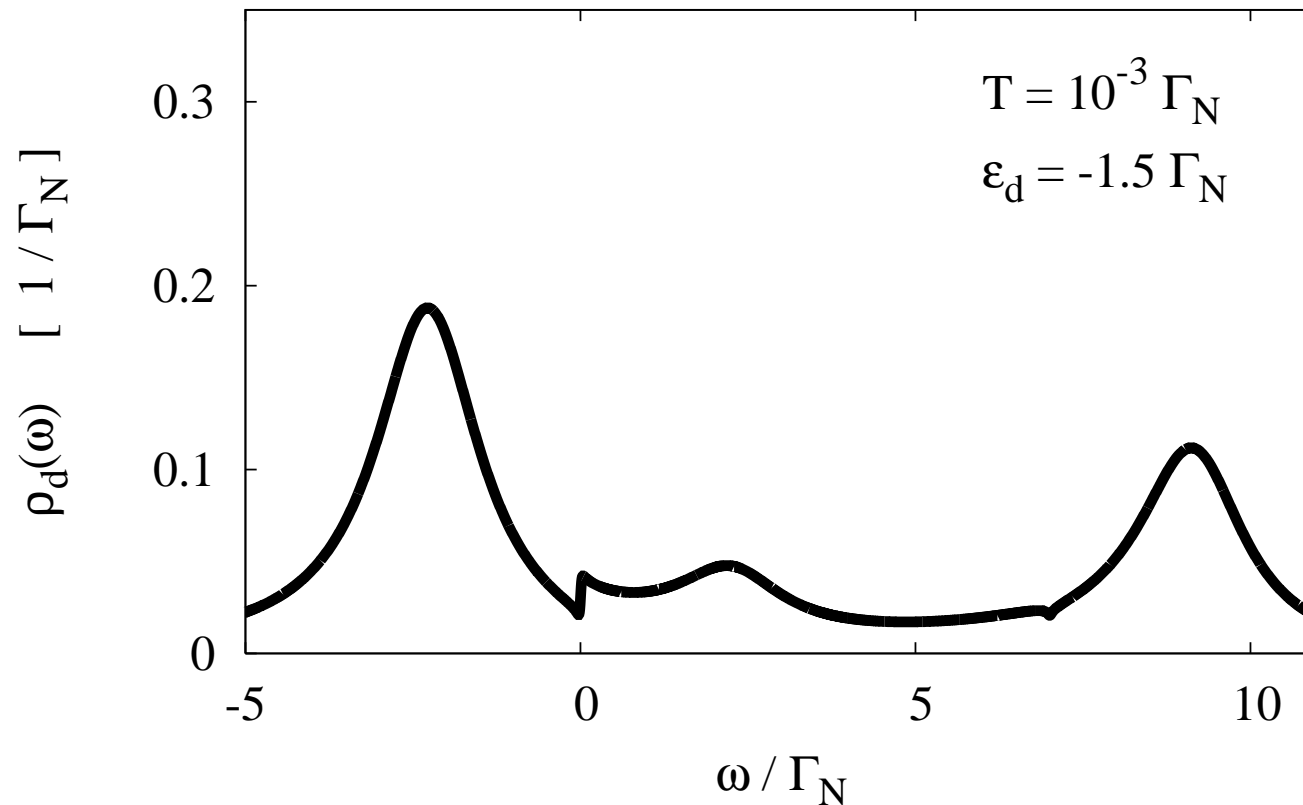


$$\Gamma_S/\Gamma_N = 5$$

Correlated QD

– effect of the asymmetry Γ_S/Γ_N

Spectral function obtained below T_K for $U = 10\Gamma_N$

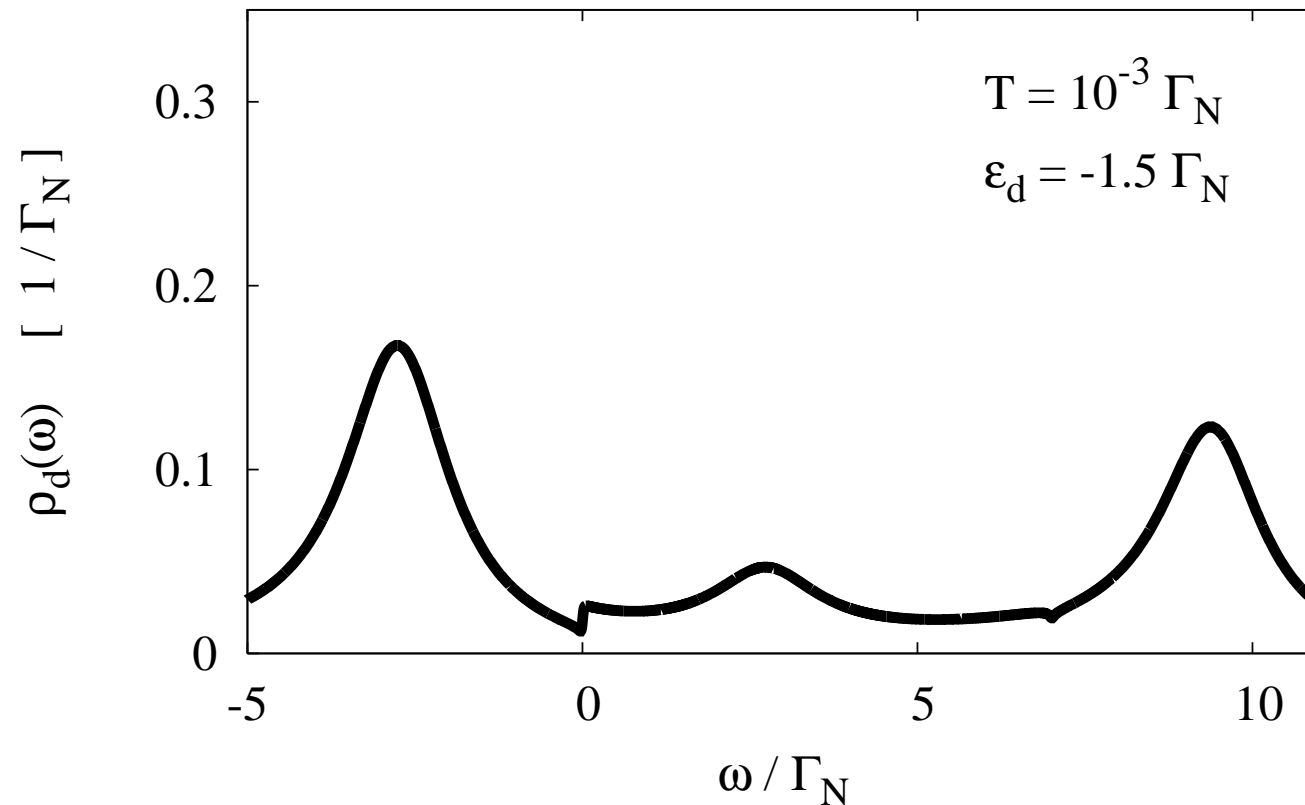


$$\Gamma_S/\Gamma_N = 6$$

Correlated QD

– effect of the asymmetry Γ_S/Γ_N

Spectral function obtained below T_K for $U = 10\Gamma_N$

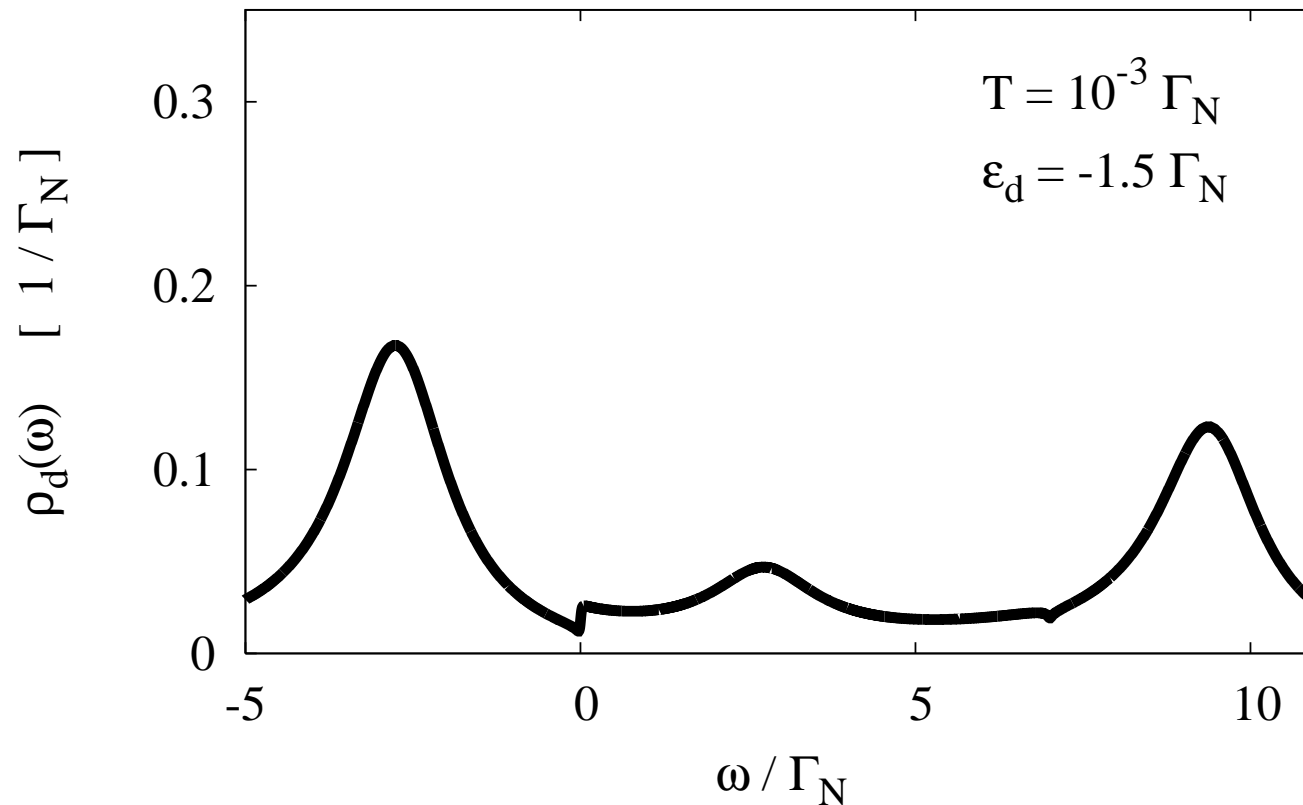


$$\Gamma_S/\Gamma_N = 8$$

Correlated QD

– effect of the asymmetry Γ_S/Γ_N

Spectral function obtained below T_K for $U = 10\Gamma_N$



Superconductivity suppresses the Kondo resonance

Correlated QD – effect of the asymmetry Γ_S/Γ_N

Andreev conductance $G_A(V)$ for:

$$U = 10\Gamma_N$$

Correlated QD – effect of the asymmetry Γ_S/Γ_N

Andreev conductance $G_A(V)$ for:

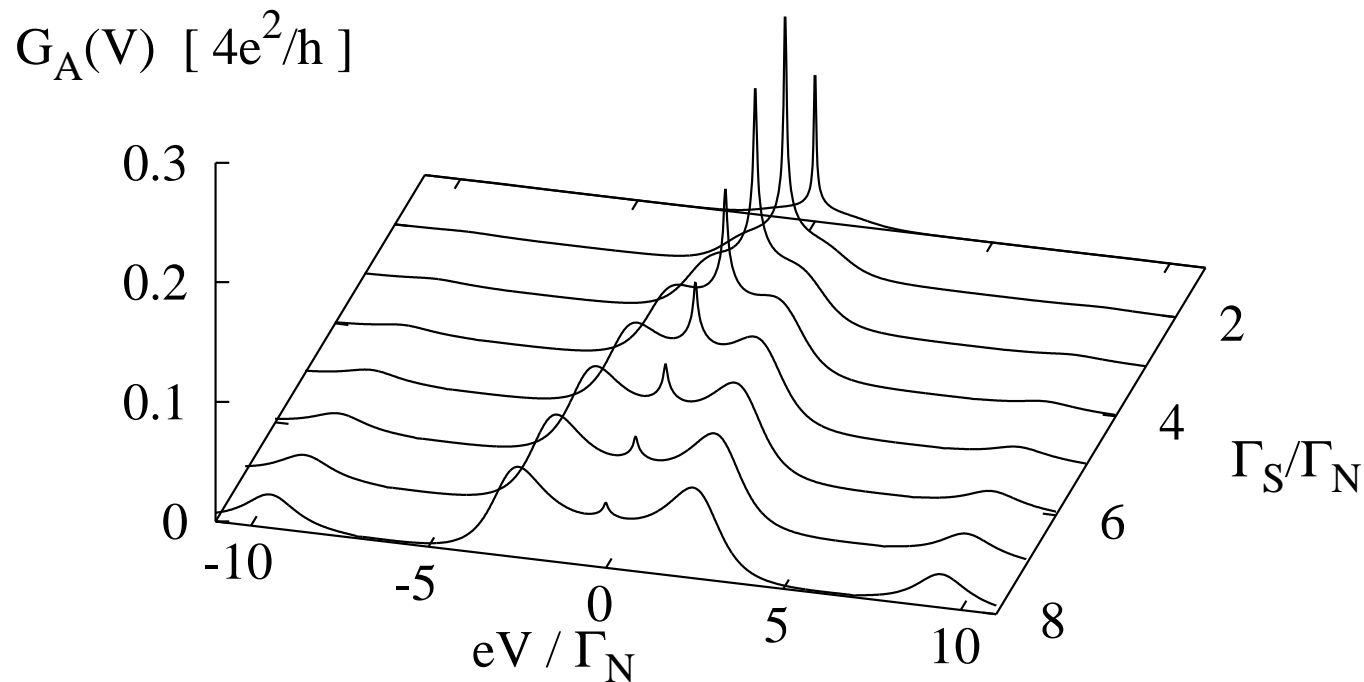
$$U = 10\Gamma_N$$

T. Domański and A. Donabidowicz, PRB **78**, 073105 (2008).

Correlated QD – effect of the asymmetry Γ_S/Γ_N

Andreev conductance $G_A(V)$ for:

$$U = 10\Gamma_N$$



T. Domański and A. Donabidowicz, PRB **78**, 073105 (2008).

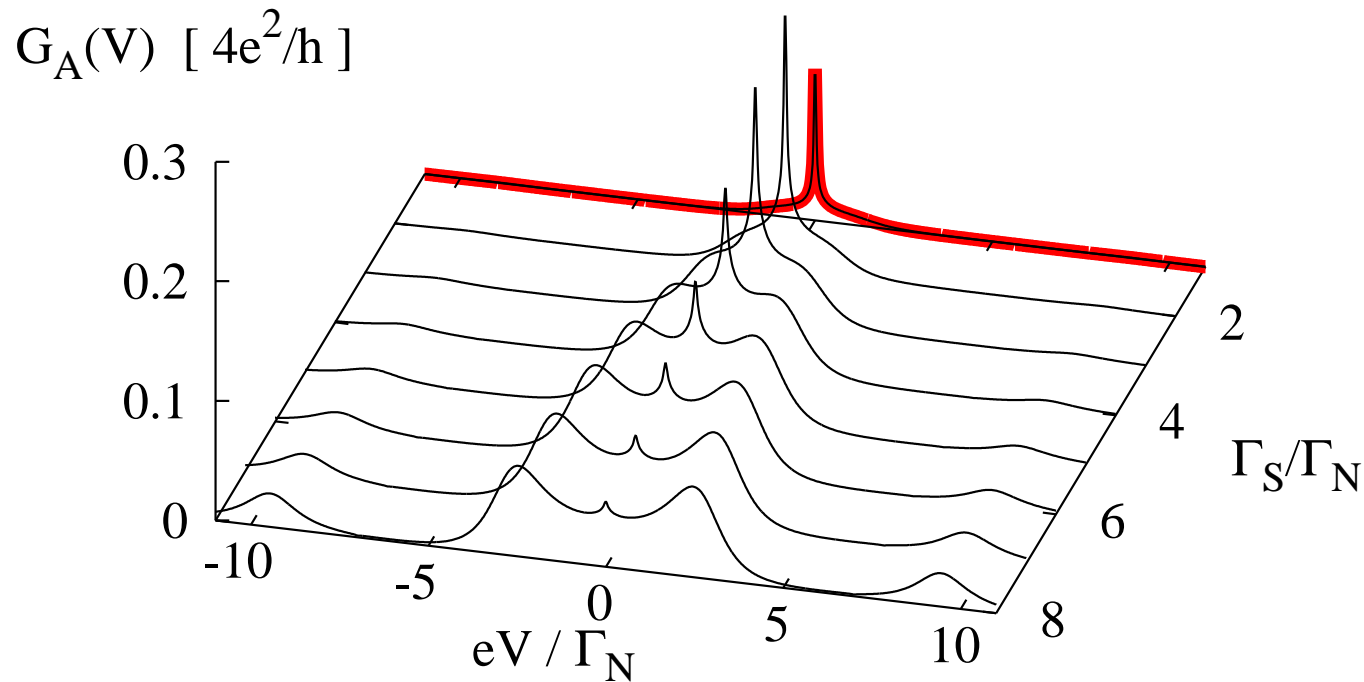
Correlated QD

– effect of the asymmetry Γ_S/Γ_N

Andreev conductance $G_A(V)$ for:

$$U = 10\Gamma_N$$

$$\Gamma_S / \Gamma_N = 1$$



T. Domański and A. Donabidowicz, PRB **78**, 073105 (2008).

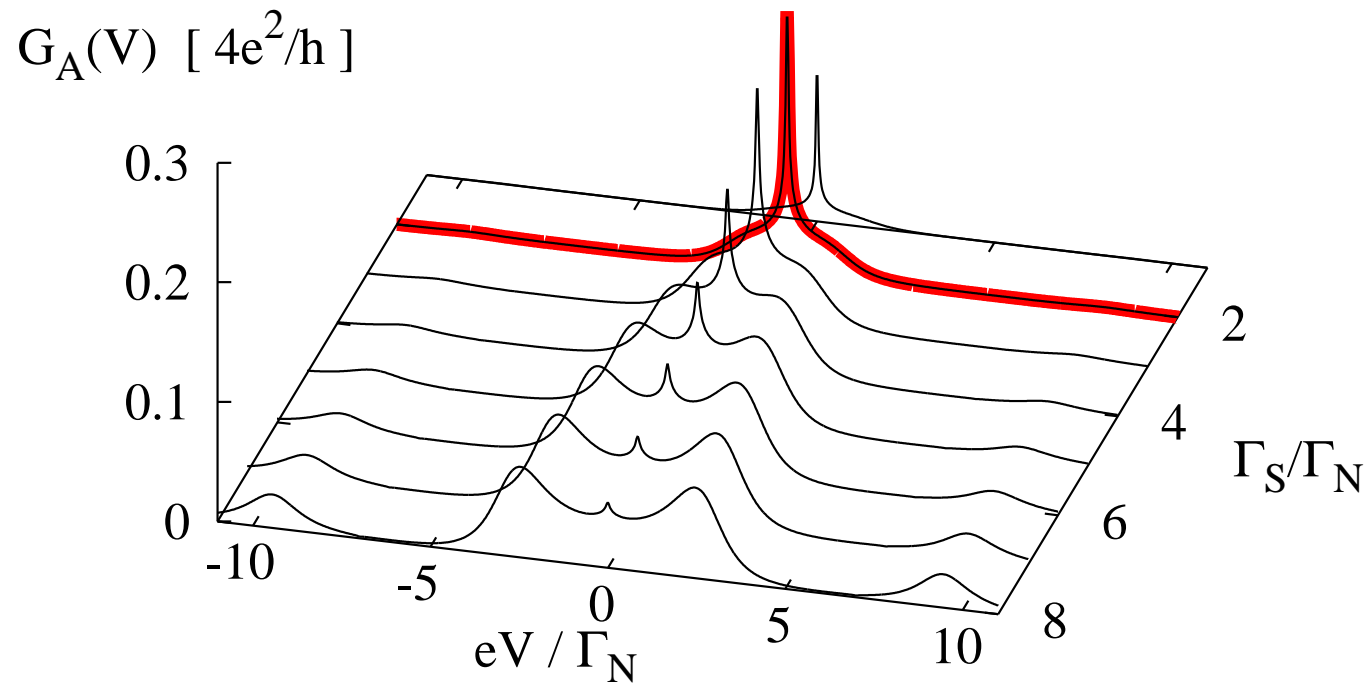
Correlated QD

– effect of the asymmetry Γ_S/Γ_N

Andreev conductance $G_A(V)$ for:

$$U = 10\Gamma_N$$

$$\Gamma_S / \Gamma_N = 2$$



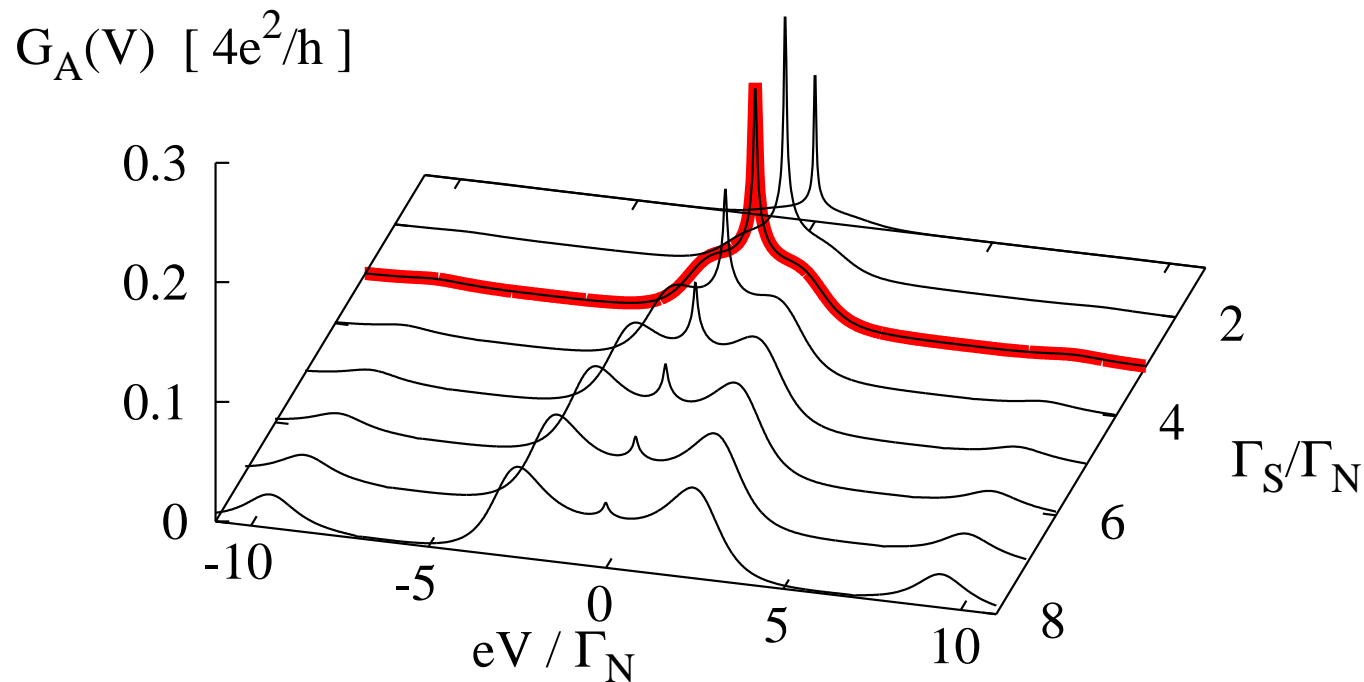
T. Domański and A. Donabidowicz, PRB **78**, 073105 (2008).

Correlated QD – effect of the asymmetry Γ_S/Γ_N

Andreev conductance $G_A(V)$ for:

$$U = 10\Gamma_N$$

$$\Gamma_S / \Gamma_N = 3$$



T. Domański and A. Donabidowicz, PRB **78**, 073105 (2008).

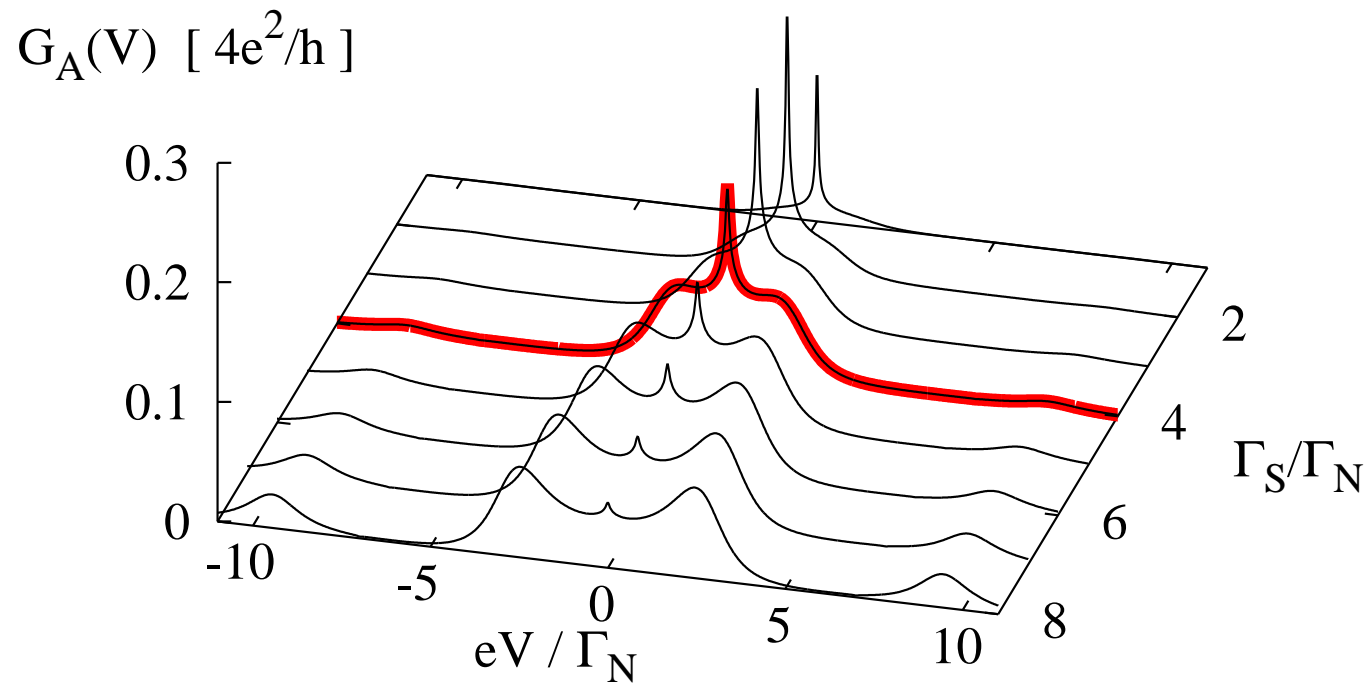
Correlated QD

– effect of the asymmetry Γ_S/Γ_N

Andreev conductance $G_A(V)$ for:

$$U = 10\Gamma_N$$

$$\Gamma_S / \Gamma_N = 4$$



T. Domański and A. Donabidowicz, PRB **78**, 073105 (2008).

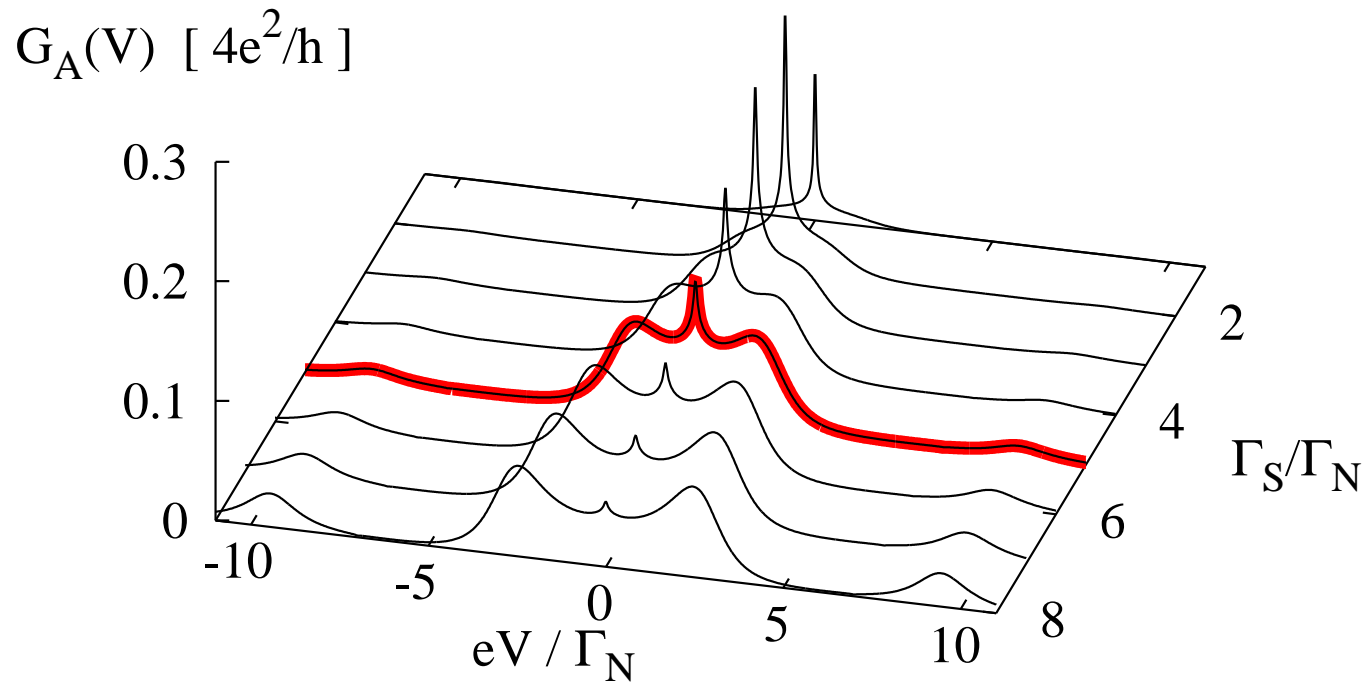
Correlated QD

– effect of the asymmetry Γ_S/Γ_N

Andreev conductance $G_A(V)$ for:

$$U = 10\Gamma_N$$

$$\Gamma_S / \Gamma_N = 5$$



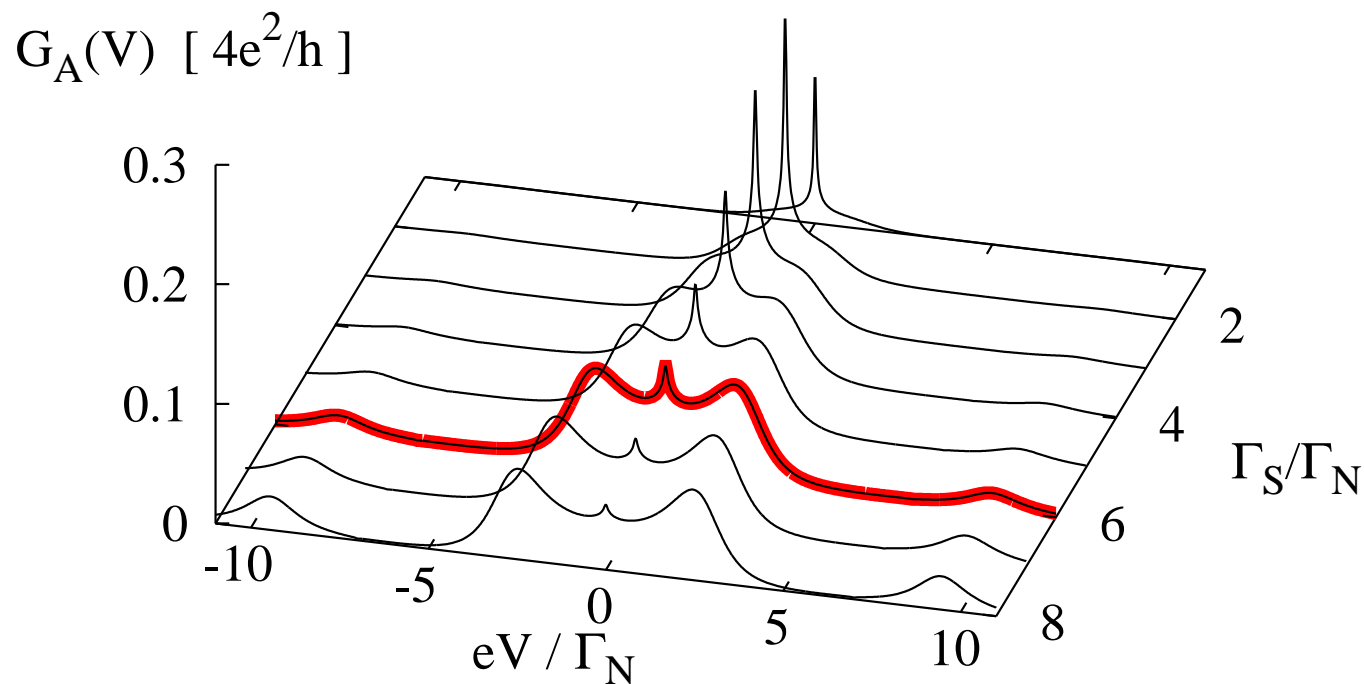
T. Domański and A. Donabidowicz, PRB **78**, 073105 (2008).

Correlated QD – effect of the asymmetry Γ_S/Γ_N

Andreev conductance $G_A(V)$ for:

$$U = 10\Gamma_N$$

$$\Gamma_S / \Gamma_N = 6$$



T. Domański and A. Donabidowicz, PRB **78**, 073105 (2008).

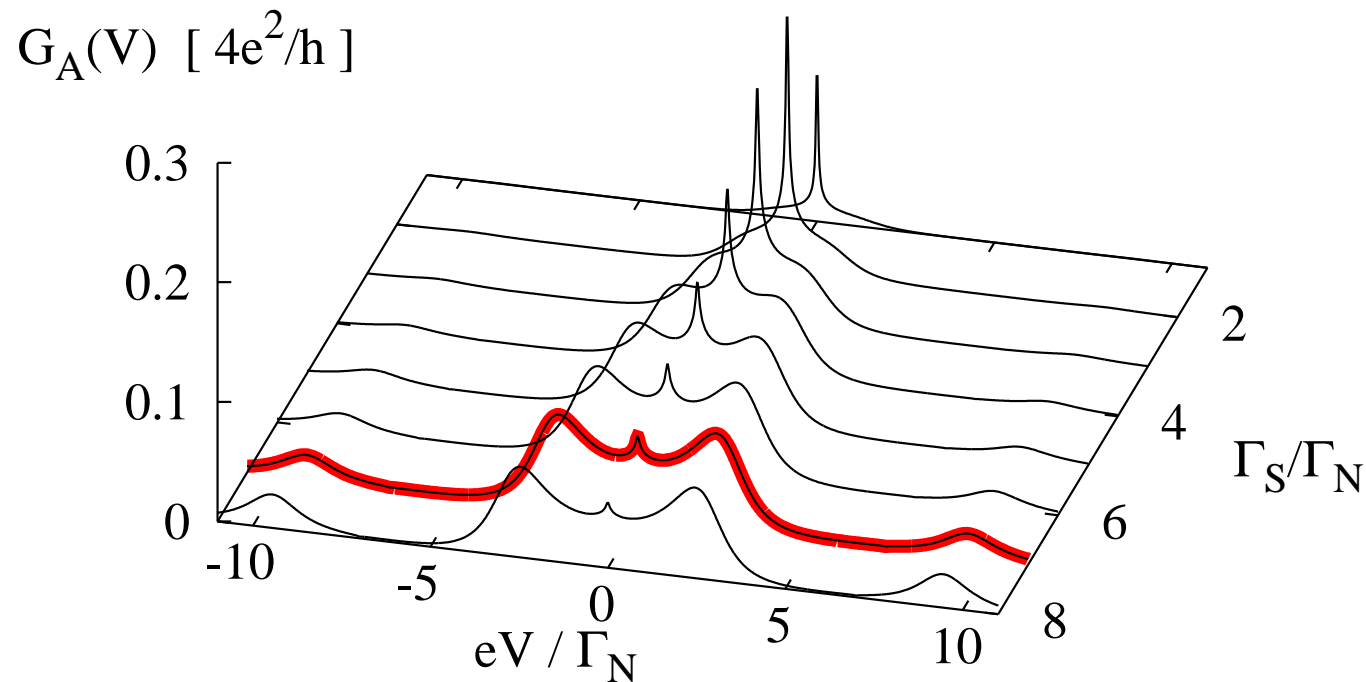
Correlated QD

– effect of the asymmetry Γ_S/Γ_N

Andreev conductance $G_A(V)$ for:

$$U = 10\Gamma_N$$

$$\Gamma_S / \Gamma_N = 7$$



T. Domański and A. Donabidowicz, PRB **78**, 073105 (2008).

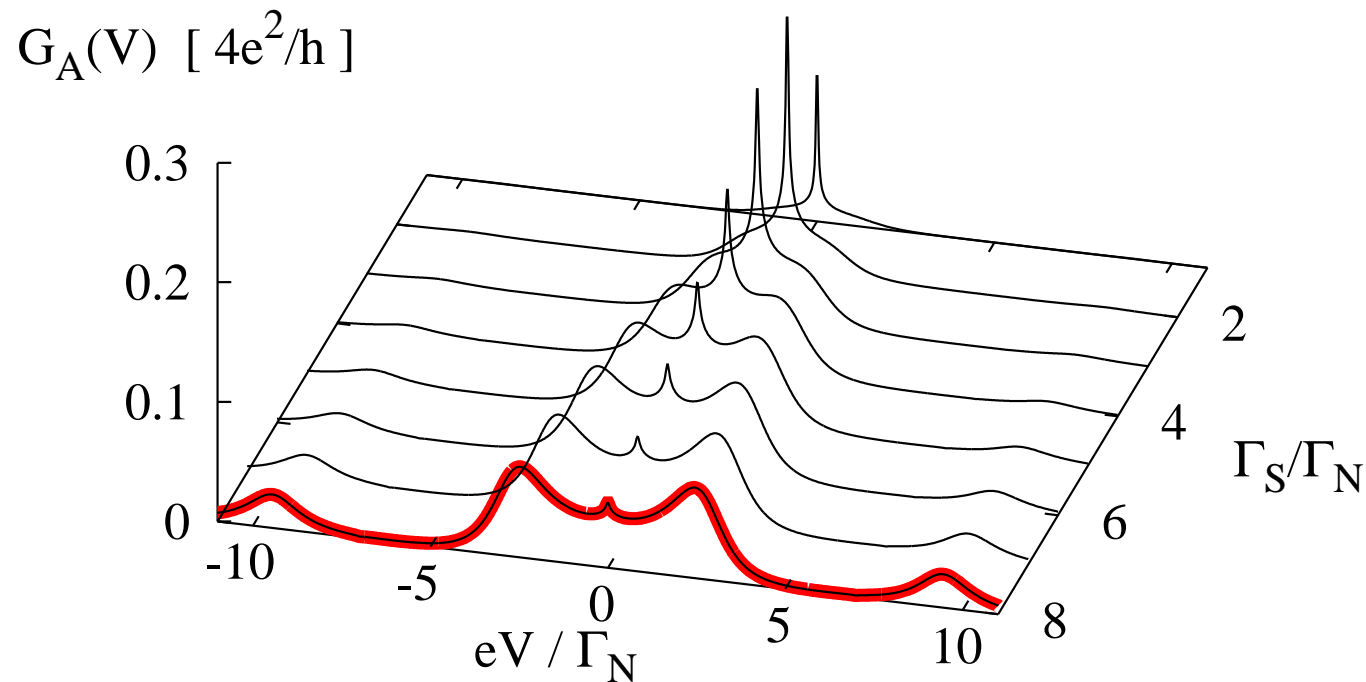
Correlated QD

– effect of the asymmetry Γ_S/Γ_N

Andreev conductance $G_A(V)$ for:

$$U = 10\Gamma_N$$

$$\Gamma_S / \Gamma_N = 8$$



T. Domański and A. Donabidowicz, PRB **78**, 073105 (2008).

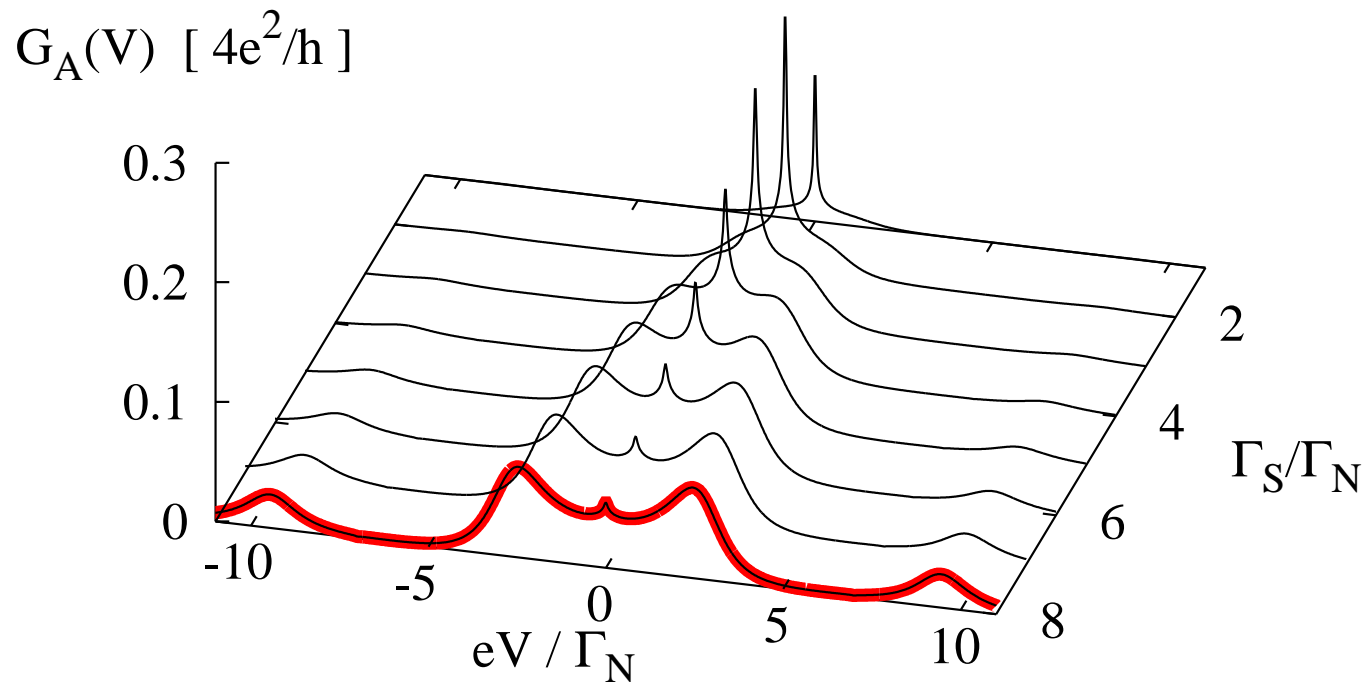
Correlated QD

– effect of the asymmetry Γ_S/Γ_N

Andreev conductance $G_A(V)$ for:

$$U = 10\Gamma_N$$

$$\Gamma_S / \Gamma_N = 8$$



T. Domański and A. Donabidowicz, PRB **78**, 073105 (2008).

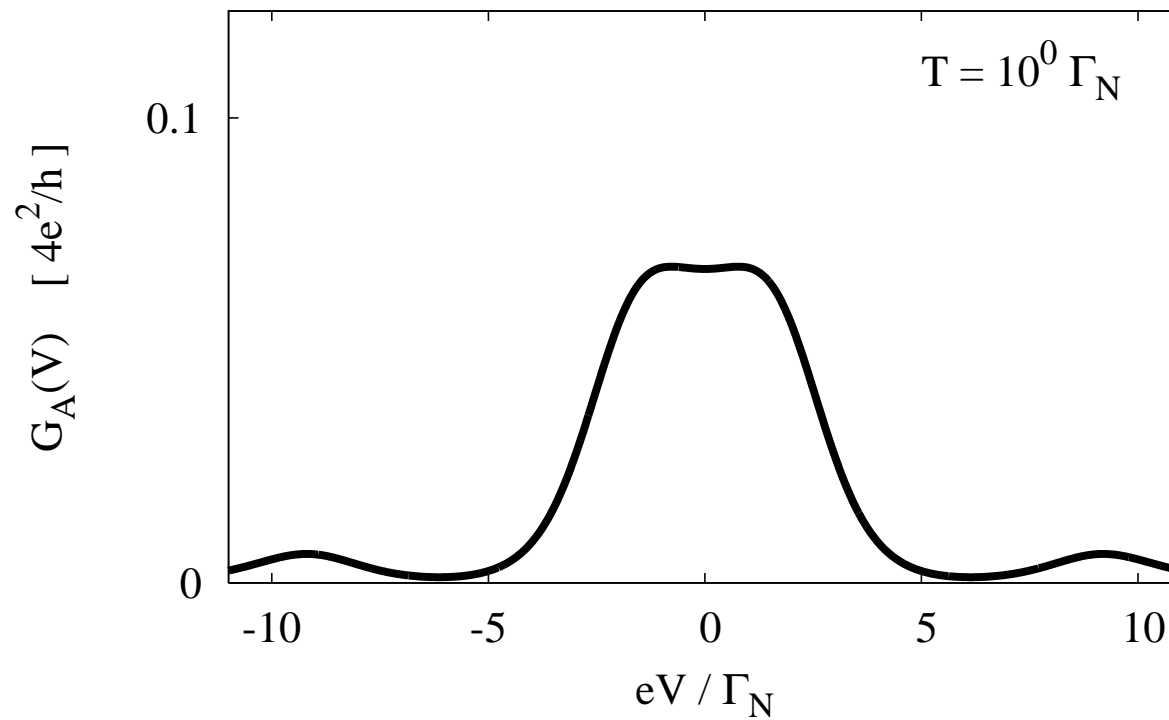
**Kondo resonance slightly enhances the zero-bias
Andreev conductance, especially for $\Gamma_S \sim \Gamma_N$!**

Strongly correlated QD – influence of temperature

Temperature dependence of $G_A(V)$ for: $U = 10\Gamma_N$

Strongly correlated QD – influence of temperature

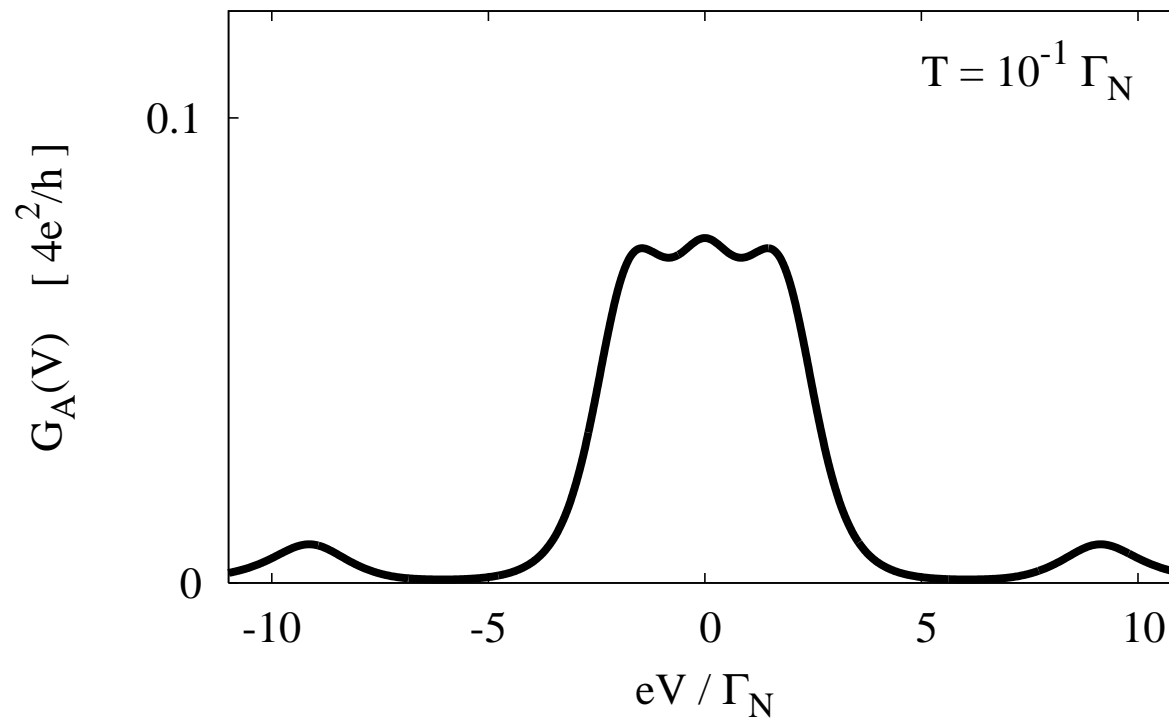
Temperature dependence of $G_A(V)$ for: $U = 10\Gamma_N$



$$k_B T = \Gamma_N$$

Strongly correlated QD – influence of temperature

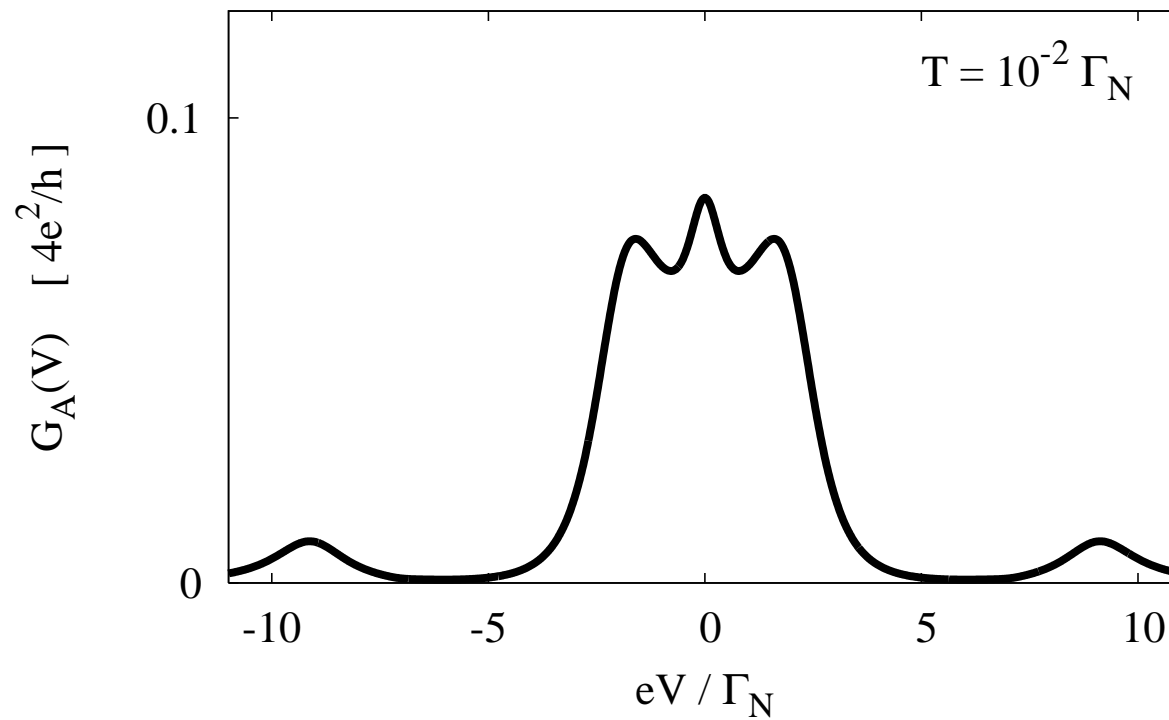
Temperature dependence of $G_A(V)$ for: $U = 10\Gamma_N$



$$k_B T = \Gamma_N / 10$$

Strongly correlated QD – influence of temperature

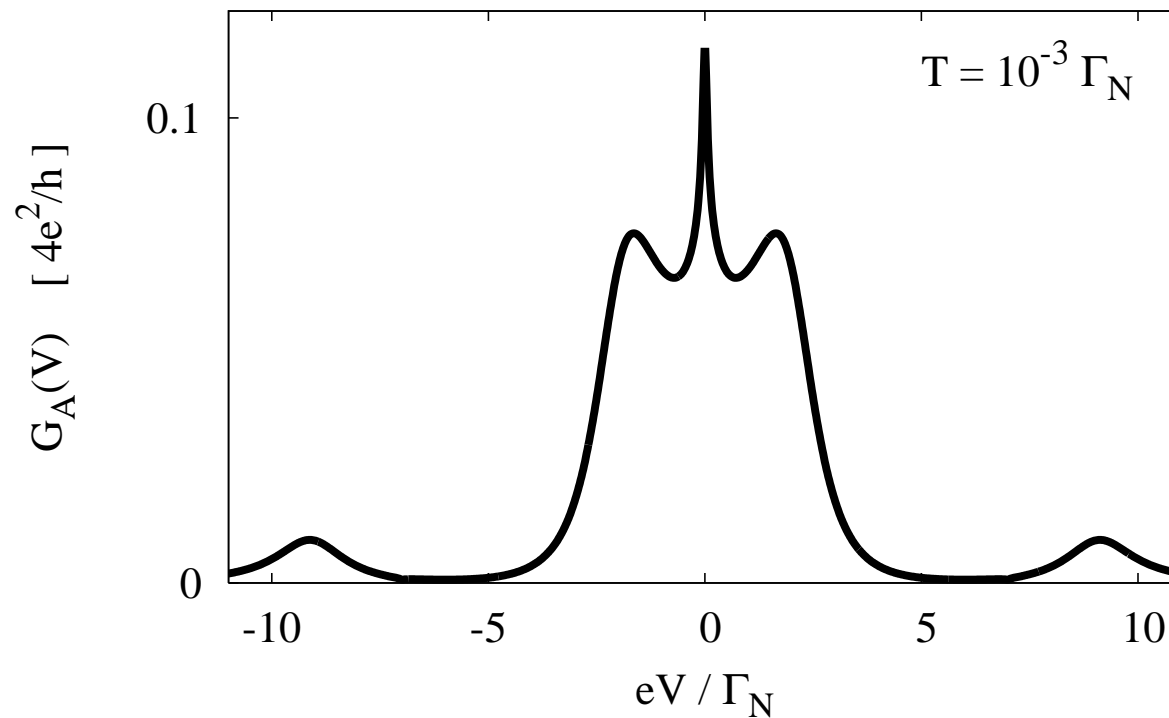
Temperature dependence of $G_A(V)$ for: $U = 10\Gamma_N$



$$k_B T = \Gamma_N / 100$$

Strongly correlated QD – influence of temperature

Temperature dependence of $G_A(V)$ for: $U = 10\Gamma_N$



$$k_B T = \Gamma_N / 1000$$

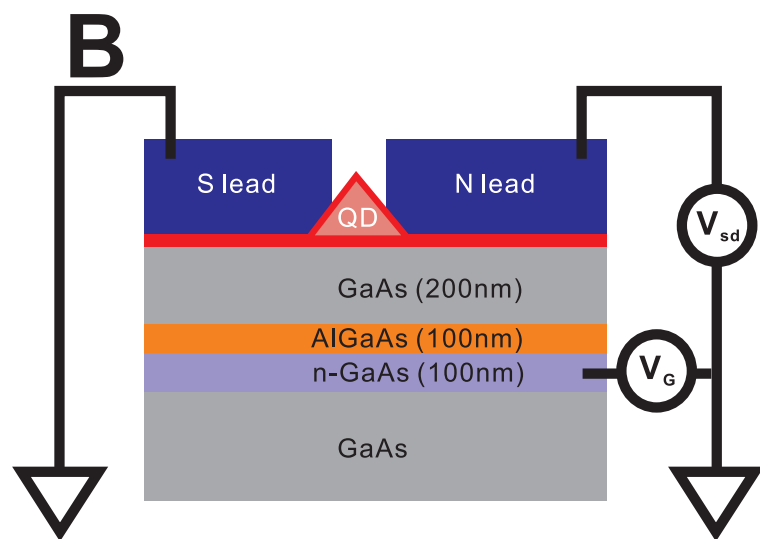
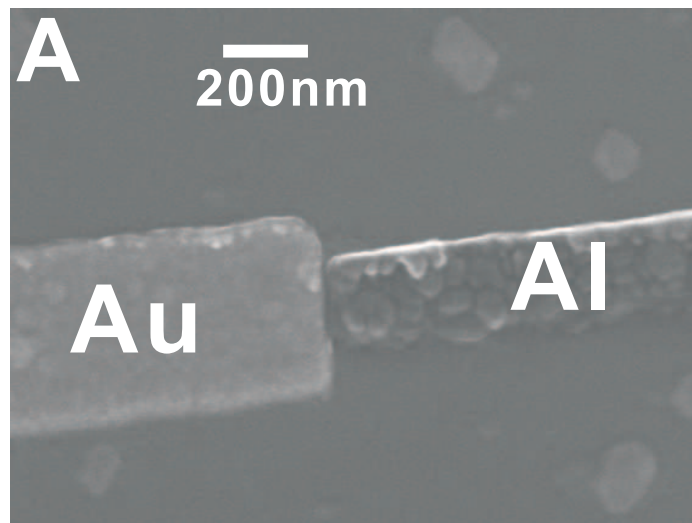
T. Domański and A. Donabidowicz, PRB **78**, 073105 (2008).

Experimental setup

/ University of Tokyo /

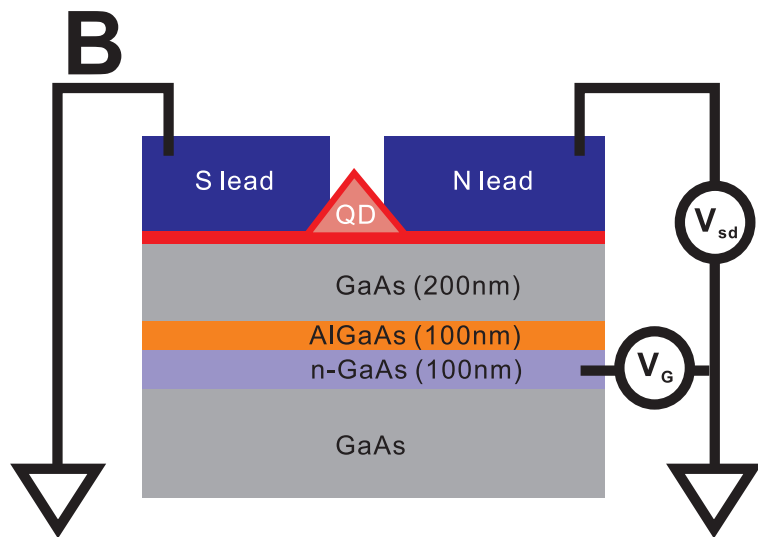
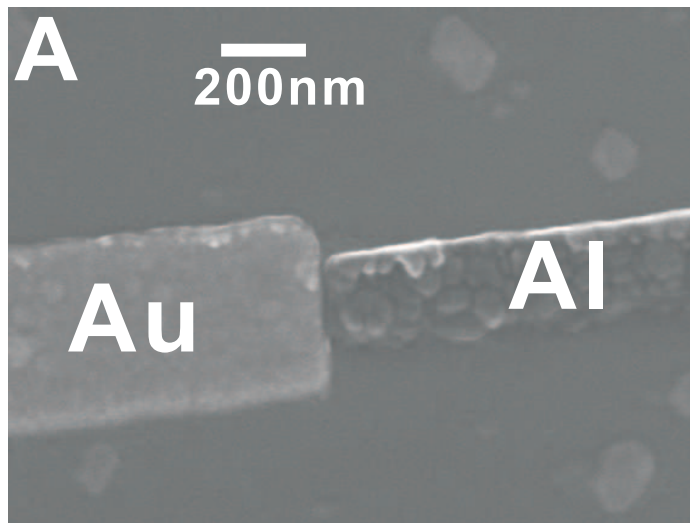
Experimental setup

/ University of Tokyo /



Experimental setup

/ University of Tokyo /



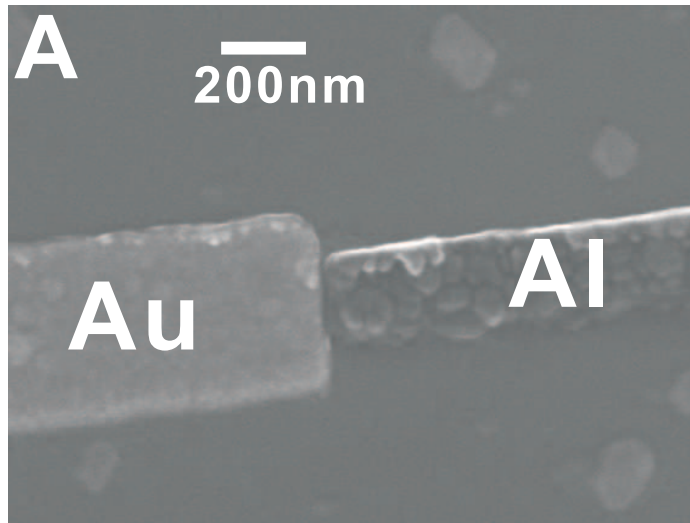
QD : self-assembled InAs

diameter \sim 100 nm

backgate : Si-doped GaAs

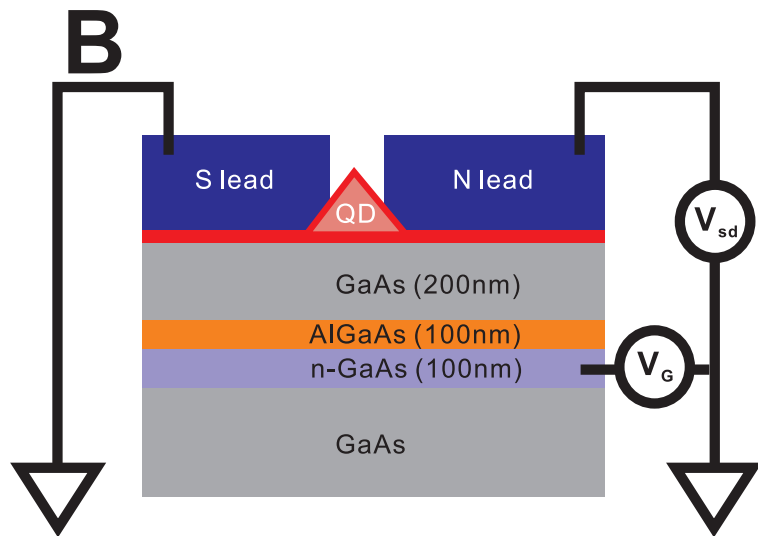
Experimental setup

/ University of Tokyo /



$$T_c \simeq 1\text{K}$$

$$\Delta \simeq 152\mu\text{eV}$$



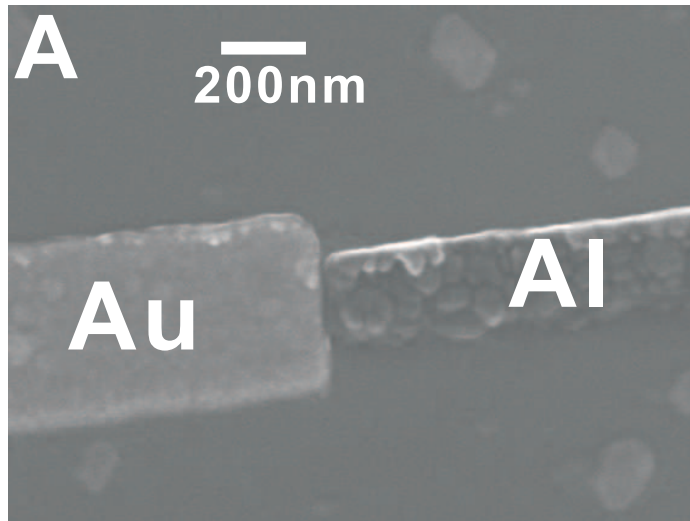
QD : self-assembled InAs

diameter ~ 100 nm

backgate : Si-doped GaAs

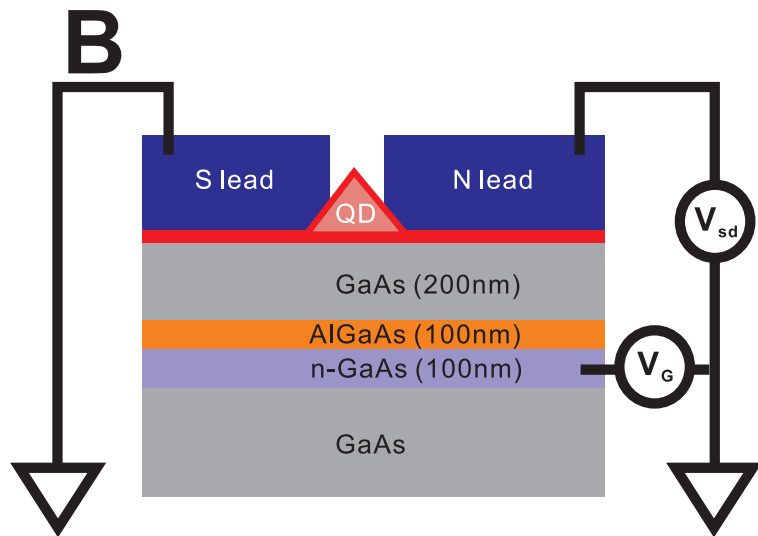
Experimental setup

/ University of Tokyo /



$$T_c \simeq 1\text{K}$$

$$\Delta \simeq 152\mu\text{eV}$$



QD : self-assembled InAs

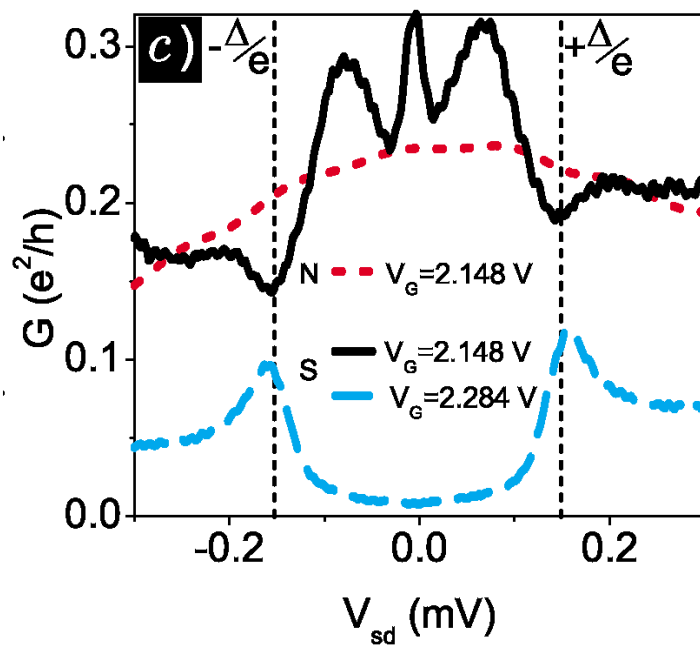
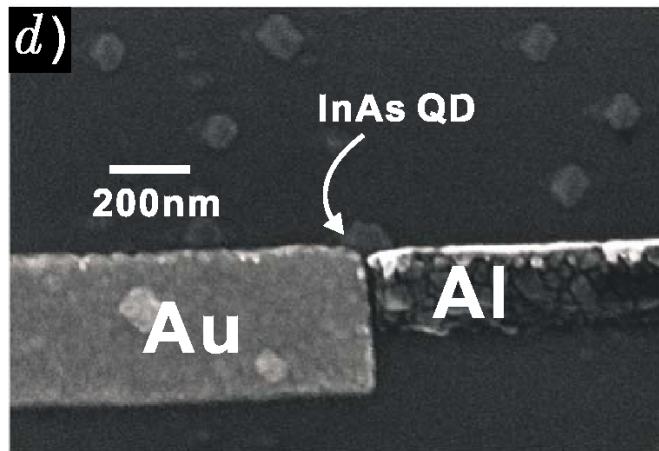
diameter ~ 100 nm

backgate : Si-doped GaAs

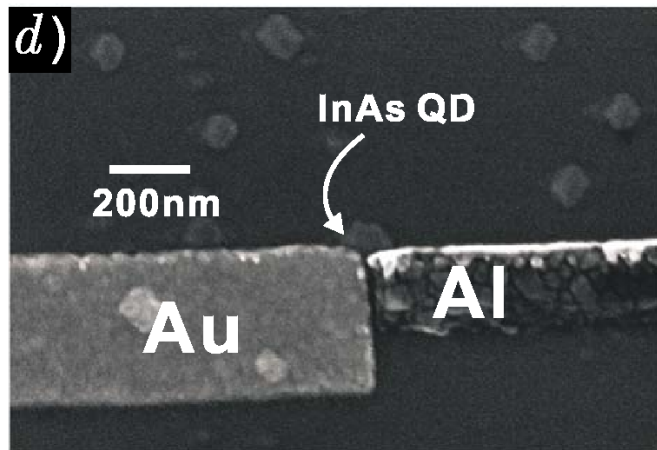
*R.S. Deacon et al, Phys. Rev. Lett. **104**, 076805 (2010).*

Interplay with the Kondo effect

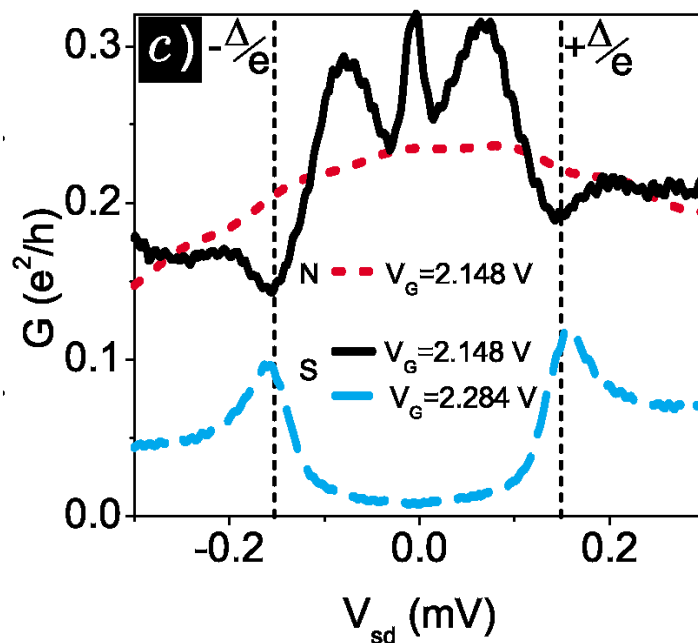
Interplay with the Kondo effect



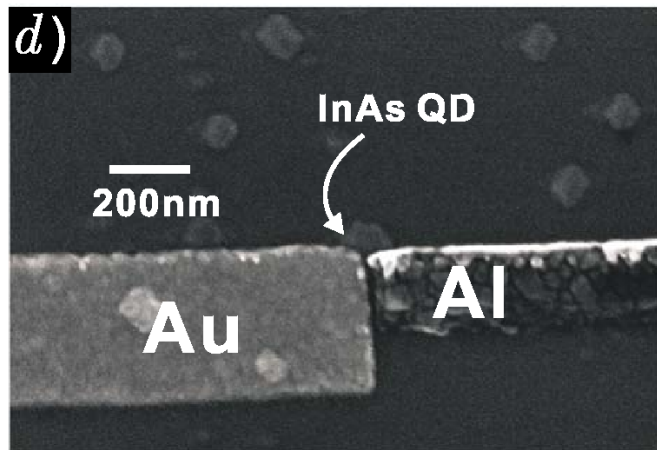
Interplay with the Kondo effect



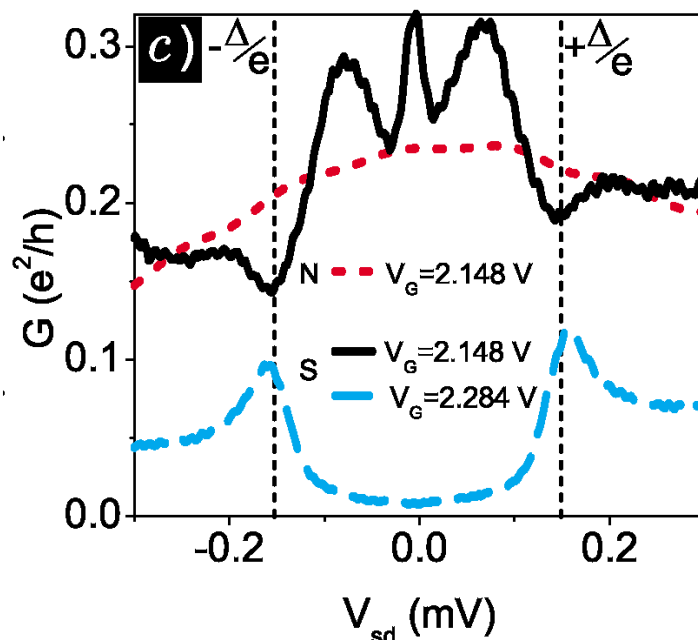
"The zero-bias conductance peak is consistent with Andreev transport enhanced by the Kondo singlet state"



Interplay with the Kondo effect



"The zero-bias conductance peak is consistent with Andreev transport enhanced by the Kondo singlet state"



"We note that the feature exhibits excellent qualitative agreement with a recent theoretical treatment by Domanski et al"

Summary

/ for the part 2 /

Summary

/ for the part 2 /

QD coupled between N and S electrodes:

Summary

/ for the part 2 /

QD coupled between N and S electrodes:

⇒ **absorbs the superconducting order** / proximity effect /

Summary

/ for the part 2 /

QD coupled between N and S electrodes:

- ⇒ **absorbs the superconducting order** / proximity effect /
- ⇒ **is affected by the correlations** / Kondo & charging effects /

Summary

/ for the part 2 /

QD coupled between N and S electrodes:

- ⇒ **absorbs the superconducting order** / proximity effect /
- ⇒ **is affected by the correlations** / Kondo & charging effects /

**Interplay between the proximity and correlation effects
is manifested in the subgap Andreev transport by:**

Summary

/ for the part 2 /

QD coupled between N and S electrodes:

- ⇒ absorbs the superconducting order / proximity effect /
- ⇒ is affected by the correlations / Kondo & charging effects /

Interplay between the proximity and correlation effects is manifested in the subgap Andreev transport by:

- ⇒ the particle-hole splitting / when $\varepsilon_d \sim \mu_S$ /

Summary

/ for the part 2 /

QD coupled between N and S electrodes:

- ⇒ absorbs the superconducting order / proximity effect /
- ⇒ is affected by the correlations / Kondo & charging effects /

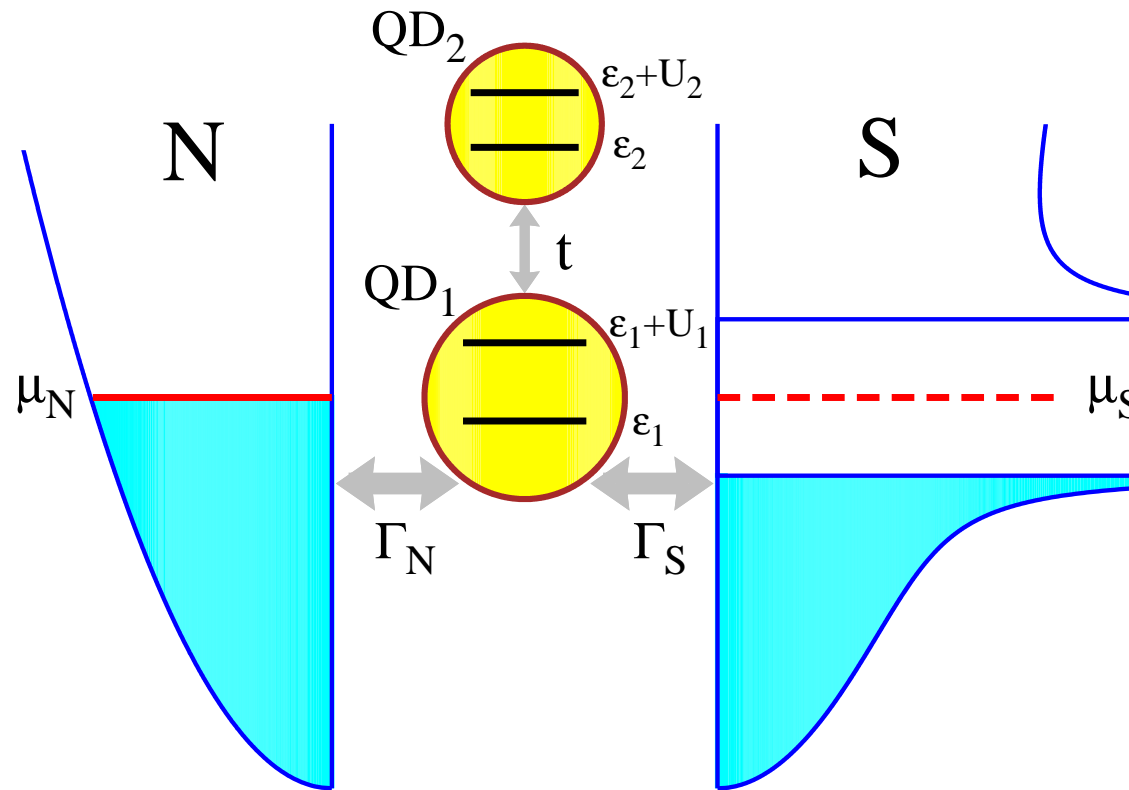
Interplay between the proximity and correlation effects is manifested in the subgap Andreev transport by:

- ⇒ the particle-hole splitting / when $\varepsilon_d \sim \mu_S$ /
- ⇒ the zero-bias enhancement / below T_K /

3. Further extensions

Double QD

– between a metal and superconductor



(T-shape configuration)

Relevant issues:

- ⇒ induced on-dot pairing (due to Γ_S)
- ⇒ Coulomb blockade & Kondo effect (via U_1 and Γ_N)
- ⇒ quantum interference (because of t)

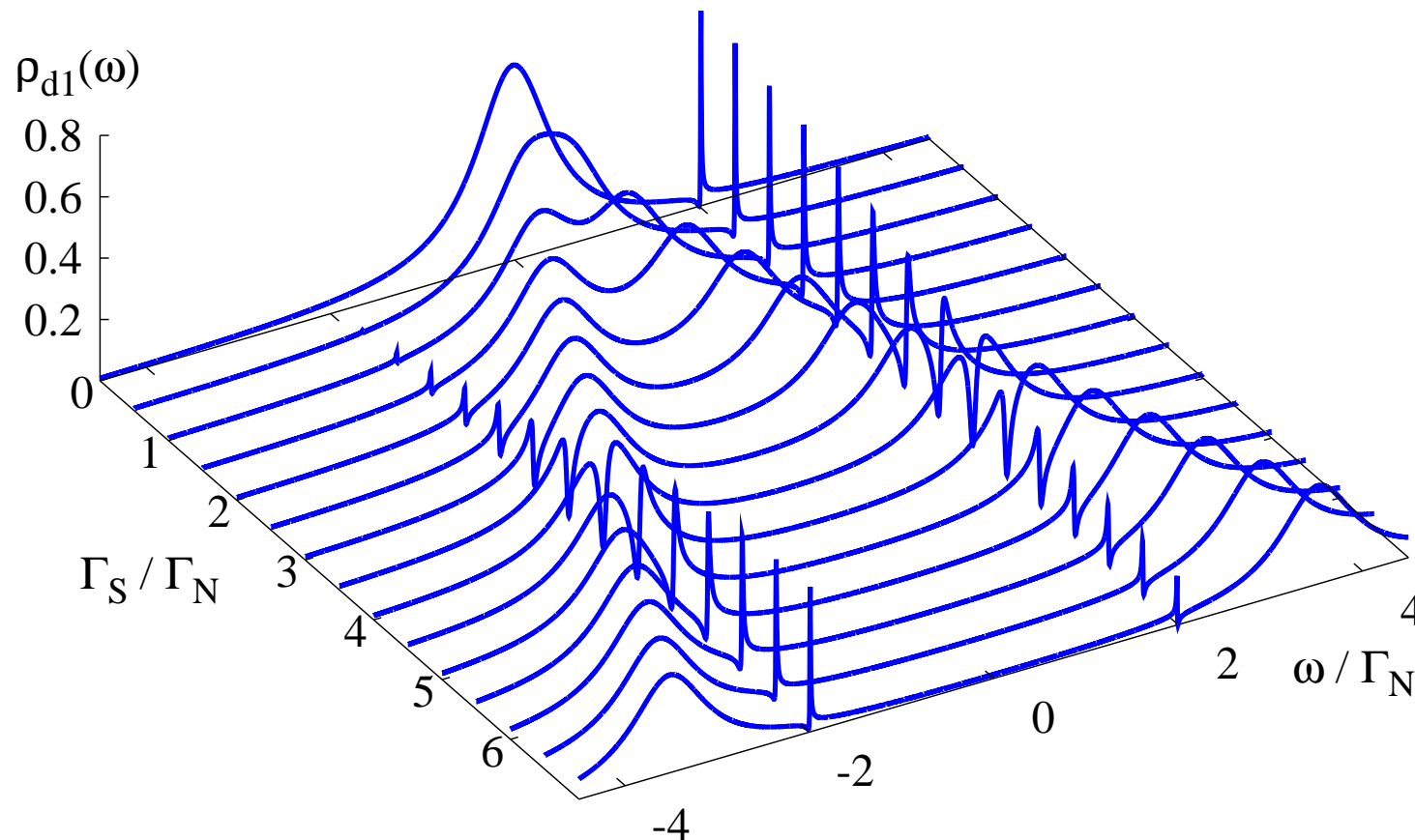
Quantum interference

– in the particle and hole channels

Quantum interference

– in the particle and hole channels

Fano-type lineshapes appear simultaneously at $\pm\varepsilon_2$



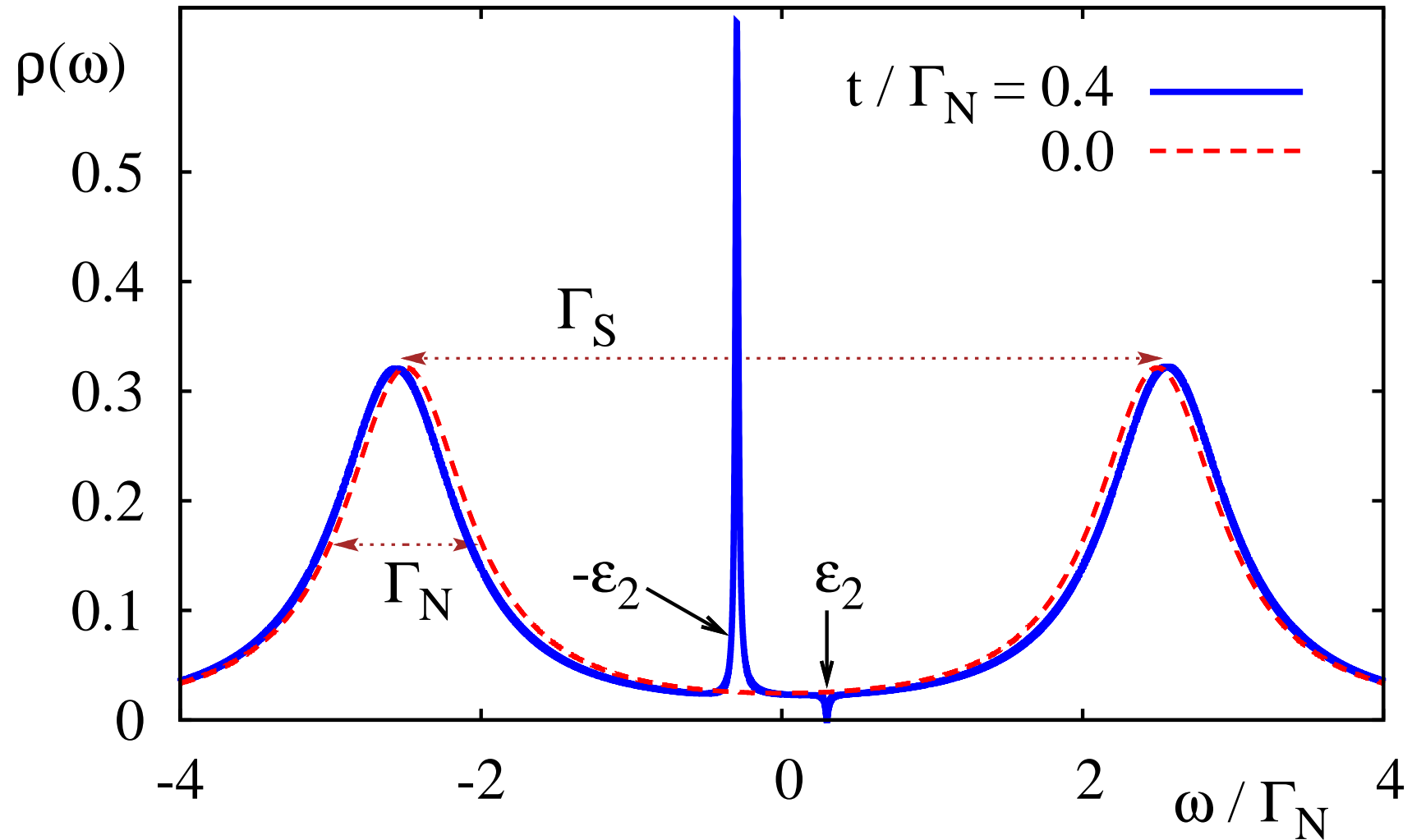
/ The case: $U_1 = 0$ and $U_2 = 0$ /

J. Barański and T. Domański, Phys. Rev. B (2012).

Quantum interference

– in the particle and hole channels

Fano-type lineshapes appear simultaneously at $\pm \varepsilon_2$

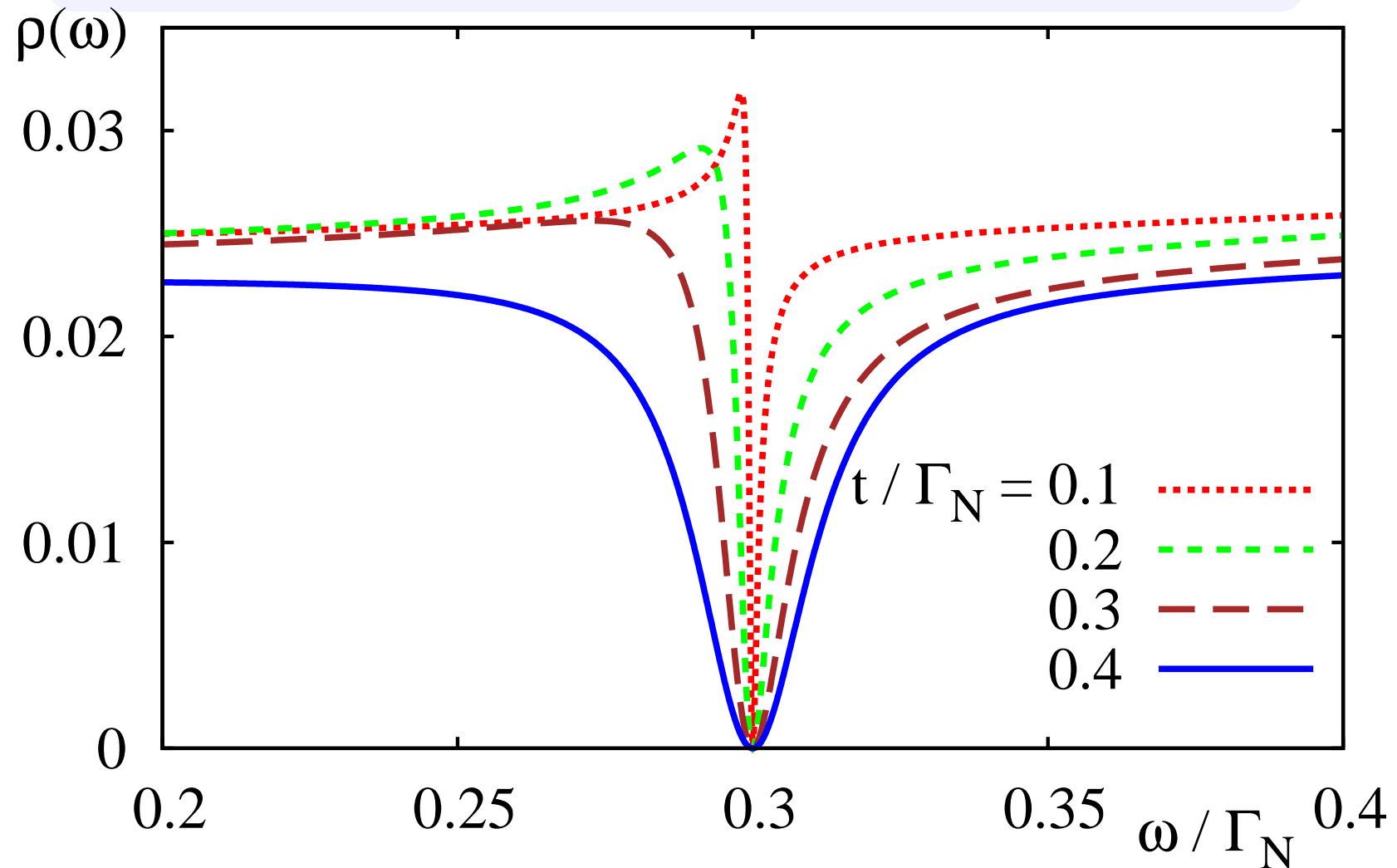


J. Barański and T. Domański, Phys. Rev. B **84**, 195424 (2011).

Quantum interference

– in the particle and hole channels

Fano-type lineshapes appear simultaneously at $\pm \varepsilon_2$

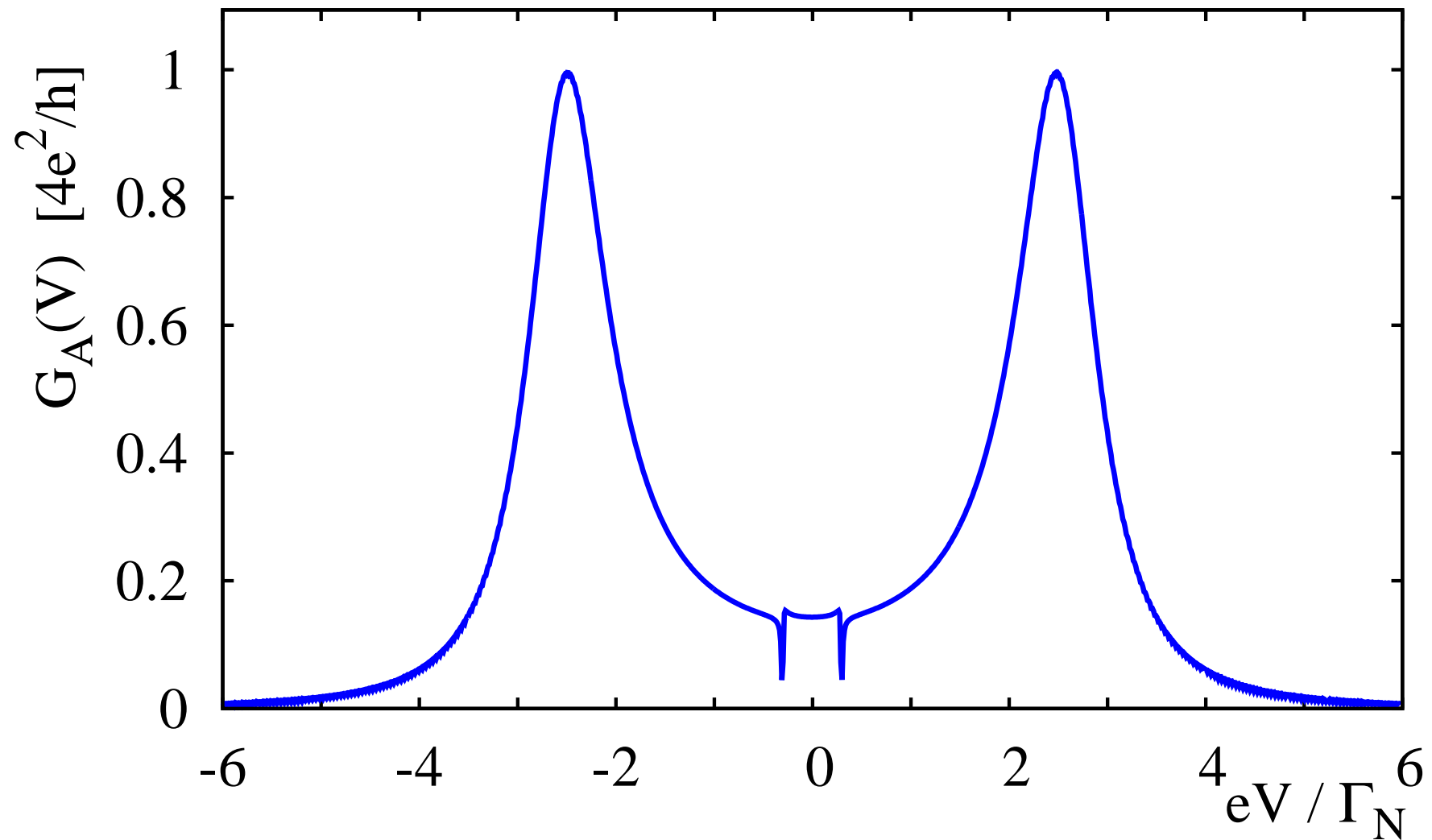


J. Barański and T. Domański, Phys. Rev. B **84**, 195424 (2011).

Quantum interference

– in the particle and hole channels

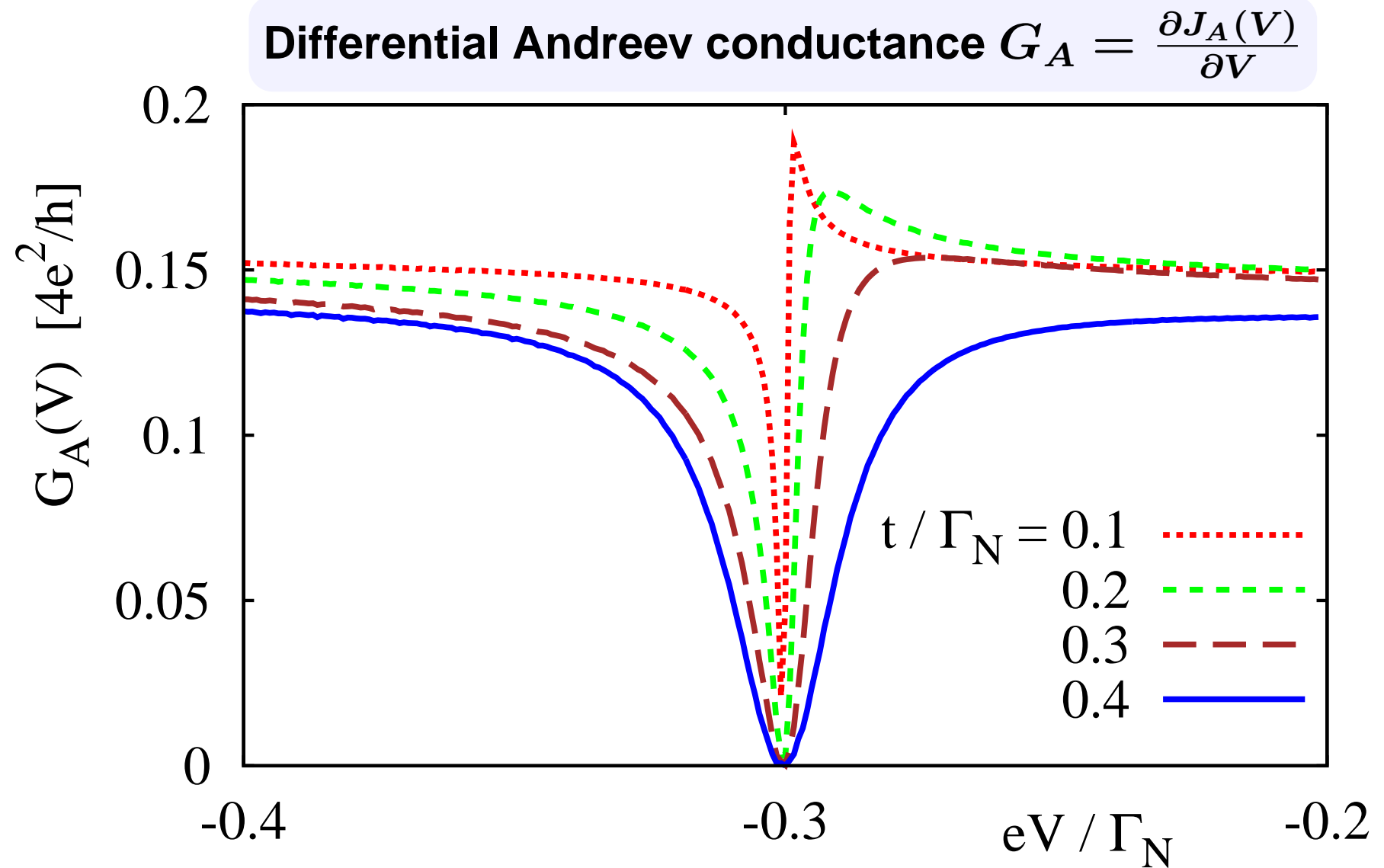
Differential Andreev conductance $G_A = \frac{\partial J_A(V)}{\partial V}$



J. Barański and T. Domański, Phys. Rev. B **84**, 195424 (2011).

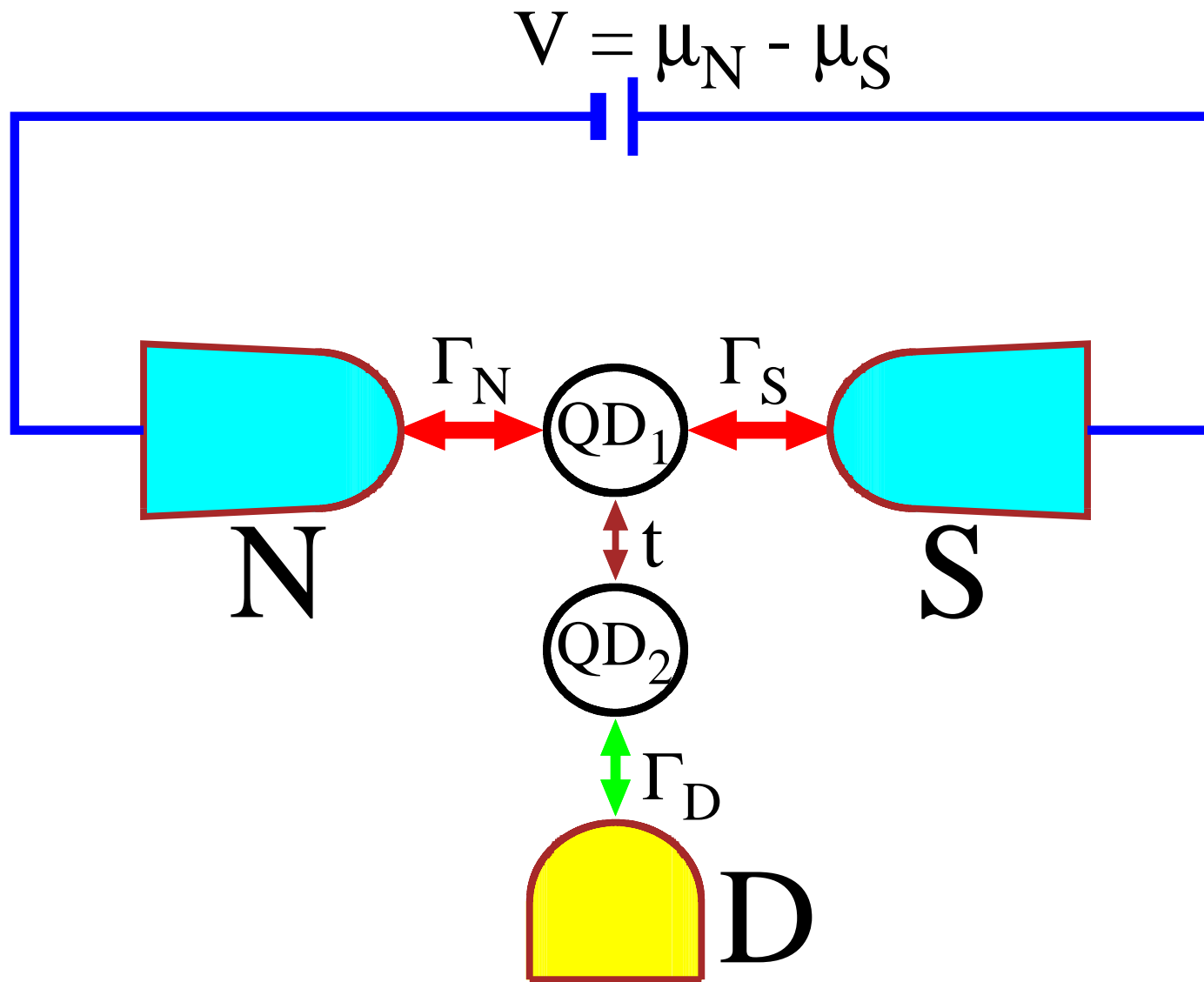
Quantum interference

– in the particle and hole channels



Double QD

– decoherence effects



Floating lead (D) does not contribute any current but it serves as a source of decoherence.

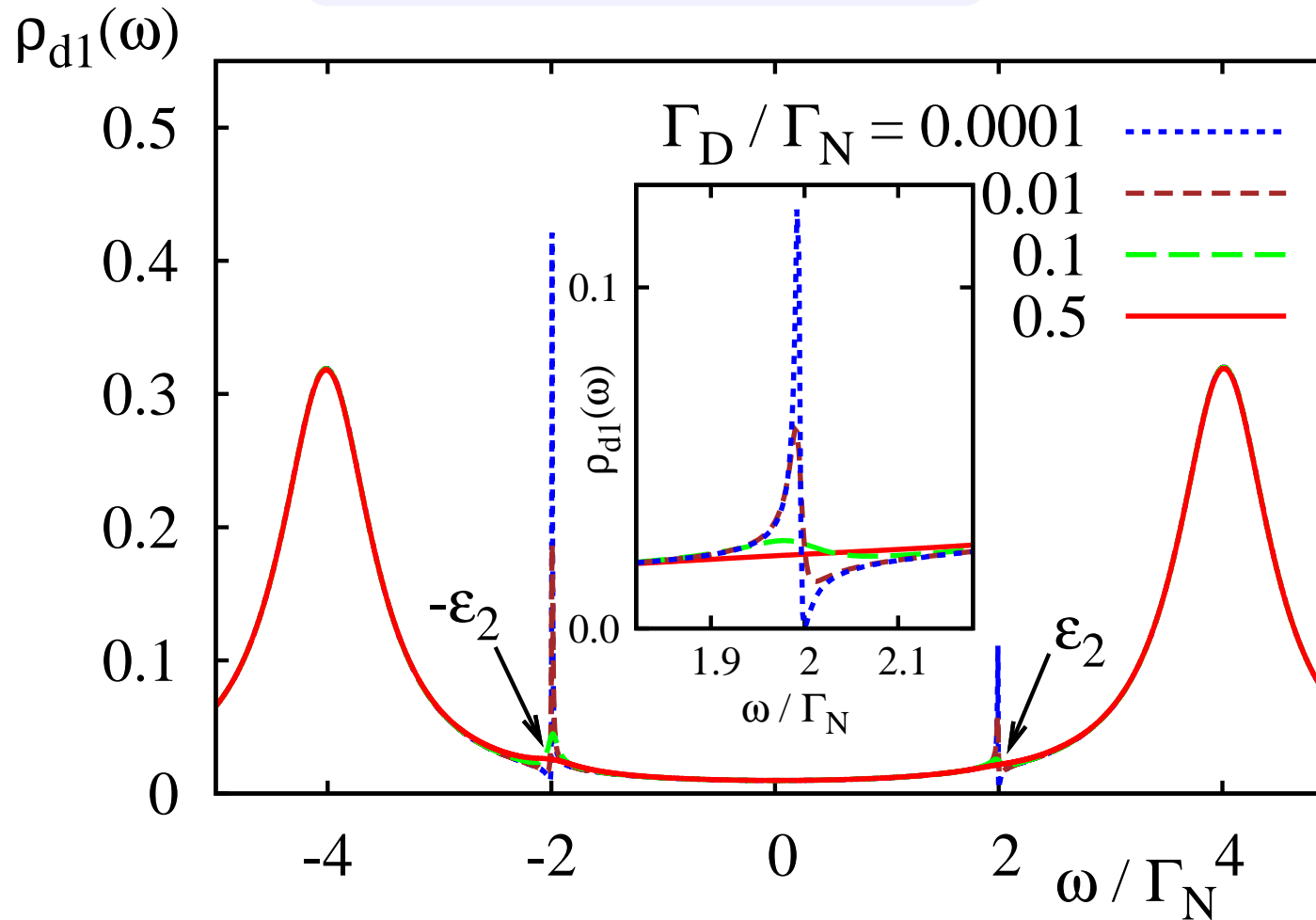
Quantum interference

– influence of the decoherence

Quantum interference

– influence of the decoherence

Density of states $\rho_{d1}(\omega)$

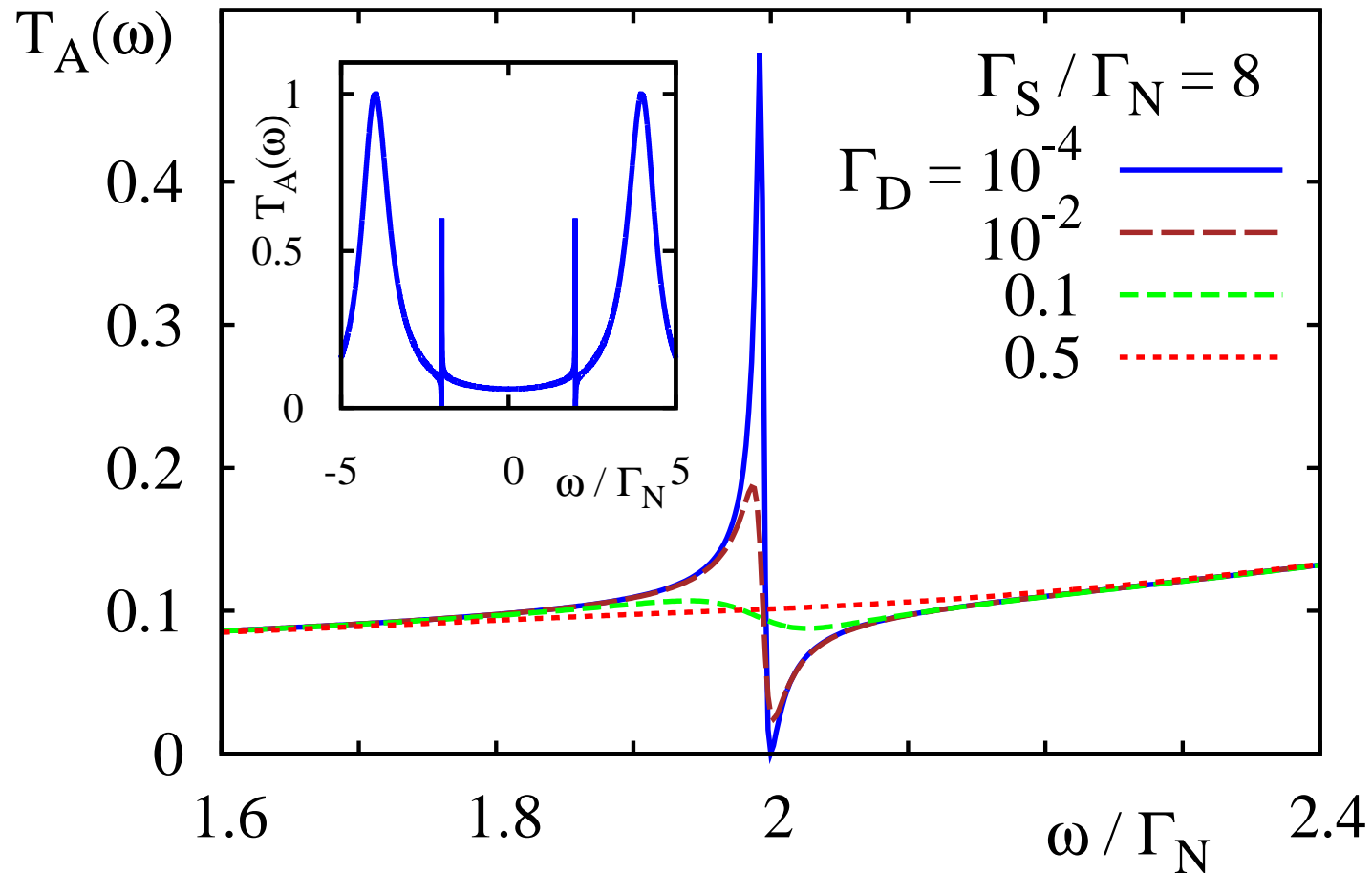


J. Barański and T. Domański, Phys. Rev. B (2012).

Quantum interference

— influence of the decoherence

Andreev conductance $T_A(\omega)$

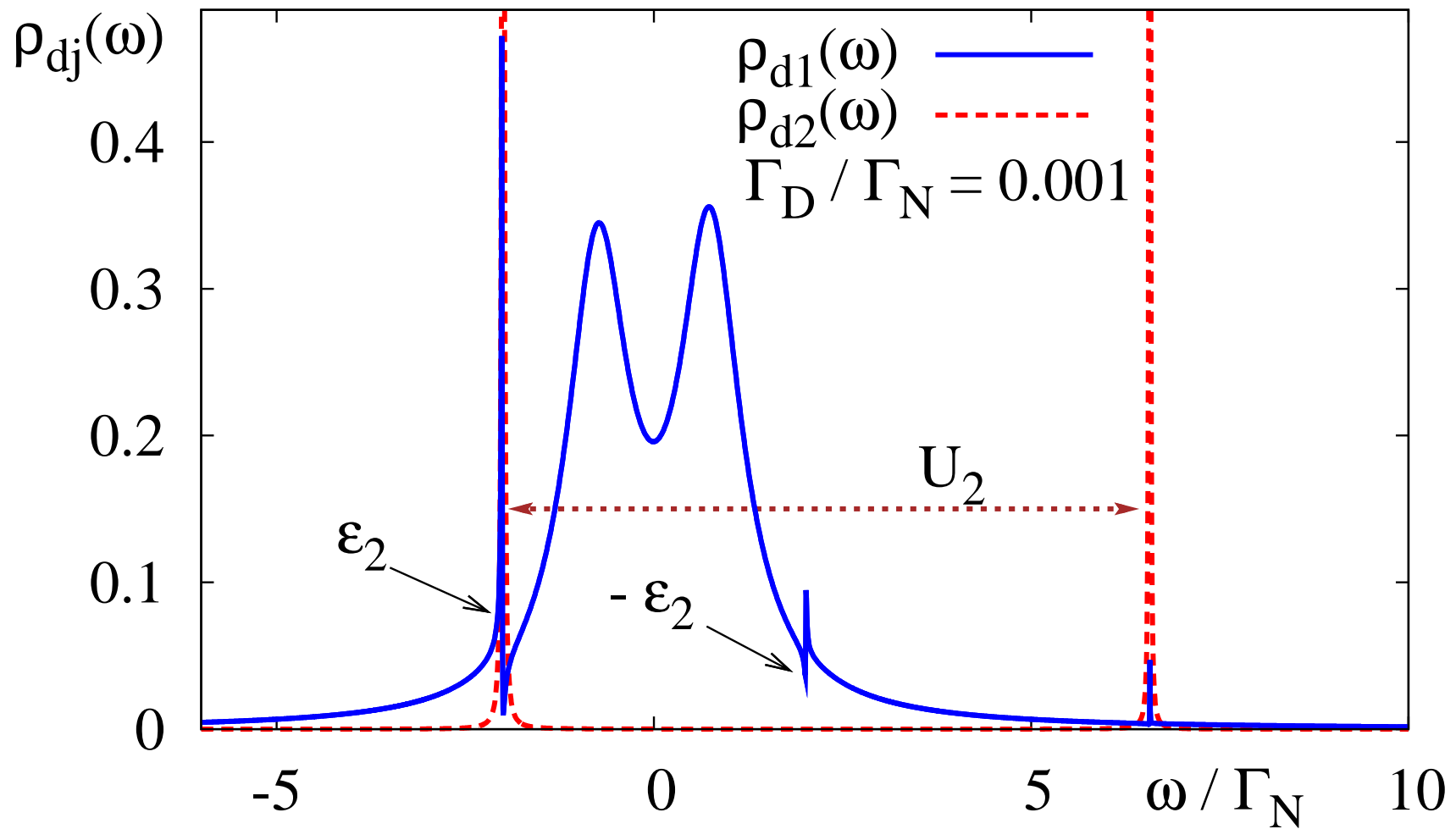


J. Barański and T. Domański, Phys. Rev. B (2012).

Quantum interference

— influence of the decoherence

Effect of U_2 and the coupling Γ_D

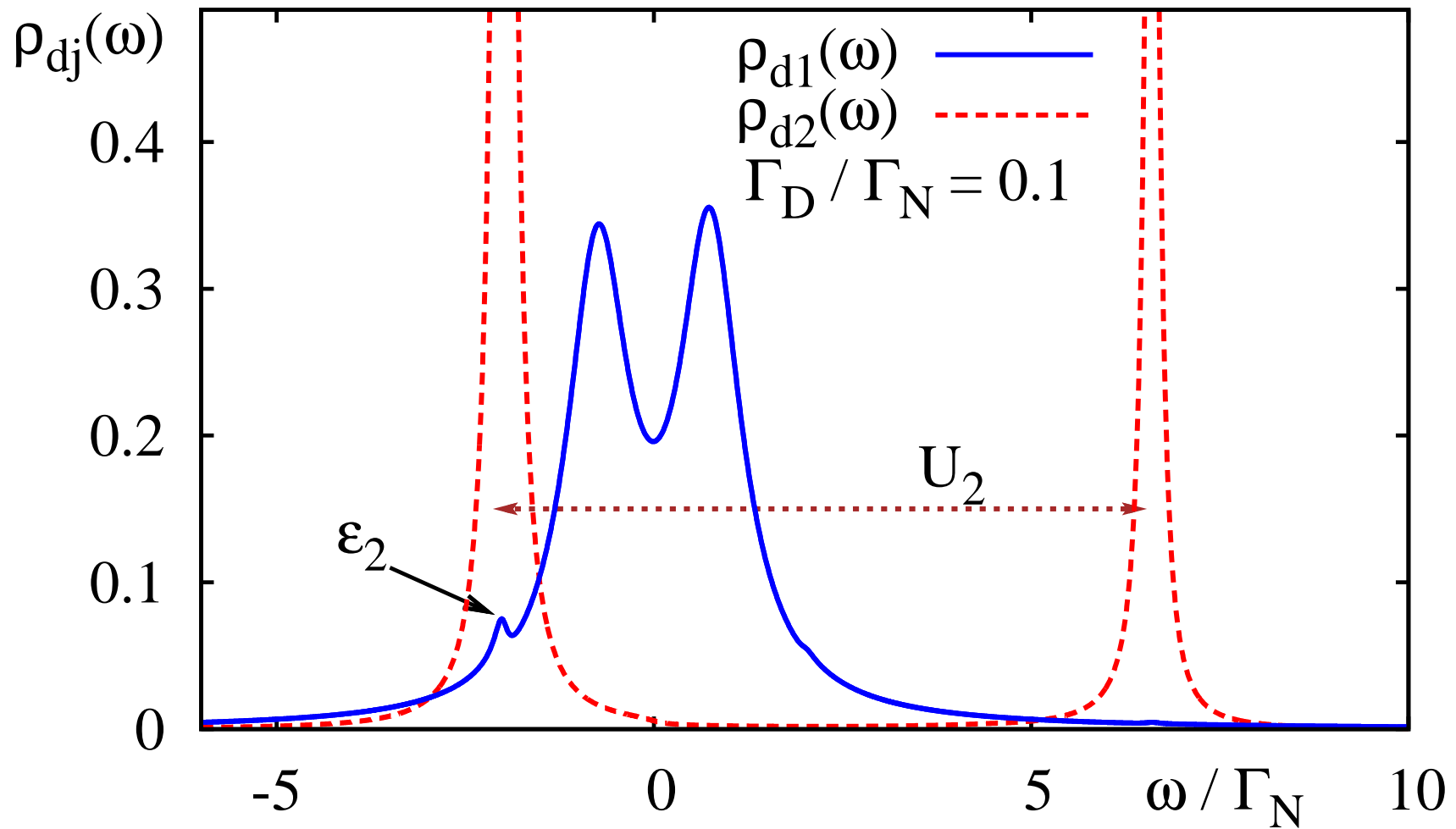


J. Barański and T. Domański, Phys. Rev. B (2012).

Quantum interference

— influence of the decoherence

Effect of U_2 and the coupling Γ_D

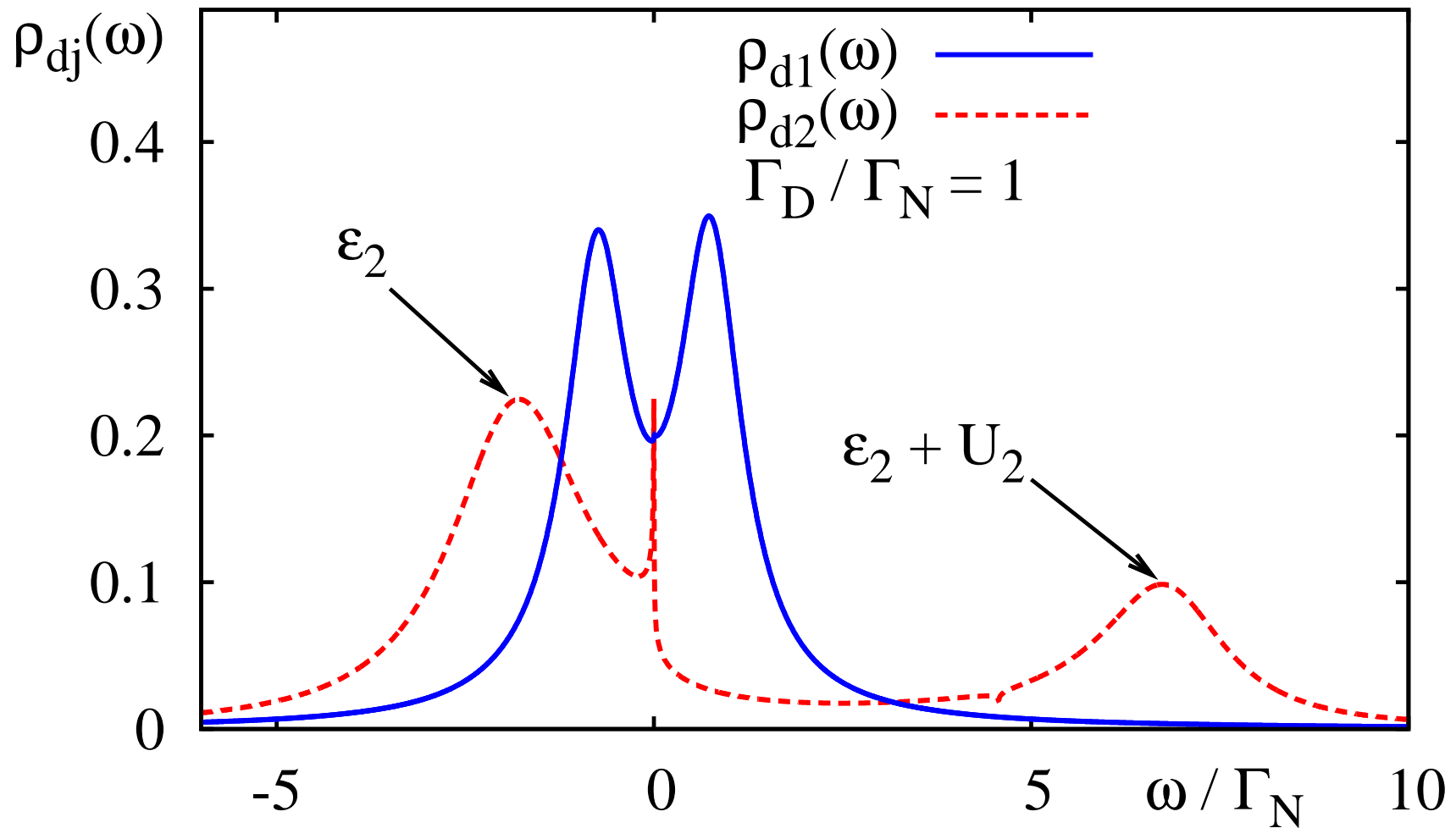


J. Barański and T. Domański, Phys. Rev. B (2012).

Quantum interference

— influence of the decoherence

Effect of U_2 and the coupling Γ_D



J. Barański and T. Domański, Phys. Rev. B (2012).

Conclusions

/ for the 3rd part /

Conclusions / for the 3rd part /

Double QD between the N and S electrodes:

Conclusions / for the 3rd part /

Double QD between the N and S electrodes:

⇒ **is affected by the quantum interference**
/ Fano-type lineshapes /

Conclusions / for the 3rd part /

Double QD between the N and S electrodes:

- ⇒ **is affected by the quantum interference**
/ Fano-type lineshapes /
- ⇒ **simultaneously in the particle and hole channels**
/ particle-hole Fano structures /

Conclusions / for the 3rd part /

Double QD between the N and S electrodes:

- ⇒ **is affected by the quantum interference**
/ Fano-type lineshapes /
- ⇒ **simultaneously in the particle and hole channels**
/ particle-hole Fano structures /

Furthermore:

Conclusions / for the 3rd part /

Double QD between the N and S electrodes:

⇒ **is affected by the quantum interference**
/ Fano-type lineshapes /

⇒ **simultaneously in the particle and hole channels**
/ particle-hole Fano structures /

Furthermore:

⇒ **Fano structure can suppress the Kondo resonance** / below T_K /

Conclusions / for the 3rd part /

Double QD between the N and S electrodes:

- ⇒ **is affected by the quantum interference**
/ Fano-type lineshapes /
- ⇒ **simultaneously in the particle and hole channels**
/ particle-hole Fano structures /

Furthermore:

- ⇒ **Fano structure can suppress the Kondo resonance** / below T_K /
- ⇒ **decoherence has a detrimental effect on the Fano lineshapes**
/ already for a weak coupling /

4. Bulk superconductors

Andreev spectroscopy

– **for bulk superconductors**

Andreev spectroscopy

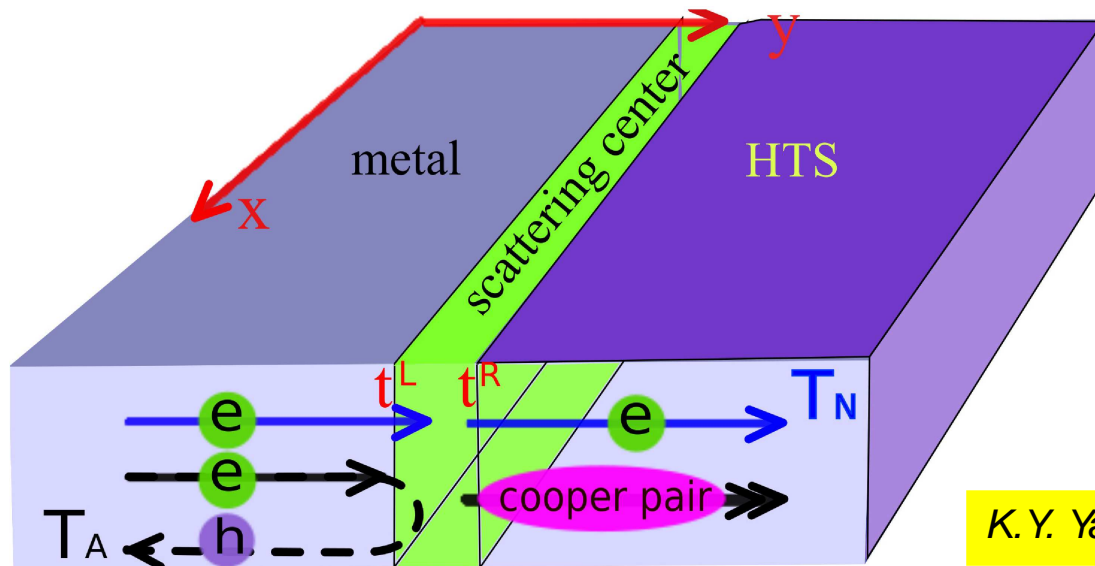
– **for bulk superconductors**

The subgap Andreev spectroscopy is also a valuable tool for studying various superconducting compounds.

Andreev spectroscopy

— for bulk superconductors

The subgap Andreev spectroscopy is also a valuable tool for studying various superconducting compounds.



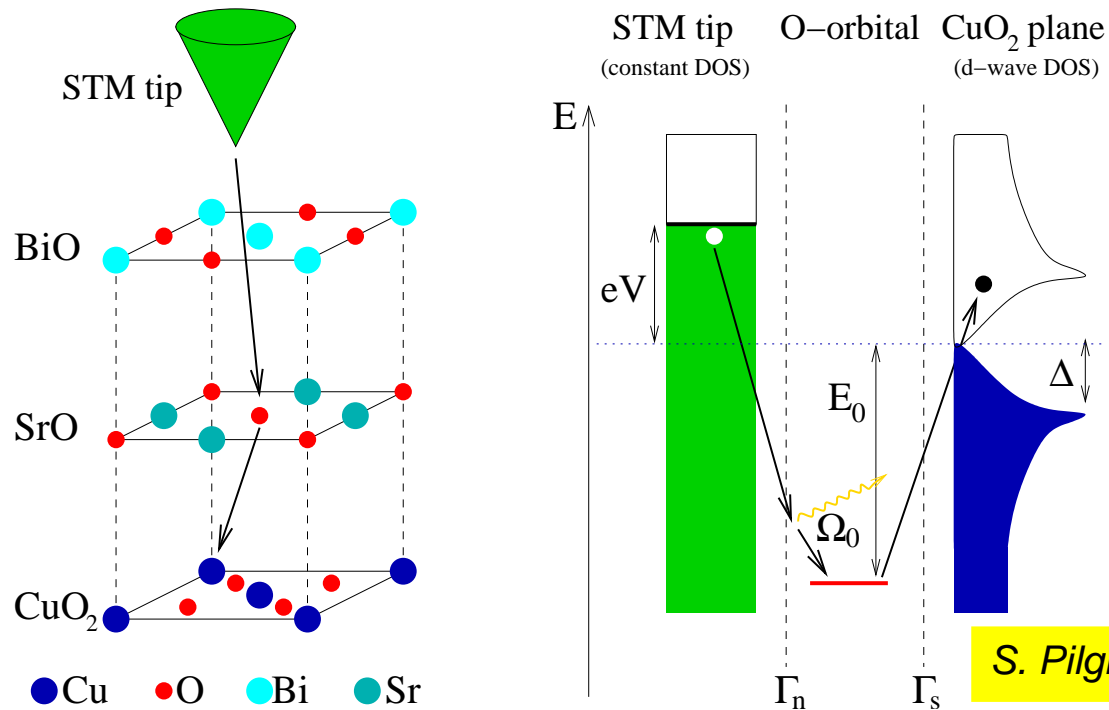
K.Y. Yang et al, Phys. Rev. Lett. 105, 167004 (2010).

For practical experimental realizations one can e.g. use an insulating barrier sandwiched between the conducting (N) and the probed superconductor (S).

Andreev spectroscopy

— for bulk superconductors

The subgap Andreev spectroscopy is also a valuable tool for studying various superconducting compounds.



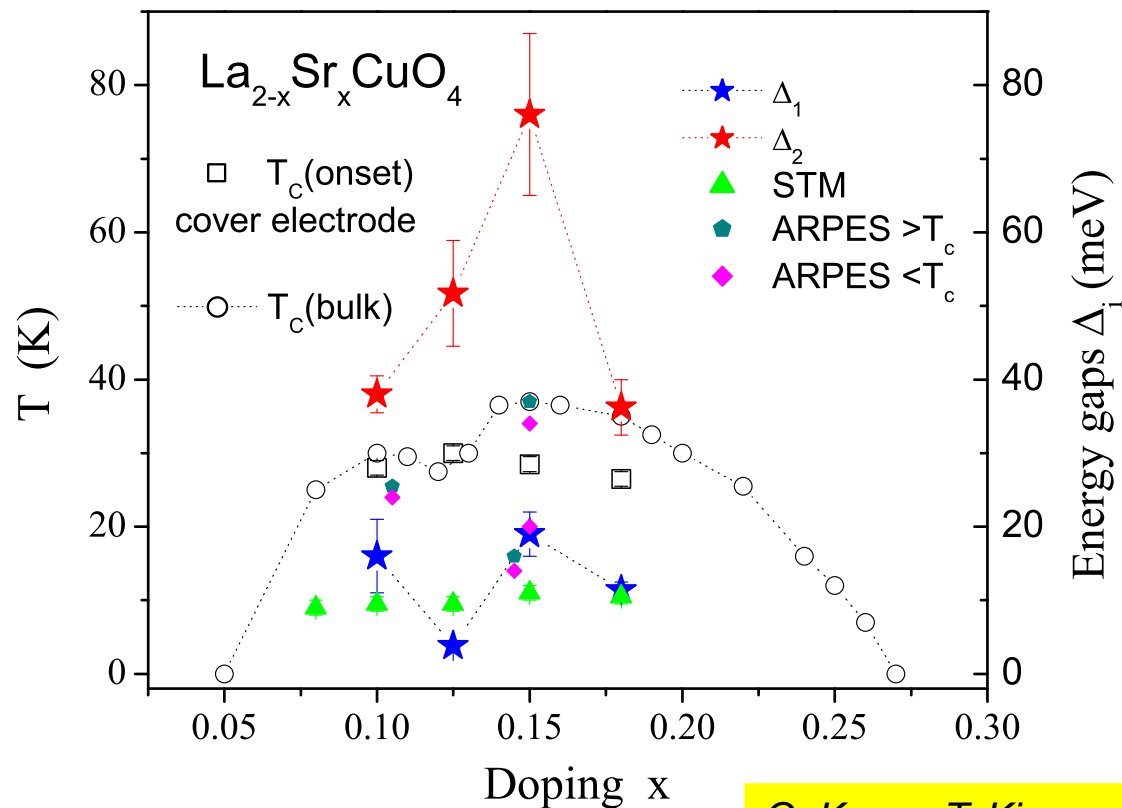
S. Pilgram et al, Phys. Rev. Lett. 97, 117003 (2006).

Other experimental realizations are also possible in the STM configuration, where the apex oxygen atoms play a role similar to QD in the N-QD-S setup.

Andreev spectroscopy

— for bulk superconductors

The subgap Andreev spectroscopy is also a valuable tool for studying various superconducting compounds.



G. Koren, T. Kirzner, *Phys. Rev. Lett.* **106**, 017002 (2011).

Such Andreev spectroscopy has revealed the intriguing two-gap feature.

Andreev scattering

– **on a microscopic level**

Andreev scattering

–

on a microscopic level

Besides the specific Andreev-type spectroscopy we can, however, think of the Andreev scattering in a much broader perspective.

Strongly correlated systems

/ Hubbard-Stratonovich transf. /

Strongly correlated systems

/ Hubbard-Stratonovich transf. /

We consider the strongly correlated fermion system

$$\hat{H} = \hat{T}_{kin} + U \int d\vec{r} \hat{c}_{\uparrow}^{\dagger}(\vec{r}) \hat{c}_{\downarrow}^{\dagger}(\vec{r}) \hat{c}_{\downarrow}(\vec{r}) \hat{c}_{\uparrow}(\vec{r})$$

Strongly correlated systems

/ Hubbard-Stratonovich transf. /

We consider the strongly correlated fermion system

$$\hat{H} = \hat{T}_{kin} + U \int d\vec{r} \hat{c}_{\uparrow}^{\dagger}(\vec{r}) \hat{c}_{\downarrow}^{\dagger}(\vec{r}) \hat{c}_{\downarrow}(\vec{r}) \hat{c}_{\uparrow}(\vec{r})$$

In a basis of **the coherent states** and using **the Grassmann fields**

Strongly correlated systems

/ Hubbard-Stratonovich transf. /

We consider the strongly correlated fermion system

$$\hat{H} = \hat{T}_{kin} + U \int d\vec{r} \hat{c}_{\uparrow}^{\dagger}(\vec{r}) \hat{c}_{\downarrow}^{\dagger}(\vec{r}) \hat{c}_{\downarrow}(\vec{r}) \hat{c}_{\uparrow}(\vec{r})$$

In a basis of **the coherent states** and using **the Grassmann fields**

$$\hat{c} |\psi\rangle = \psi |\psi\rangle \quad \text{and} \quad \langle\psi| \hat{c}^{\dagger} = \langle\psi| \bar{\psi}$$

Strongly correlated systems

/ Hubbard-Stratonovich transf. /

We consider the strongly correlated fermion system

$$\hat{H} = \hat{T}_{kin} + U \int d\vec{r} \hat{c}_{\uparrow}^{\dagger}(\vec{r}) \hat{c}_{\downarrow}^{\dagger}(\vec{r}) \hat{c}_{\downarrow}(\vec{r}) \hat{c}_{\uparrow}(\vec{r})$$

In a basis of **the coherent states** and using **the Grassmann fields**

$$\hat{c}|\psi\rangle = \psi|\psi\rangle \quad \text{and} \quad \langle\psi|\hat{c}^{\dagger} = \langle\psi|\bar{\psi}$$

we can express the partition function by the path integral

$$Z = \int D[\bar{\psi}, \psi] e^{-S[\bar{\psi}, \psi]}$$

Strongly correlated systems

/ Hubbard-Stratonovich transf. /

We consider the strongly correlated fermion system

$$\hat{H} = \hat{T}_{kin} + U \int d\vec{r} \hat{c}_{\uparrow}^{\dagger}(\vec{r}) \hat{c}_{\downarrow}^{\dagger}(\vec{r}) \hat{c}_{\downarrow}(\vec{r}) \hat{c}_{\uparrow}(\vec{r})$$

In a basis of **the coherent states** and using **the Grassmann fields**

$$\hat{c} |\psi\rangle = \psi |\psi\rangle \quad \text{and} \quad \langle\psi| \hat{c}^{\dagger} = \langle\psi| \bar{\psi}$$

we can express the partition function by the path integral

$$Z = \int D[\bar{\psi}, \psi] e^{-S[\bar{\psi}, \psi]}$$

where the imaginary-time fermionic action

$$S[\bar{\psi}, \psi] = \int_0^{\beta} d\tau \int d\vec{r} \left[\sum_{\sigma} \bar{\psi}_{\sigma}(\vec{r}, \tau) \left(\partial_{\tau} + \hat{\xi} \right) \psi_{\sigma}(\vec{r}, \tau) - g \bar{\psi}_{\uparrow}(\vec{r}, \tau) \bar{\psi}_{\downarrow}(\vec{r}, \tau) \psi_{\downarrow}(\vec{r}, \tau) \psi_{\uparrow}(\vec{r}, \tau) \right]$$

Strongly correlated systems

/ Hubbard-Stratonovich transf. /

We consider the strongly correlated fermion system

$$\hat{H} = \hat{T}_{kin} + U \int d\vec{r} \hat{c}_{\uparrow}^{\dagger}(\vec{r}) \hat{c}_{\downarrow}^{\dagger}(\vec{r}) \hat{c}_{\downarrow}(\vec{r}) \hat{c}_{\uparrow}(\vec{r})$$

In a basis of **the coherent states** and using **the Grassmann fields**

$$\hat{c} |\psi\rangle = \psi |\psi\rangle \quad \text{and} \quad \langle\psi| \hat{c}^{\dagger} = \langle\psi| \bar{\psi}$$

we can express the partition function by the path integral

$$Z = \int D[\bar{\psi}, \psi] e^{-S[\bar{\psi}, \psi]}$$

where the imaginary-time fermionic action

$$S[\bar{\psi}, \psi] = \int_0^{\beta} d\tau \int d\vec{r} \left[\sum_{\sigma} \bar{\psi}_{\sigma}(\vec{r}, \tau) \left(\partial_{\tau} + \hat{\xi} \right) \psi_{\sigma}(\vec{r}, \tau) - g \bar{\psi}_{\uparrow}(\vec{r}, \tau) \bar{\psi}_{\downarrow}(\vec{r}, \tau) \psi_{\downarrow}(\vec{r}, \tau) \psi_{\uparrow}(\vec{r}, \tau) \right]$$

and $\hat{\xi} \equiv -\hbar^2 \nabla^2 / 2m - \mu$, $g = -U$.

Hubbard-Stratonovich – continued

Hubbard-Stratonovich – continued

To eliminate the quartic term we can introduce the auxiliary pairing fields

$$Z = \int D [\bar{\Delta}, \Delta, \bar{\psi}, \psi] e^{-S[\bar{\Delta}, \Delta, \bar{\psi}, \psi]}$$

Hubbard-Stratonovich – continued

To eliminate the quartic term we can introduce the auxiliary pairing fields

$$Z = \int D [\bar{\Delta}, \Delta, \bar{\psi}, \psi] e^{-S[\bar{\Delta}, \Delta, \bar{\psi}, \psi]}$$

simplifying the action to a bi-linear form

$$S = \int_0^\beta d\tau \int d\vec{r} \left[\sum_\sigma \bar{\psi}_\sigma(\vec{r}, \tau) \left(\partial_\tau + \hat{\xi} \right) \psi_\sigma(\vec{r}, \tau) + \frac{|\Delta(\vec{r}, \tau)|^2}{g} \right. \\ \left. - \bar{\Delta}(\vec{r}, \tau) \psi_\downarrow(\vec{r}, \tau) \psi_\uparrow(\vec{r}, \tau) - \Delta(\vec{r}, \tau) \bar{\psi}_\uparrow(\vec{r}, \tau) \bar{\psi}_\downarrow(\vec{r}, \tau) \right]$$

Hubbard-Stratonovich – continued

To eliminate the quartic term we can introduce the auxiliary pairing fields

$$Z = \int D [\bar{\Delta}, \Delta, \bar{\psi}, \psi] e^{-S[\bar{\Delta}, \Delta, \bar{\psi}, \psi]}$$

simplifying the action to a bi-linear form

$$S = \int_0^\beta d\tau \int d\vec{r} \left[\sum_\sigma \bar{\psi}_\sigma(\vec{r}, \tau) \left(\partial_\tau + \hat{\xi} \right) \psi_\sigma(\vec{r}, \tau) + \frac{|\Delta(\vec{r}, \tau)|^2}{g} \right. \\ \left. - \bar{\Delta}(\vec{r}, \tau) \psi_\downarrow(\vec{r}, \tau) \psi_\uparrow(\vec{r}, \tau) - \Delta(\vec{r}, \tau) \bar{\psi}_\uparrow(\vec{r}, \tau) \bar{\psi}_\downarrow(\vec{r}, \tau) \right]$$

The mean field (*saddle point*) solution usually relies on the assumption of a static and uniform pairing field

$$\Delta(\vec{r}, \tau) = \Delta, \quad \bar{\Delta}(\vec{r}, \tau) = \bar{\Delta}.$$

Hubbard-Stratonovich – continued

To eliminate the quartic term we can introduce the auxiliary pairing fields

$$Z = \int D [\bar{\Delta}, \Delta, \bar{\psi}, \psi] e^{-S[\bar{\Delta}, \Delta, \bar{\psi}, \psi]}$$

simplifying the action to a bi-linear form

$$S = \int_0^\beta d\tau \int d\vec{r} \left[\sum_\sigma \bar{\psi}_\sigma(\vec{r}, \tau) \left(\partial_\tau + \hat{\xi} \right) \psi_\sigma(\vec{r}, \tau) + \frac{|\Delta(\vec{r}, \tau)|^2}{g} \right. \\ \left. - \bar{\Delta}(\vec{r}, \tau) \psi_\downarrow(\vec{r}, \tau) \psi_\uparrow(\vec{r}, \tau) - \Delta(\vec{r}, \tau) \bar{\psi}_\uparrow(\vec{r}, \tau) \bar{\psi}_\downarrow(\vec{r}, \tau) \right]$$

The mean field (*saddle point*) solution usually relies on the assumption of a static and uniform pairing field

$$\Delta(\vec{r}, \tau) = \Delta, \quad \bar{\Delta}(\vec{r}, \tau) = \bar{\Delta}.$$

We tried to go beyond this scheme treating the fermionic and bosonic degrees of freedom on an equal footing !

Boson-Fermion scenario

[in the lattice representation]

$$\begin{aligned}\hat{H} &= \sum_{i,j,\sigma} (t_{ij} - \mu \delta_{i,j}) \hat{c}_{i\sigma}^\dagger \hat{c}_{j\sigma} + \sum_l \left(E_l^{(B)} - 2\mu \right) \hat{b}_l^\dagger \hat{b}_l \\ &+ \sum_{i,j} g_{ij} \left[\hat{b}_l^\dagger \hat{c}_{i,\downarrow} \hat{c}_{j,\uparrow} + \text{h.c.} \right]\end{aligned}$$

Boson-Fermion scenario

[in the lattice representation]

$$\begin{aligned}\hat{H} &= \sum_{i,j,\sigma} (t_{ij} - \mu \delta_{i,j}) \hat{c}_{i\sigma}^\dagger \hat{c}_{j\sigma} + \sum_l \left(E_l^{(B)} - 2\mu \right) \hat{b}_l^\dagger \hat{b}_l \\ &+ \sum_{i,j} g_{ij} \left[\hat{b}_l^\dagger \hat{c}_{i,\downarrow} \hat{c}_{j,\uparrow} + \text{h.c.} \right]\end{aligned}$$

$$\vec{R}_l = (\vec{r}_i + \vec{r}_j)/2$$

Boson-Fermion scenario

[in the lattice representation]

$$\begin{aligned}\hat{H} = & \sum_{i,j,\sigma} (t_{ij} - \mu \delta_{i,j}) \hat{c}_{i\sigma}^\dagger \hat{c}_{j\sigma} + \sum_l \left(E_l^{(B)} - 2\mu \right) \hat{b}_l^\dagger \hat{b}_l \\ & + \sum_{i,j} g_{ij} \left[\hat{b}_l^\dagger \hat{c}_{i,\downarrow} \hat{c}_{j,\uparrow} + \text{h.c.} \right]\end{aligned}$$

$$\vec{R}_l = (\vec{r}_i + \vec{r}_j)/2$$

describes a two-component system consisting of:

Boson-Fermion scenario

[in the lattice representation]

$$\begin{aligned}\hat{H} = & \sum_{i,j,\sigma} (t_{ij} - \mu \delta_{i,j}) \hat{c}_{i\sigma}^\dagger \hat{c}_{j\sigma} + \sum_l \left(E_l^{(B)} - 2\mu \right) \hat{b}_l^\dagger \hat{b}_l \\ & + \sum_{i,j} g_{ij} \left[\hat{b}_l^\dagger \hat{c}_{i,\downarrow} \hat{c}_{j,\uparrow} + \text{h.c.} \right]\end{aligned}$$

$$\vec{R}_l = (\vec{r}_i + \vec{r}_j)/2$$

describes a two-component system consisting of:

$\hat{c}_{i\sigma}^{(\dagger)}$ itinerant fermions (e.g. holes near the Mott insulator)

Boson-Fermion scenario

[in the lattice representation]

$$\begin{aligned}\hat{H} = & \sum_{i,j,\sigma} (t_{ij} - \mu \delta_{i,j}) \hat{c}_{i\sigma}^\dagger \hat{c}_{j\sigma} + \sum_l \left(E_l^{(B)} - 2\mu \right) \hat{b}_l^\dagger \hat{b}_l \\ & + \sum_{i,j} g_{ij} \left[\hat{b}_l^\dagger \hat{c}_{i,\downarrow} \hat{c}_{j,\uparrow} + \text{h.c.} \right]\end{aligned}$$

$$\vec{R}_l = (\vec{r}_i + \vec{r}_j)/2$$

describes a two-component system consisting of:

$\hat{c}_{i\sigma}^{(\dagger)}$ itinerant fermions (e.g. holes near the Mott insulator)

$\hat{b}_l^{(\dagger)}$ local pairs (RVB defines them on the bonds)

Boson-Fermion scenario

[in the lattice representation]

$$\begin{aligned}\hat{H} = & \sum_{i,j,\sigma} (t_{ij} - \mu \delta_{i,j}) \hat{c}_{i\sigma}^\dagger \hat{c}_{j\sigma} + \sum_l \left(E_l^{(B)} - 2\mu \right) \hat{b}_l^\dagger \hat{b}_l \\ & + \sum_{i,j} g_{ij} \left[\hat{b}_l^\dagger \hat{c}_{i,\downarrow} \hat{c}_{j,\uparrow} + \text{h.c.} \right]\end{aligned}$$

$$\vec{R}_l = (\vec{r}_i + \vec{r}_j)/2$$

describes a two-component system consisting of:

$\hat{c}_{i\sigma}^{(\dagger)}$ itinerant fermions (e.g. holes near the Mott insulator)

$\hat{b}_l^{(\dagger)}$ local pairs (RVB defines them on the bonds)

interacting via:

Boson-Fermion scenario

[in the lattice representation]

$$\begin{aligned}\hat{H} = & \sum_{i,j,\sigma} (t_{ij} - \mu \delta_{i,j}) \hat{c}_{i\sigma}^\dagger \hat{c}_{j\sigma} + \sum_l \left(E_l^{(B)} - 2\mu \right) \hat{b}_l^\dagger \hat{b}_l \\ & + \sum_{i,j} g_{ij} \left[\hat{b}_l^\dagger \hat{c}_{i,\downarrow} \hat{c}_{j,\uparrow} + \text{h.c.} \right]\end{aligned}$$

$$\vec{R}_l = (\vec{r}_i + \vec{r}_j)/2$$

describes a two-component system consisting of:

$\hat{c}_{i\sigma}^{(\dagger)}$ itinerant fermions (e.g. holes near the Mott insulator)

$\hat{b}_l^{(\dagger)}$ local pairs (RVB defines them on the bonds)

interacting via:

$\hat{b}_l^\dagger \hat{c}_{i,\downarrow} \hat{c}_{j,\uparrow} + \text{h.c.}$ (Andreev-type conversion)

Boson-Fermion scenario

[in the lattice representation]

$$\begin{aligned}\hat{H} = & \sum_{i,j,\sigma} (t_{ij} - \mu \delta_{i,j}) \hat{c}_{i\sigma}^\dagger \hat{c}_{j\sigma} + \sum_l \left(E_l^{(B)} - 2\mu \right) \hat{b}_l^\dagger \hat{b}_l \\ & + \sum_{i,j} g_{ij} \left[\hat{b}_l^\dagger \hat{c}_{i,\downarrow} \hat{c}_{j,\uparrow} + \text{h.c.} \right]\end{aligned}$$

$$\vec{R}_l = (\vec{r}_i + \vec{r}_j)/2$$

describes a two-component system consisting of:

$\hat{c}_{i\sigma}^{(\dagger)}$ itinerant fermions (e.g. holes near the Mott insulator)

$\hat{b}_l^{(\dagger)}$ local pairs (RVB defines them on the bonds)

interacting via:

$\hat{b}_l^\dagger \hat{c}_{i,\downarrow} \hat{c}_{j,\uparrow} + \text{h.c.}$ (Andreev-type conversion)

For a more specific recent
derivation see for instance:

E. Altman and A. Auerbach, *Phys. Rev. B* **65**, 104508 (2002).

or Y. Yildirim and Wei Ku, *Phys. Rev. X* **1**, 011011 (2011).

Outline of the procedure

Outline of the procedure

For studying the quantum many-body feedback effects we construct the continuous unitary transformation

Outline of the procedure

For studying the quantum many-body feedback effects we construct the continuous unitary transformation

$$\hat{H} \longrightarrow \hat{H}(l_1) \longrightarrow \hat{H}(l_2) \longrightarrow \dots \longrightarrow \hat{H}(\infty)$$

Outline of the procedure

For studying the quantum many-body feedback effects we construct the continuous unitary transformation

$$\hat{H} \longrightarrow \hat{H}(l_1) \longrightarrow \hat{H}(l_2) \longrightarrow \dots \longrightarrow \hat{H}(\infty)$$

gradually decoupling the boson from fermion degrees of freedom.

Outline of the procedure

For studying the quantum many-body feedback effects we construct the continuous unitary transformation

$$\hat{H} \longrightarrow \hat{H}(l_1) \longrightarrow \hat{H}(l_2) \longrightarrow \dots \longrightarrow \hat{H}(\infty)$$

gradually decoupling the boson from fermion degrees of freedom.

F. Wegner (1994); K.G. Wilson (1994) - inventors of this RG-like scheme

Outline of the procedure

For studying the quantum many-body feedback effects we construct the continuous unitary transformation

$$\hat{H} \longrightarrow \hat{H}(l_1) \longrightarrow \hat{H}(l_2) \longrightarrow \dots \longrightarrow \hat{H}(\infty)$$

gradually decoupling the boson from fermion degrees of freedom.

F. Wegner (1994); K.G. Wilson (1994) - inventors of this RG-like scheme

Hamiltonian at $l = 0$

$$\hat{H}_F + \hat{H}_B + \hat{V}_{BF}$$

Outline of the procedure

For studying the quantum many-body feedback effects we construct the continuous unitary transformation

$$\hat{H} \longrightarrow \hat{H}(l_1) \longrightarrow \hat{H}(l_2) \longrightarrow \dots \longrightarrow \hat{H}(\infty)$$

gradually decoupling the boson from fermion degrees of freedom.

F. Wegner (1994); K.G. Wilson (1994) - inventors of this RG-like scheme

Hamiltonian at $0 < l < \infty$

$$\hat{H}_F(l) + \hat{H}_B(l) + \hat{V}_{BF}(l)$$

Outline of the procedure

For studying the quantum many-body feedback effects we construct the continuous unitary transformation

$$\hat{H} \longrightarrow \hat{H}(l_1) \longrightarrow \hat{H}(l_2) \longrightarrow \dots \longrightarrow \hat{H}(\infty)$$

gradually decoupling the boson from fermion degrees of freedom.

F. Wegner (1994); K.G. Wilson (1994) - inventors of this RG-like scheme

Hamiltonian at $l = \infty$

$$\hat{H}_F(\infty) + \hat{H}_B(\infty) + 0$$

Outline of the procedure

For studying the quantum many-body feedback effects we construct the continuous unitary transformation

$$\hat{H} \longrightarrow \hat{H}(l_1) \longrightarrow \hat{H}(l_2) \longrightarrow \dots \longrightarrow \hat{H}(\infty)$$

gradually decoupling the boson from fermion degrees of freedom.

F. Wegner (1994); K.G. Wilson (1994) - inventors of this RG-like scheme

Hamiltonian at $l = \infty$

$$\hat{H}_F(\infty) + \hat{H}_B(\infty) + 0$$

T. Domański and J. Ranninger, Phys. Rev. B 63, 134505 (2001).

Beyond BCS approximation

Beyond BCS approximation

We generalized the Bogoliubov-Valatin transformation, taking into account the non-condensed (preformed) pairs

Beyond BCS approximation

We generalized the Bogoliubov-Valatin transformation, taking into account the non-condensed (preformed) pairs

$$\begin{aligned}\hat{c}_{\mathbf{k}\uparrow}(l) &= u_{\mathbf{k}}(l) \hat{c}_{\mathbf{k}\uparrow} + v_{\mathbf{k}}(l) \hat{c}_{-\mathbf{k}\downarrow}^\dagger + \\ &\quad \frac{1}{\sqrt{N}} \sum_{\mathbf{q} \neq 0} \left[u_{\mathbf{k},\mathbf{q}}(l) \hat{b}_{\mathbf{q}}^\dagger \hat{c}_{\mathbf{q}+\mathbf{k}\uparrow} + v_{\mathbf{k},\mathbf{q}}(l) \hat{b}_{\mathbf{q}} \hat{c}_{\mathbf{q}-\mathbf{k}\downarrow}^\dagger \right], \\ \hat{c}_{-\mathbf{k}\downarrow}^\dagger(l) &= -v_{\mathbf{k}}^*(l) \hat{c}_{\mathbf{k}\uparrow} + u_{\mathbf{k}}^*(l) \hat{c}_{-\mathbf{k}\downarrow}^\dagger + \\ &\quad \frac{1}{\sqrt{N}} \sum_{\mathbf{q} \neq 0} \left[-v_{\mathbf{k},\mathbf{q}}^*(l) \hat{b}_{\mathbf{q}}^\dagger \hat{c}_{\mathbf{q}+\mathbf{k}\uparrow} + u_{\mathbf{k},\mathbf{q}}^*(l) \hat{b}_{\mathbf{q}} \hat{c}_{\mathbf{q}-\mathbf{k}\downarrow}^\dagger \right],\end{aligned}$$

Beyond BCS approximation

We generalized the Bogoliubov-Valatin transformation, taking into account the non-condensed (preformed) pairs

$$\begin{aligned}\hat{c}_{\mathbf{k}\uparrow}(l) &= u_{\mathbf{k}}(l) \hat{c}_{\mathbf{k}\uparrow} + v_{\mathbf{k}}(l) \hat{c}_{-\mathbf{k}\downarrow}^{\dagger} + \\ &\quad \frac{1}{\sqrt{N}} \sum_{\mathbf{q} \neq 0} \left[u_{\mathbf{k},\mathbf{q}}(l) \hat{b}_{\mathbf{q}}^{\dagger} \hat{c}_{\mathbf{q}+\mathbf{k}\uparrow} + v_{\mathbf{k},\mathbf{q}}(l) \hat{b}_{\mathbf{q}} \hat{c}_{\mathbf{q}-\mathbf{k}\downarrow}^{\dagger} \right], \\ \hat{c}_{-\mathbf{k}\downarrow}^{\dagger}(l) &= -v_{\mathbf{k}}^*(l) \hat{c}_{\mathbf{k}\uparrow} + u_{\mathbf{k}}^*(l) \hat{c}_{-\mathbf{k}\downarrow}^{\dagger} + \\ &\quad \frac{1}{\sqrt{N}} \sum_{\mathbf{q} \neq 0} \left[-v_{\mathbf{k},\mathbf{q}}^*(l) \hat{b}_{\mathbf{q}}^{\dagger} \hat{c}_{\mathbf{q}+\mathbf{k}\uparrow} + u_{\mathbf{k},\mathbf{q}}^*(l) \hat{b}_{\mathbf{q}} \hat{c}_{\mathbf{q}-\mathbf{k}\downarrow}^{\dagger} \right],\end{aligned}$$

with the boundary conditions

$$u_{\mathbf{k}}(0) = 1 \quad \text{and} \quad v_{\mathbf{k}}(0) = v_{\mathbf{k},\mathbf{q}}(0) = u_{\mathbf{k},\mathbf{q}}(0) = 0.$$

Beyond BCS approximation

We generalized the Bogoliubov-Valatin transformation, taking into account the non-condensed (preformed) pairs

$$\begin{aligned}\hat{c}_{\mathbf{k}\uparrow}(l) &= u_{\mathbf{k}}(l) \hat{c}_{\mathbf{k}\uparrow} + v_{\mathbf{k}}(l) \hat{c}_{-\mathbf{k}\downarrow}^{\dagger} + \\ &\quad \frac{1}{\sqrt{N}} \sum_{\mathbf{q} \neq 0} \left[u_{\mathbf{k},\mathbf{q}}(l) \hat{b}_{\mathbf{q}}^{\dagger} \hat{c}_{\mathbf{q}+\mathbf{k}\uparrow} + v_{\mathbf{k},\mathbf{q}}(l) \hat{b}_{\mathbf{q}} \hat{c}_{\mathbf{q}-\mathbf{k}\downarrow}^{\dagger} \right], \\ \hat{c}_{-\mathbf{k}\downarrow}^{\dagger}(l) &= -v_{\mathbf{k}}^*(l) \hat{c}_{\mathbf{k}\uparrow} + u_{\mathbf{k}}^*(l) \hat{c}_{-\mathbf{k}\downarrow}^{\dagger} + \\ &\quad \frac{1}{\sqrt{N}} \sum_{\mathbf{q} \neq 0} \left[-v_{\mathbf{k},\mathbf{q}}^*(l) \hat{b}_{\mathbf{q}}^{\dagger} \hat{c}_{\mathbf{q}+\mathbf{k}\uparrow} + u_{\mathbf{k},\mathbf{q}}^*(l) \hat{b}_{\mathbf{q}} \hat{c}_{\mathbf{q}-\mathbf{k}\downarrow}^{\dagger} \right],\end{aligned}$$

with the boundary conditions

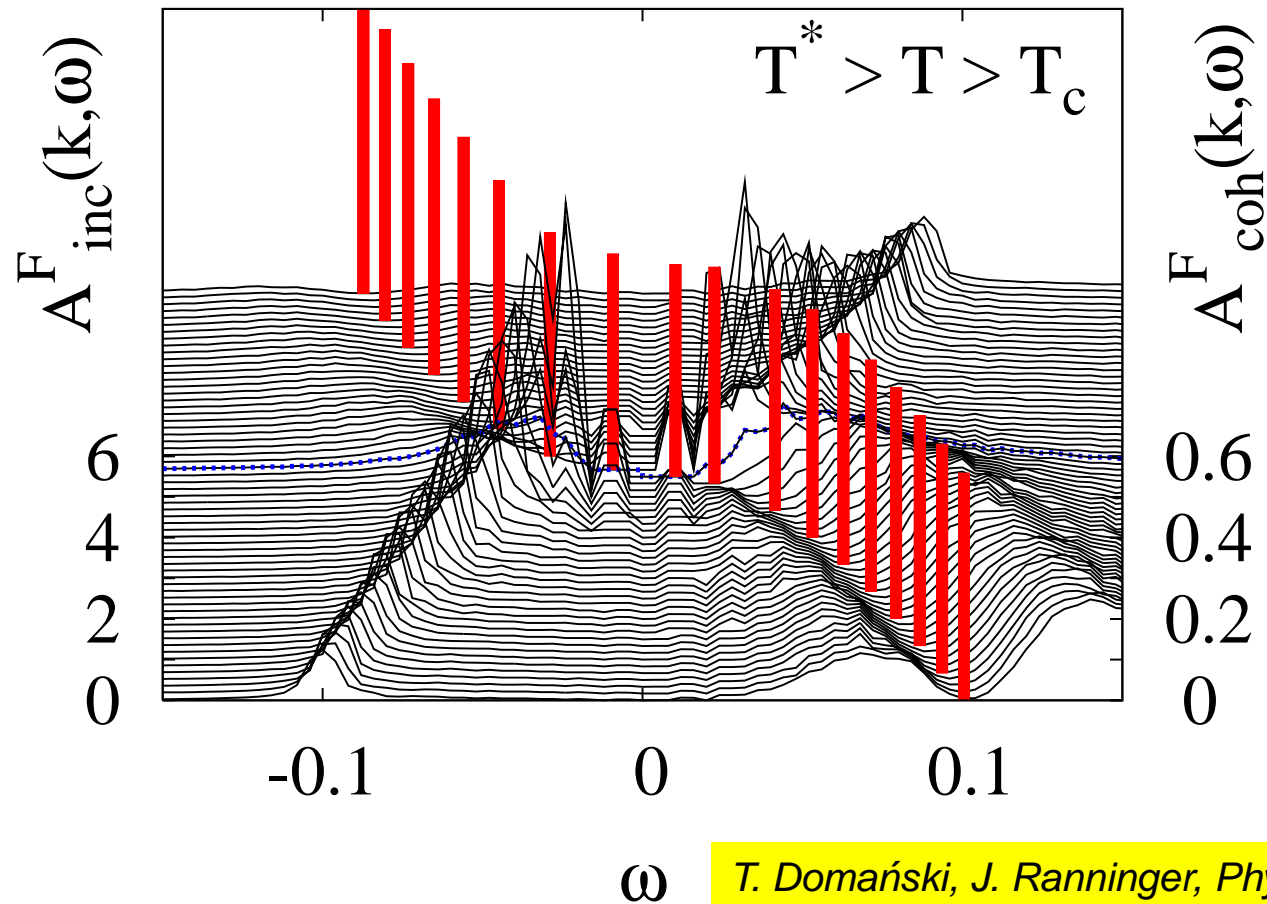
$$u_{\mathbf{k}}(0) = 1 \quad \text{and} \quad v_{\mathbf{k}}(0) = v_{\mathbf{k},\mathbf{q}}(0) = u_{\mathbf{k},\mathbf{q}}(0) = 0.$$

The corresponding **fixed point** values $\lim_{l \rightarrow \infty} u_{\mathbf{k}}(l)$ (and other parameters) have to be determined from the set of coupled flow equations

$$\frac{\partial}{\partial l} u_{\mathbf{k}}(l), \quad \frac{\partial}{\partial l} v_{\mathbf{k}}(l), \quad \frac{\partial}{\partial l} u_{\mathbf{k},\mathbf{q}}(l), \quad \frac{\partial}{\partial l} v_{\mathbf{k},\mathbf{q}}(l).$$

Single particle spectrum above T_c

Single particle spectrum above T_c



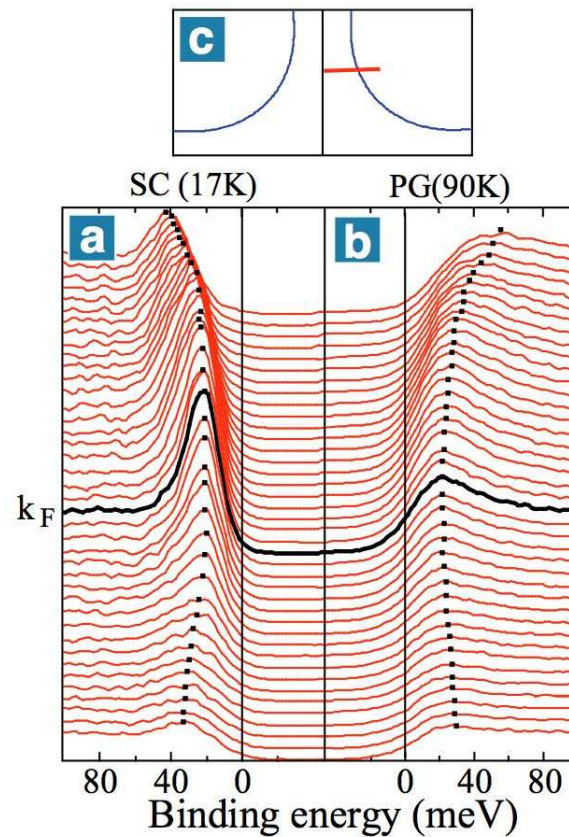
T. Domański, J. Ranninger, Phys. Rev. Lett. 91, 255301 (2003).

The Bogoliubov-type quasiparticles survive above T_c , being responsible for a partial destruction of the Fermi surface.

Evidence for Bogoliubov QPs above T_c

Evidence for Bogoliubov QPs above T_c

J. Campuzano group (Chicago, USA)

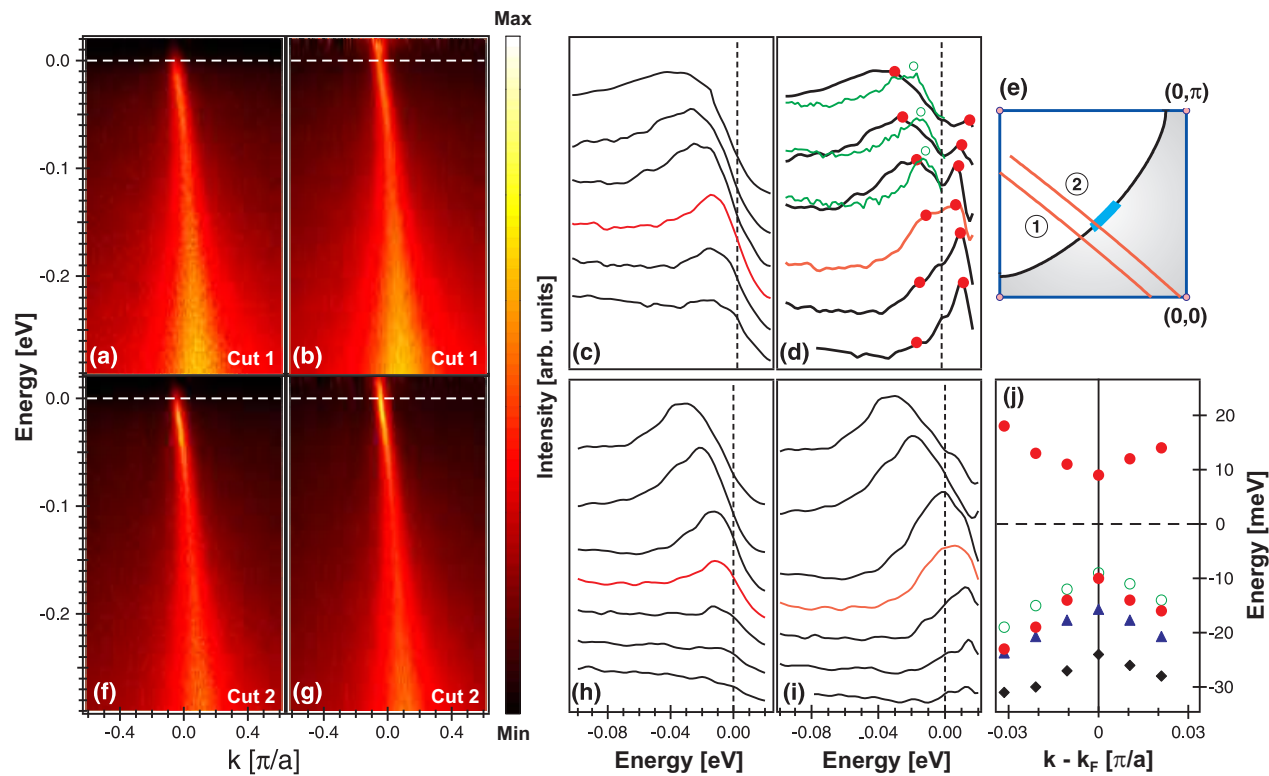


Results for: $\text{Bi}_2\text{Sr}_2\text{CaCu}_2\text{O}_8$

A. Kanigel et al, *Phys. Rev. Lett.* **101**, 137002 (2008).

Evidence for Bogoliubov QPs above T_c

PSI group (Villigen, Switzerland)



Results for: $\text{La}_{1.895}\text{Sr}_{0.105}\text{CuO}_4$

M. Shi et al, Eur. Phys. Lett. 88, 27008 (2009).

5. Ultracold gasses

Andreev spectroscopy

–

for ultracold atoms

Andreev spectroscopy

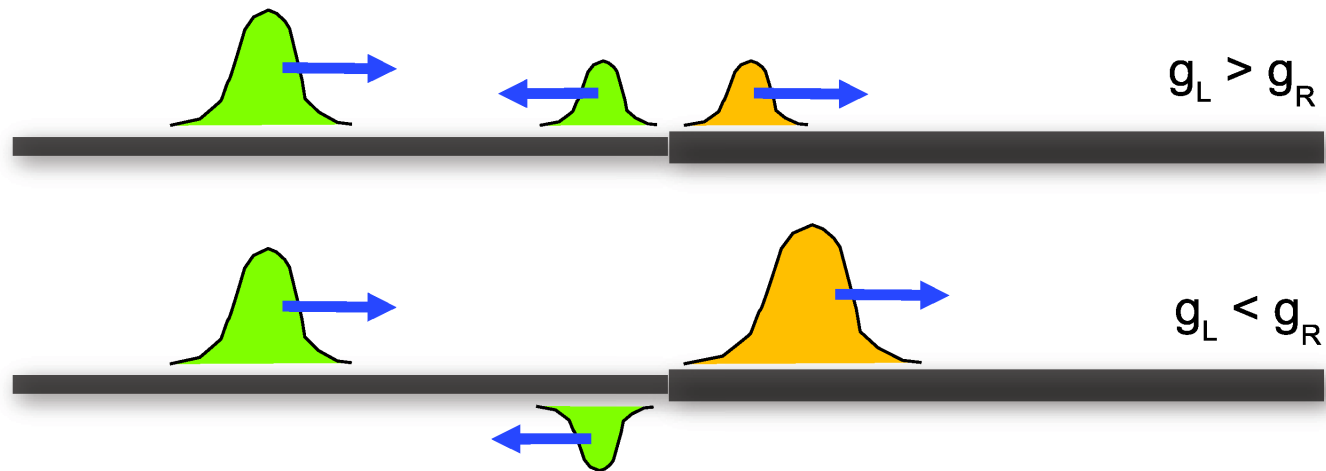
– **for ultracold atoms**

Proposal for the Andreev-type spectroscopy has been discussed also in a context of the superfluid ultracold fermion atom systems.

Andreev spectroscopy

– for ultracold atoms

Proposal for the Andreev-type spectroscopy has been discussed also in a context of the superfluid ultracold fermion atom systems.



*A.J. Daley, P. Zoller, and B. Trauzettel, Phys. Rev. Lett. **100**, 110404 (2008).*

The wave packet propagating along the 1-dimensional optical lattice can be scattered at an interaction boundary in the Andreev-type fashion.

Feshbach resonance

[local problem]

$$\begin{aligned}\hat{H}_{loc}(\mathbf{r}) = & \sum_{\sigma} \varepsilon(\mathbf{r}) \hat{c}_{\sigma}^{\dagger}(\mathbf{r}) \hat{c}_{\sigma}(\mathbf{r}) + E(\mathbf{r}) \hat{b}^{\dagger}(\mathbf{r}) \hat{b}(\mathbf{r}) \\ & + g \left(\hat{b}^{\dagger}(\mathbf{r}) \hat{c}_{\downarrow}(\mathbf{r}) \hat{c}_{\uparrow}(\mathbf{r}) + \hat{c}_{\uparrow}^{\dagger}(\mathbf{r}) \hat{c}_{\downarrow}^{\dagger}(\mathbf{r}) \hat{b}(\mathbf{r}) \right)\end{aligned}$$

Feshbach resonance

[local problem]

$$\begin{aligned}\hat{H}_{loc}(\mathbf{r}) = & \sum_{\sigma} \varepsilon(\mathbf{r}) \hat{c}_{\sigma}^{\dagger}(\mathbf{r}) \hat{c}_{\sigma}(\mathbf{r}) + E(\mathbf{r}) \hat{b}^{\dagger}(\mathbf{r}) \hat{b}(\mathbf{r}) \\ & + g \left(\hat{b}^{\dagger}(\mathbf{r}) \hat{c}_{\downarrow}(\mathbf{r}) \hat{c}_{\uparrow}(\mathbf{r}) + \hat{c}_{\uparrow}^{\dagger}(\mathbf{r}) \hat{c}_{\downarrow}^{\dagger}(\mathbf{r}) \hat{b}(\mathbf{r}) \right)\end{aligned}$$

describes:

Feshbach resonance

[local problem]

$$\begin{aligned}\hat{H}_{loc}(\mathbf{r}) = & \sum_{\sigma} \varepsilon(\mathbf{r}) \hat{c}_{\sigma}^{\dagger}(\mathbf{r}) \hat{c}_{\sigma}(\mathbf{r}) + E(\mathbf{r}) \hat{b}^{\dagger}(\mathbf{r}) \hat{b}(\mathbf{r}) \\ & + g \left(\hat{b}^{\dagger}(\mathbf{r}) \hat{c}_{\downarrow}(\mathbf{r}) \hat{c}_{\uparrow}(\mathbf{r}) + \hat{c}_{\uparrow}^{\dagger}(\mathbf{r}) \hat{c}_{\downarrow}^{\dagger}(\mathbf{r}) \hat{b}(\mathbf{r}) \right)\end{aligned}$$

describes:

$\hat{c}_{\sigma}^{(\dagger)}(\mathbf{r})$ fermion atoms (*open channel*)

Feshbach resonance

[local problem]

$$\begin{aligned}\hat{H}_{loc}(\mathbf{r}) = & \sum_{\sigma} \varepsilon(\mathbf{r}) \hat{c}_{\sigma}^{\dagger}(\mathbf{r}) \hat{c}_{\sigma}(\mathbf{r}) + E(\mathbf{r}) \hat{b}^{\dagger}(\mathbf{r}) \hat{b}(\mathbf{r}) \\ & + g \left(\hat{b}^{\dagger}(\mathbf{r}) \hat{c}_{\downarrow}(\mathbf{r}) \hat{c}_{\uparrow}(\mathbf{r}) + \hat{c}_{\uparrow}^{\dagger}(\mathbf{r}) \hat{c}_{\downarrow}^{\dagger}(\mathbf{r}) \hat{b}(\mathbf{r}) \right)\end{aligned}$$

describes:

$\hat{c}_{\sigma}^{(\dagger)}(\mathbf{r})$ fermion atoms (*open channel*)

$\hat{b}^{(\dagger)}(\mathbf{r})$ molecules (*closed channel*)

Feshbach resonance

[local problem]

$$\begin{aligned}\hat{H}_{loc}(\mathbf{r}) = & \sum_{\sigma} \varepsilon(\mathbf{r}) \hat{c}_{\sigma}^{\dagger}(\mathbf{r}) \hat{c}_{\sigma}(\mathbf{r}) + E(\mathbf{r}) \hat{b}^{\dagger}(\mathbf{r}) \hat{b}(\mathbf{r}) \\ & + g \left(\hat{b}^{\dagger}(\mathbf{r}) \hat{c}_{\downarrow}(\mathbf{r}) \hat{c}_{\uparrow}(\mathbf{r}) + \hat{c}_{\uparrow}^{\dagger}(\mathbf{r}) \hat{c}_{\downarrow}^{\dagger}(\mathbf{r}) \hat{b}(\mathbf{r}) \right)\end{aligned}$$

describes:

$\hat{c}_{\sigma}^{(\dagger)}(\mathbf{r})$ fermion atoms (*open channel*)

$\hat{b}^{(\dagger)}(\mathbf{r})$ molecules (*closed channel*)

resonantly interacting via:

Feshbach resonance

[local problem]

$$\begin{aligned}\hat{H}_{loc}(\mathbf{r}) = & \sum_{\sigma} \varepsilon(\mathbf{r}) \hat{c}_{\sigma}^{\dagger}(\mathbf{r}) \hat{c}_{\sigma}(\mathbf{r}) + E(\mathbf{r}) \hat{b}^{\dagger}(\mathbf{r}) \hat{b}(\mathbf{r}) \\ & + g \left(\hat{b}^{\dagger}(\mathbf{r}) \hat{c}_{\downarrow}(\mathbf{r}) \hat{c}_{\uparrow}(\mathbf{r}) + \hat{c}_{\uparrow}^{\dagger}(\mathbf{r}) \hat{c}_{\downarrow}^{\dagger}(\mathbf{r}) \hat{b}(\mathbf{r}) \right)\end{aligned}$$

describes:

$\hat{c}_{\sigma}^{(\dagger)}(\mathbf{r})$ fermion atoms (*open channel*)

$\hat{b}^{(\dagger)}(\mathbf{r})$ molecules (*closed channel*)

resonantly interacting via:

$\hat{b}^{\dagger} \hat{c}_{\downarrow} \hat{c}_{\uparrow} + h.c.$ (*Feshbach resonance*)

Feshbach resonance

[local problem]

$$\hat{H}_{loc}(\mathbf{r}) = \sum_{\sigma} \varepsilon(\mathbf{r}) \hat{c}_{\sigma}^{\dagger}(\mathbf{r}) \hat{c}_{\sigma}(\mathbf{r}) + E(\mathbf{r}) \hat{b}^{\dagger}(\mathbf{r}) \hat{b}(\mathbf{r}) \\ + g \left(\hat{b}^{\dagger}(\mathbf{r}) \hat{c}_{\downarrow}(\mathbf{r}) \hat{c}_{\uparrow}(\mathbf{r}) + \hat{c}_{\uparrow}^{\dagger}(\mathbf{r}) \hat{c}_{\downarrow}^{\dagger}(\mathbf{r}) \hat{b}(\mathbf{r}) \right)$$

describes:

$\hat{c}_{\sigma}^{(\dagger)}(\mathbf{r})$ fermion atoms (*open channel*)

$\hat{b}^{(\dagger)}(\mathbf{r})$ molecules (*closed channel*)

resonantly interacting via:

$\hat{b}^{\dagger} \hat{c}_{\downarrow} \hat{c}_{\uparrow} + h.c.$ (*Feshbach resonance*)

M.L. Chiofalo, S.J.J.M.F. Kokkelmans, J.N. Milstein, and M.J. Holland, *Phys. Rev. Lett.* **88**, 090402 (2002).

Local solution

[exact]

$$\mathcal{G}_{loc}(i\omega_n) = [1 - Z(T)] \left(\frac{u^2}{i\omega_n - \varepsilon_+} + \frac{v^2}{i\omega_n - \varepsilon_-} \right) + \frac{Z(T)}{i\omega_n - \varepsilon}$$

Local solution

[exact]

$$\mathcal{G}_{loc}(i\omega_n) = [1 - Z(T)] \left(\frac{u^2}{i\omega_n - \varepsilon_+} + \frac{v^2}{i\omega_n - \varepsilon_-} \right) + \frac{Z(T)}{i\omega_n - \varepsilon}$$

where

Local solution

[exact]

$$\mathcal{G}_{loc}(i\omega_n) = [1 - Z(T)] \left(\frac{u^2}{i\omega_n - \varepsilon_+} + \frac{v^2}{i\omega_n - \varepsilon_-} \right) + \frac{Z(T)}{i\omega_n - \varepsilon}$$

where

ε

..... energy of non-bonding state

Local solution

[exact]

$$\mathcal{G}_{loc}(i\omega_n) = [1 - Z(T)] \left(\frac{u^2}{i\omega_n - \varepsilon_+} + \frac{v^2}{i\omega_n - \varepsilon_-} \right) + \frac{Z(T)}{i\omega_n - \varepsilon}$$

where

ε energy of non-bonding state

$Z(T)$ the spectral weight

Local solution

[exact]

$$\mathcal{G}_{loc}(i\omega_n) = [1 - Z(T)] \left(\frac{u^2}{i\omega_n - \varepsilon_+} + \frac{v^2}{i\omega_n - \varepsilon_-} \right) + \frac{Z(T)}{i\omega_n - \varepsilon}$$

where

ε energy of non-bonding state

$Z(T)$ the spectral weight

$\varepsilon_{\pm} = E/2 \pm \sqrt{(\varepsilon - E/2)^2 + g^2}$ BCS-like excitation energies

Local solution

[exact]

$$\mathcal{G}_{loc}(i\omega_n) = [1 - Z(T)] \left(\frac{u^2}{i\omega_n - \varepsilon_+} + \frac{v^2}{i\omega_n - \varepsilon_-} \right) + \frac{Z(T)}{i\omega_n - \varepsilon}$$

where

ε energy of non-bonding state

$Z(T)$ the spectral weight

$\varepsilon_{\pm} = E/2 \pm \sqrt{(\varepsilon - E/2)^2 + g^2}$ BCS-like excitation energies

$u^2, v^2 = \frac{1}{2} \left[1 \pm (\varepsilon - E/2) / \sqrt{(\varepsilon - E/2)^2 + g^2} \right]$ BCS-like coefficients

Local solution

[exact]

$$\mathcal{G}_{loc}(i\omega_n) = [1 - Z(T)] \left(\frac{u^2}{i\omega_n - \varepsilon_+} + \frac{v^2}{i\omega_n - \varepsilon_-} \right) + \frac{Z(T)}{i\omega_n - \varepsilon}$$

where

ε energy of non-bonding state

$Z(T)$ the spectral weight

$\varepsilon_{\pm} = E/2 \pm \sqrt{(\varepsilon - E/2)^2 + g^2}$ BCS-like excitation energies

$u^2, v^2 = \frac{1}{2} \left[1 \pm (\varepsilon - E/2) / \sqrt{(\varepsilon - E/2)^2 + g^2} \right]$ BCS-like coefficients

T. Domański, Eur. Phys. J. B **33**, 41 (2003);

T. Domański et al, Sol. State Commun. **105**, 473 (1998).

Approximate general solution

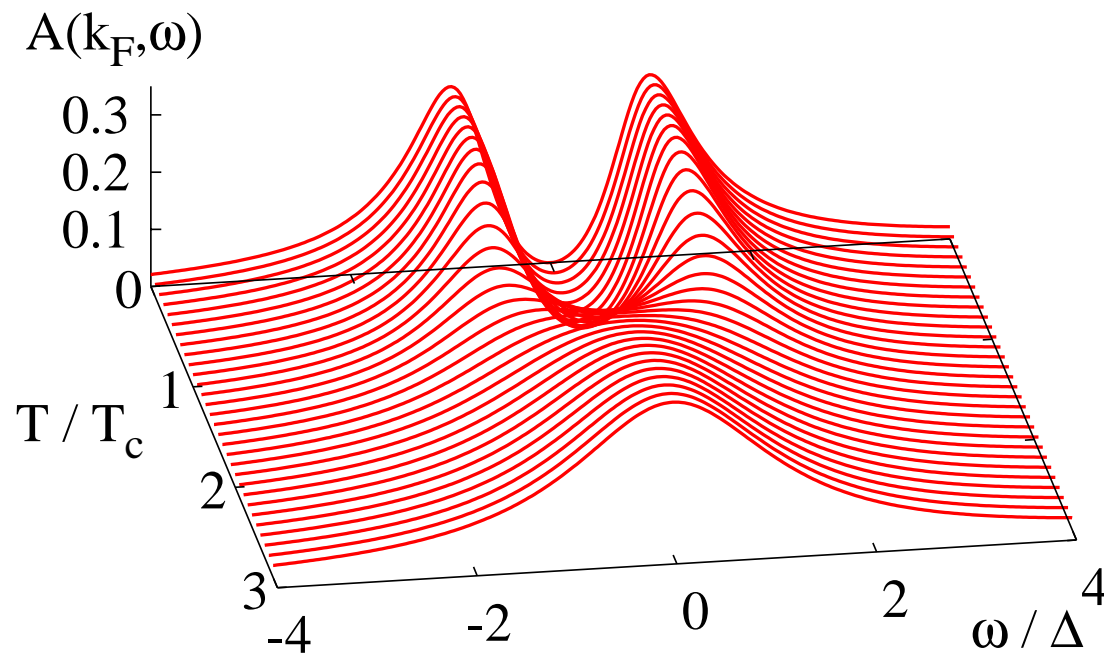
[near the unitary limit]

$$\hat{H} = \int dr \left(\hat{T}_{kin}(r) + \hat{H}_{loc}(r) \right)$$

Approximate general solution

[near the unitary limit]

$$\hat{H} = \int dr \left(\hat{T}_{kin}(r) + \hat{H}_{loc}(r) \right)$$

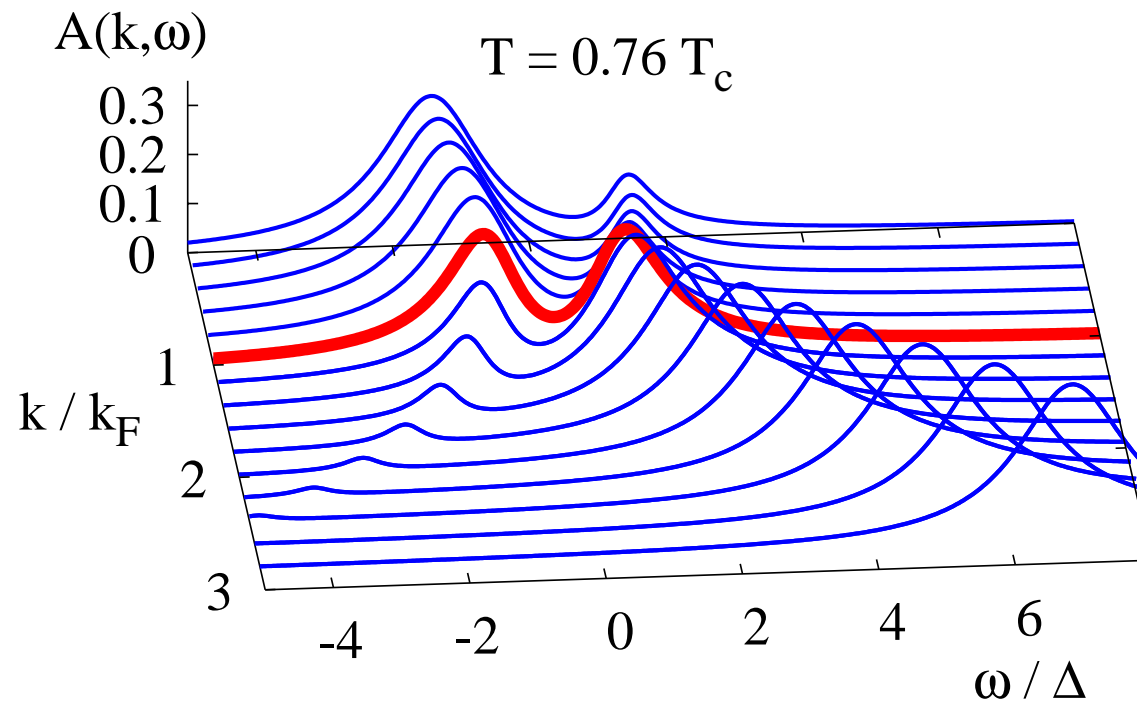


T. Domański, Phys. Rev. A **84**, 023634 (2011).

Approximate general solution

[near the unitary limit]

$$\hat{H} = \int dr \left(\hat{T}_{kin}(r) + \hat{H}_{loc}(r) \right)$$

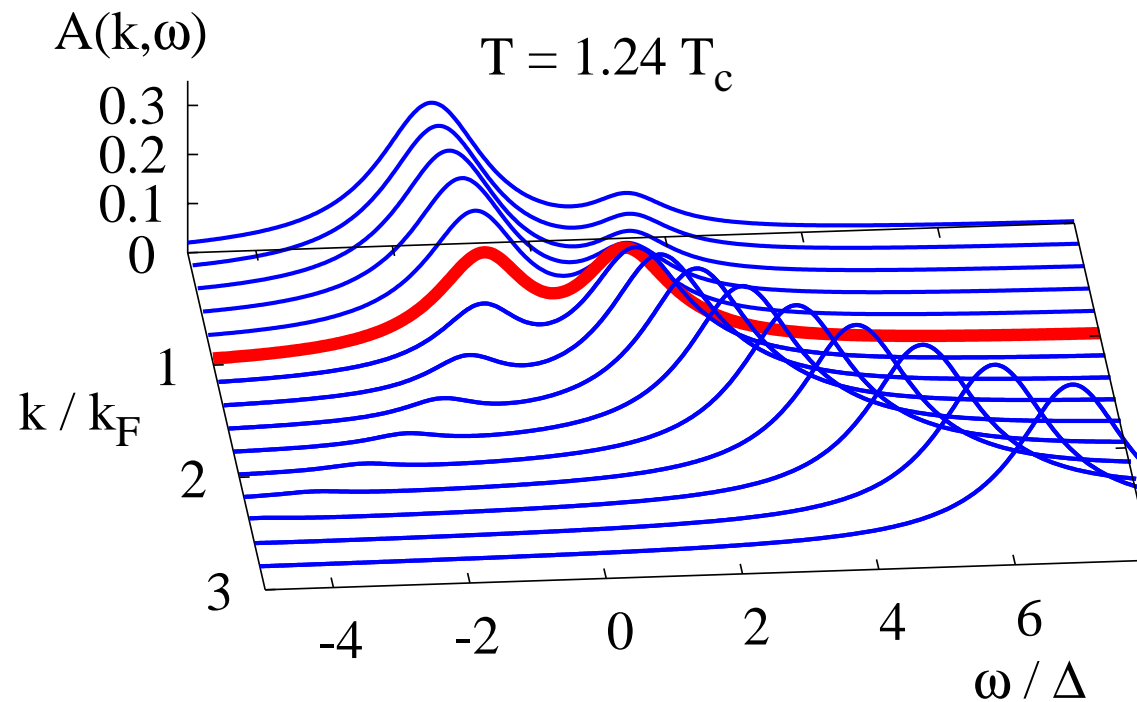


T. Domański, Phys. Rev. A **84**, 023634 (2011).

Approximate general solution

[near the unitary limit]

$$\hat{H} = \int dr \left(\hat{T}_{kin}(r) + \hat{H}_{loc}(r) \right)$$

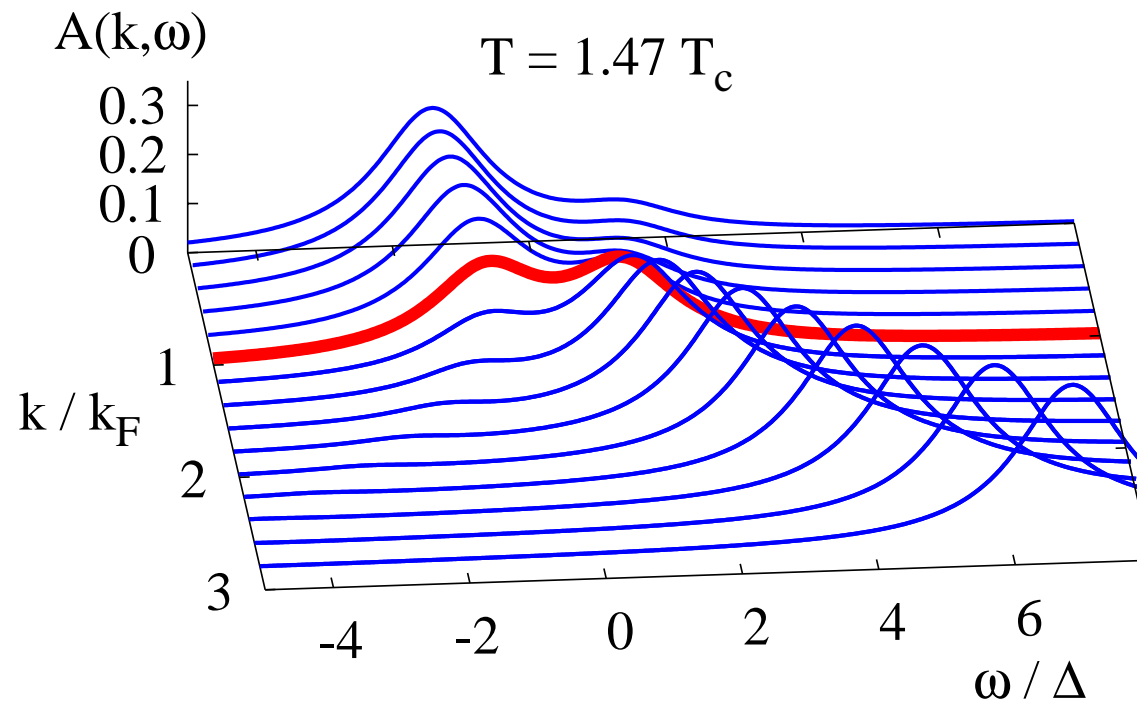


T. Domański, Phys. Rev. A **84**, 023634 (2011).

Approximate general solution

[near the unitary limit]

$$\hat{H} = \int dr \left(\hat{T}_{kin}(r) + \hat{H}_{loc}(r) \right)$$

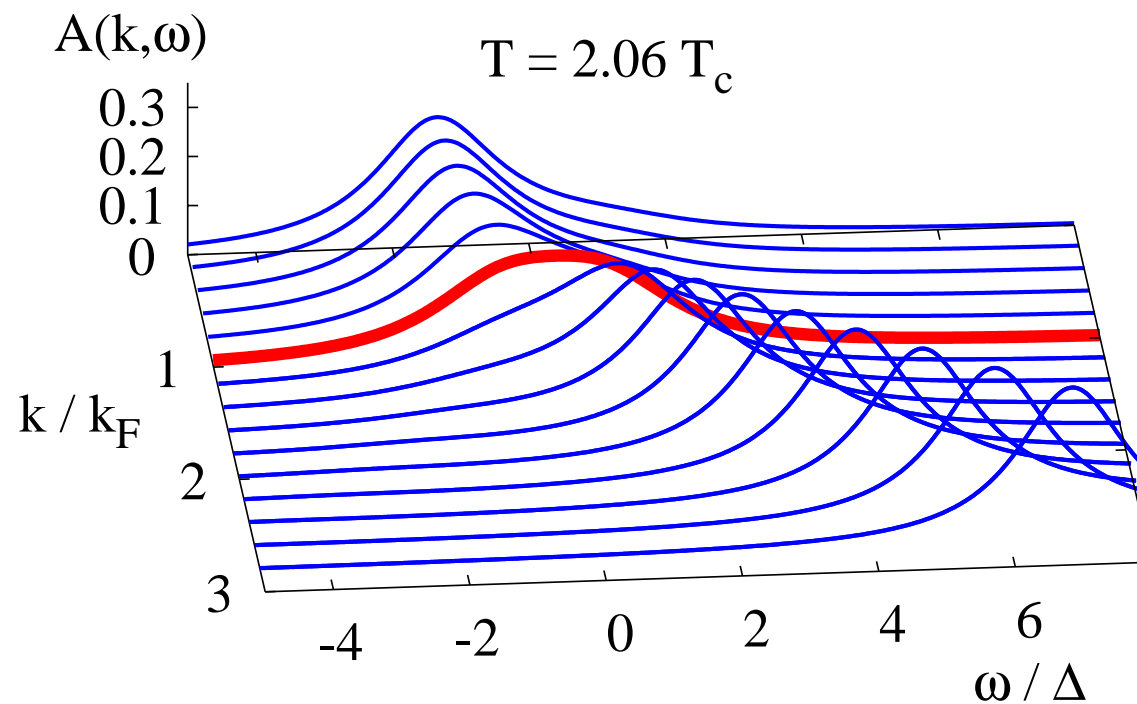


T. Domański, Phys. Rev. A **84**, 023634 (2011).

Approximate general solution

[near the unitary limit]

$$\hat{H} = \int dr \left(\hat{T}_{kin}(r) + \hat{H}_{loc}(r) \right)$$

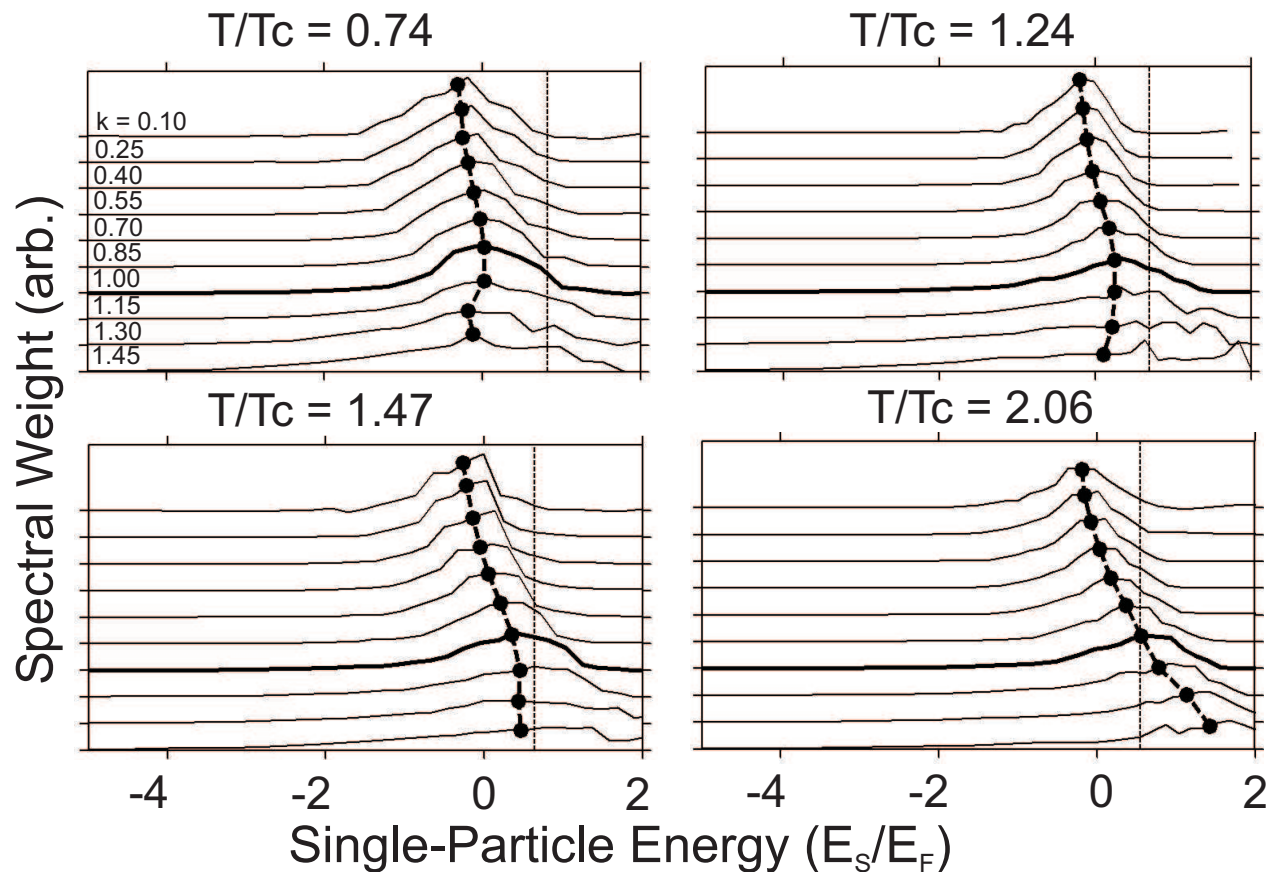


T. Domański, Phys. Rev. A **84**, 023634 (2011).

Evidence for Bogoliubov QPs above T_c

Evidence for Bogoliubov QPs above T_c

D. Jin group (Boulder, USA)



Results for the ultracold ^{40}K atoms

J.P. Gaebler et al, Nature Phys. 6, 569 (2010).

Conclusions

/ for parts 4 & 5 /

Conclusions

/ for parts 4 & 5 /

- Andreev-type scattering on the (preformed) pairs

Conclusions

/ for parts 4 & 5 /

- Andreev-type scattering on the (preformed) pairs

⇒ can lead to the superconducting features

Conclusions

/ for parts 4 & 5 /

- Andreev-type scattering on the (preformed) pairs

⇒ can lead to the superconducting features

⇒ manifested even above T_c / in absence of the ODLRO /

Conclusions

/ for parts 4 & 5 /

- Andreev-type scattering on the (preformed) pairs

⇒ can lead to the superconducting features

⇒ manifested even above T_c / in absence of the ODLRO /

- This fact is indeed observed experimentally by:

Conclusions

/ for parts 4 & 5 /

- Andreev-type scattering on the (preformed) pairs

⇒ can lead to the superconducting features

⇒ manifested even above T_c / in absence of the ODLRO /

- This fact is indeed observed experimentally by:

⇒ the Bogoliubov-type quasiparticles

/ ARPES, FT-STM, Josephson effect /

Conclusions

/ for parts 4 & 5 /

- Andreev-type scattering on the (preformed) pairs

⇒ can lead to the superconducting features

⇒ manifested even above T_c / in absence of the ODLRO /

- This fact is indeed observed experimentally by:

⇒ the Bogoliubov-type quasiparticles

/ ARPES, FT-STM, Josephson effect /

⇒ the residual diamagnetism

/ torque magnetometry, proximity induced Meissner state /

Conclusions

/ for parts 4 & 5 /

- Andreev-type scattering on the (preformed) pairs

⇒ can lead to the superconducting features

⇒ manifested even above T_c / in absence of the ODLRO /

- This fact is indeed observed experimentally by:

⇒ the Bogoliubov-type quasiparticles

/ ARPES, FT-STM, Josephson effect /

⇒ the residual diamagnetism

/ torque magnetometry, proximity induced Meissner state /

<http://kft.umcs.lublin.pl/doman/lectures>